



Heliostat Cost Down Scoping Study

Final Report

ANU document reference: STG-3261 Rev 01

For public release

Date of issue: STG-3033 Rev 01: 20 December 2013, STG-3033 Rev 02 (in ASTRI format): 22 October 2014; STG-3261-Rev 01 (modified for public release): 12 December 2016

Heliostat Cost Down Scoping Study - Project Partners:

- (1) ANU
- (2) Flinders University
- (3) CSIRO
- (4) University of Adelaide
- (5) University of South Australia
- (6) Queensland University of Technology

Contributors: Joe Coventry¹, Jon Campbell², Yun Peng Xue⁴, Colin Hall⁵, Jin-Soo Kim³, John Pye¹, Greg Burgess¹, David Lewis², Gus Nathan⁴, Maziar Arjomandi⁴, Wes Stein³, Manuel Blanco³, John Barry⁶, Matt Doolan¹, Wojciech Lipinski¹, Andrew Beath³

ASTRI Partners:



Australian
National
University



Flinders
UNIVERSITY



University of
South Australia



THE UNIVERSITY
OF QUEENSLAND
AUSTRALIA



THE UNIVERSITY
of ADELAIDE

ASU ARIZONA STATE
UNIVERSITY

NREL
NATIONAL RENEWABLE ENERGY LABORATORY



Sandia
National
Laboratories



Australian Government

Australian Renewable
Energy Agency

Copyright and disclaimer

© 2013 ASTRI To the extent permitted by law, all rights are reserved and no part of this publication covered by copyright may be reproduced or copied in any form or by any means except with the written permission of ASTRI.

Important disclaimer

ASTRI advises that the information contained in this publication comprises general statements based on scientific research. The reader is advised and needs to be aware that such information may be incomplete or unable to be used in any specific situation. No reliance or actions must therefore be made on that information without seeking prior expert professional, scientific and technical advice. To the extent permitted by law, ASTRI (including its employees and consultants) excludes all liability to any person for any consequences, including but not limited to all losses, damages, costs, expenses and any other compensation, arising directly or indirectly from using this publication (in part or in whole) and any information or material contained in it.

1 Contents

1	Contents.....	3
2	Executive Summary.....	5
3	Introduction	8
4	Current heliostat designs and developments.....	9
	4.1 Heliostats offered commercially.....	10
	4.2 Heliostats under development	11
5	The key to LCOE reduction.....	17
	5.1 Leverage of heliostat performance	17
	5.2 The importance of O&M costs	18
6	Solar field design.....	19
7	Heliostat manufacturing and assembly	20
	7.1 Heliostat manufacturing case study 1: Brightsource Ivanpah.....	21
	7.2 Heliostat manufacturing case study 2: Brightsource FAST.....	22
8	Heliostat size.....	23
9	Wind loads	25
	9.1 Is it windy where it is sunny?.....	25
	9.2 Static wind load	28
	9.3 The dynamic wind load on the heliostats.....	33
10	Mirrors	36
	10.1 Glass mirrors.....	36
	10.2 Reflective films	38
	10.3 Polished metal	40
	10.4 Plastic mirrors.....	41
	10.5 Anti-soiling coating for glass.....	42
	10.6 Structural mirror panels	43
11	Production Methods for Mirror Supports.....	45
	11.1 Introduction.....	45
	11.2 Design	45
	11.3 Plastics	46
	11.4 Metals.....	49
	11.5 Summary of production methods for heliostat supports.....	50
	11.6 Issues to explore	51
12	Communications	52
	12.1 Autonomous heliostats.....	52
	12.2 Conventional communications systems.....	52
13	Sun tracking systems.....	53

13.1	Horizontal primary axis heliostats	54
13.2	Target aligned heliostats	55
13.3	Heliostat shape	57
13.4	Canting.....	58
13.5	Low profile mirror panels	60
14	Actuation systems.....	61
14.1	Pedestal mounted drive systems.....	61
14.2	GFC.....	64
14.3	Flextronics.....	64
14.4	Linear drive systems	64
14.5	Rim drive systems.....	65
14.6	Hydraulic drive systems.....	66
14.7	Pipe-in-pipe drive system	67
14.8	Backlash	68
15	Foundations	69
16	Cost information	71
16.1	NREL (2013)	71
16.2	Sandia (2011).....	71
16.3	Abengoa Solar (2010)	71
16.4	Sandia (2007).....	71
16.5	Heliostat cost information from SolarPACES 2013.....	72
16.6	Cost summary	73
17	Key findings.....	74
18	Acknowledgement	79
19	References	80
Appendix A Mirror Technologies used in Solar Thermal Facilities Globally		90

2 Executive Summary

The Heliostat Cost Down Scoping Study is a preliminary activity led by the ANU, part of the ASTRI Node 1 program to reduce capital expenditure across an entire CSP solar field, and is the first step in a heliostat cost-reduction project to be carried out over the 8 year ASTRI program.

The context for this report is the annual growth of the global CSP industry by 40% since 2005; it is expected that installed capacity will reach 4.5 GWe in 2013. There is unprecedented growth for power tower technology predicted for 2013, with 500 MWe expected to become operational this calendar year compared to the 65 MWe presently in operation. However, for growth to continue, the capital cost of the solar field must continue to be brought down. The cost of heliostats is presently estimated to be in the range 150-200 USD/m² and the target costs for heliostats are generally in the range 75-120 USD/m². This indicates that there is an expectation within the industry for large cost reductions.

Some of the key findings of the literature review are summarised here by topic:

Leverage of performance: heliostat performance has a strong leverage on LCOE, and as a result the use of mirror with high reflectance is important. The benchmark is 3-4 mm silvered glass mirrors with solar-weighted spectral reflectance around 93-94%, but there is the possibility of achieving higher reflectance through the use of thinner glass and reflective films.

Importance of O&M costs: O&M costs have a strong impact on LCOE when aggressive LCOE targets apply. Compatibility with low-cost cleaning systems is an important design requirement.

The influence of solar field layout: heliostats deployed in power tower plants with >50% efficient power cycles are more likely to be arranged in a polar field rather than a surround field, due to the compatibility with cavity receivers. However, a surround field is also possible. Both field layouts require optically accurate heliostats to achieve high flux at the receiver with acceptable uniformity and light spillage.

Manufacturing and assembly: it has been estimated that as much as 80% of the cost of product development and manufacture is determined by the decisions made in the initial stages of design. Concurrent engineering processes are essential for a quality, low-cost outcome for a new heliostat design, i.e. engineers across disciplines working together from the earliest stages of product design and through the design life-cycle. Make-buy decisions are important, and supplier capability is a key issue. The benefits of low-cost country sourcing cannot be overlooked.

Heliostat size: Currently operational heliostats range in size from 1.14 m² to 120 m², and there is no consensus regarding the optimal size of a heliostat. In the past, the studies indicated that heliostats should be very large to be cost effective, at least 50 m² and preferably larger. The main driver to large scale was the cost per m² of the heliostat drive system. However, as size is reduced to a scale equivalent to other volume manufactured commodity items, a number of drivers relating to manufacturing and assembly become more relevant, such as:

- a. Production volume
- b. Use of common-off-the-shelf (COTS) components
- c. Use of low-cost manufacturing processes
- d. Use of standard assembly processes
- e. Transport and logistics

These cost drivers all favour reduced scale, and have the impact of lowering specific cost.

Static wind loads: a key initial design decision is the determination of peak static wind loads, due to the sensitivity of loads (and hence material cost) to the wind specification. Design loads derived from wind tunnel tests are more accurate, and generally lower, than those derived using building codes.

The wind load on heliostats can be reduced by the application of wind barriers. In addition, inner rows are partially protected from the wind by outer rows of heliostats, and for certain heliostat orientations, they may experience a reduction in total wind load as high as 90% compared to the first row.

Another technique to reduce loads is to mount a porous fence at the edge of the mirror panel. This can reduce the overturning moment by as much as 40%.

Dynamic wind loads: where the frequency of wind induced vibration matches a natural frequency of the heliostat structure, deformation or damage of the heliostat structure may occur. Adjusting the flow field to reduce vortex formation is an attractive alternative to increasing the rigidity of the structure. Previous work on heliostat aerodynamics has mainly addressed static wind load characteristics, while the dynamics of wind loading have not been fully understood and considered in heliostat design.

Reflector technologies: mirrored glass and reflective film are the most suitable current (or near-term) options for heliostat reflectors. Polished metal and plastic mirrors both do not currently have adequate reflectance. There are around six suppliers of standard 3-4 mm low-iron mirrored glass for solar applications. Three of these can also supply thin mirrored glass (~1 mm). Glass mirrors should be considered default reflector, as they are relatively inexpensive, durable, have high reflectance and are accepted by industry. There are around four suppliers of reflective film. Reflective film technology is still evolving and continuing to improve, particularly via an active research program by 3M, and encouraging durability results.

Structural mirror panels: there is a significant renewal of development in mirror facets based on sandwich panel type constructions. Two companies offer foam cored sandwich panels commercially. Sandia is also actively working with US manufacturers to develop new sandwich panel facets. Sandwich panel constructions have the following key advantages: use of thin glass is feasible, hence there is improved reflectance; and sandwich panels are very strong and rigid, and with good design can lower the mirror support costs. Structural mirror panels may also be made incorporating structural features with the largely planar mirror facets, either as integral features or by bonding to the reflector. For example, pressed sheet metal structures support the glass at both the Gemasolar and Crescent Dunes projects. Various options exist with plastics, most likely in combination with a reflective film. For example, thermoforming or compression moulding of a pre-prepared flat sheet of a thermoplastic polymer may achieve suitable optics at a competitive cost.

Autonomous heliostats: development of autonomous heliostats – i.e. heliostats that do not require power or communication wiring – has progressed markedly in recent years and there is potential for significant cost compared to conventional wired systems.

Alternative solar tracking systems: the majority of heliostat systems have used the ‘azimuth-elevation’ style of sun tracking. However, other styles of tracking have been used in a number of recent prototypes. These include horizontal primary axis heliostats, which are suitable for linear actuators on both axes and allow denser spacing, and target aligned heliostats, which minimise astigmatic aberration to improve overall solar capture and flux uniformity.

Actuation systems: actuation systems have long been one of the key cost drivers for heliostats. The pedestal mounted azimuth drive system has been one of the main drivers to larger size heliostats. However, some technology developers believe linear drive systems are

cheaper, and can completely replace azimuth drives. Alternative drive systems, such as rim drives with cables, have been proposed to avoid the cost of pedestal mounted systems. Hydraulic drive systems have been used cost effectively on large heliostats.

The scoping study has investigated in detail the current state-of-the-art of heliostat design and found that significant potential remains for deep cost reductions.

3 Introduction

The Heliostat Cost Down Scoping Study [1] is a preliminary activity led by the ANU, part of the ASTRI Node 1 program to reduce capital expenditure across an entire CSP solar field.

The context for this report is the annual growth of the global CSP industry by 40% since 2005; it is expected that installed capacity will reach 4.5 GWe in 2013 [2]. There is unprecedented growth for power tower technology predicted for 2013, with 500 MWe expected to become operational this calendar year (2013) compared to the 65 MWe presently in operation [3]. For the CSP industry it is a period of uncertainty – with strong competition in the solar sector from PV, a moratorium on renewable energy plants in Spain, and a slow recovery from the global financial crisis – and a period of promise, with 2.9 GWe under construction and 7.3 GWe soon to commence construction [2]. Strongly funded research programs are in place, with aggressive levelised cost of energy (LCOE) targets, such as the U.S. SunShot program, with a 0.06 USD/kWh target [4], and the Australian Solar Thermal Research Initiative (ASTRI) program, with a 0.12 AUD/kWh LCOE target [5], both by 2020. This review is the first step in a heliostat cost-reduction project to be carried out as part of the 8 year ASTRI program. We discuss technology trends and examine some of the best prospects to progress the state-of-the-art technology to reduce heliostat solar field costs, which is consistent with ASTRI goals.

The history of design and deployment of heliostat fields is well documented [6, 7]. The first documented study was in the USSR in the 1950's, involving large tilted mirrors mounted on railroad carriages. Only a crude, manually operated, prototype heliostat was constructed. Early experiments were carried out in the 1960s by the University of Genoa, including construction of a field of 121 heliostats. During the 1970's six power tower plants were constructed worldwide, from 500 kWe to 10 MWe. In the early 1980s Sandia made an extensive evaluation of heliostat designs (see the vast number of references in [6]). Four different designs were produced during the program (McDonnell Douglas, Northrup, Boeing, Martin Marietta) as shown in Figure 1. All four designs were assessed as being mass manufacturable at low cost.

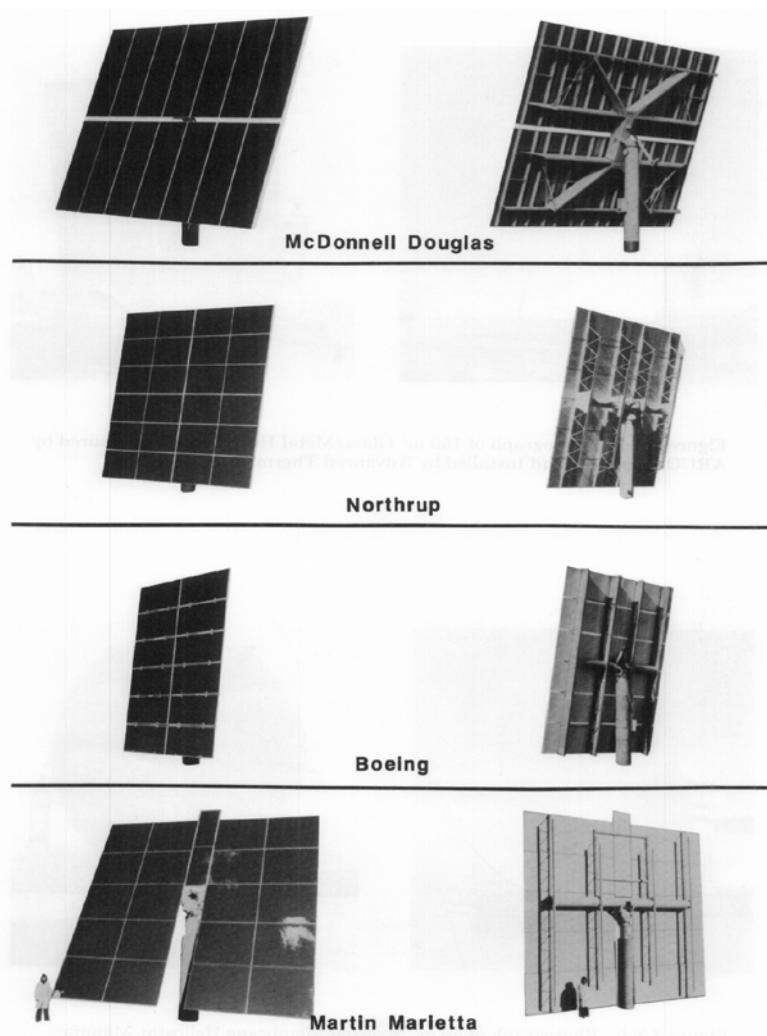


Figure 1. 'Second-generation' heliostats, developed under the 1980's Sandia led heliostat program[6].

The style of all four designs is the azimuth-elevation tracking glass/metal pedestal design, which had extensive research, development and testing throughout the 1980s, and remains the most common heliostat type operating in commercial power towers today.

The actual cost of heliostats is presently estimated to be in the range 150-200 USD/m² [8, 9] and the target costs of heliostats are generally in the range 75-120 USD/m² [4, 9, 10], indicating that there is an expectation within the industry for large cost reductions. This expectation was further validated during industry panel discussions at the recent SolarPACES conference, with expectations of 50% cost reductions and near-term achievement of the Sunshot target of 75 USD/m² expressed by companies such as Brightsource and Abengoa. Further details of the current cost estimate range are given in Section 16.

4 Current heliostat designs and developments

As described above, glass-metal, faceted T-shaped heliostats have long been the dominant technology, and continue to be deployed in the largest power tower installations using the technology of companies like Brightsource Energy, Solar Reserve, Sener and Abengoa [7, 11-15]. This style of heliostat also continues to have popularity for new heliostat designs, for

example, NEM Energy's 58 m² heliostat [16] and AORA Solar's 16 m² heliostat [17], both under test at PSA.

A recent DLR survey of a wide range of heliostat designs categorised pros and cons of the various design features in a systematic way, in order to make a series of recommendations of promising concepts [18]. Similarly, in this report we focus on those design features at a sub-system or component level that we believe have the best performance improvement and cost reduction potential.

4.1 Heliostats offered commercially

Brightsource is deploying its 15.2 m² LH 2.2 heliostats for the Ivanpah project (Figure 2) [12]. Ivanpah consists of 173,500 heliostats and 3 x 130 MWe towers in the Mojave Desert in California. Brightsource has developed a new larger heliostat design, the 19.0 m² LH2.3, which it plans to use in future projects.

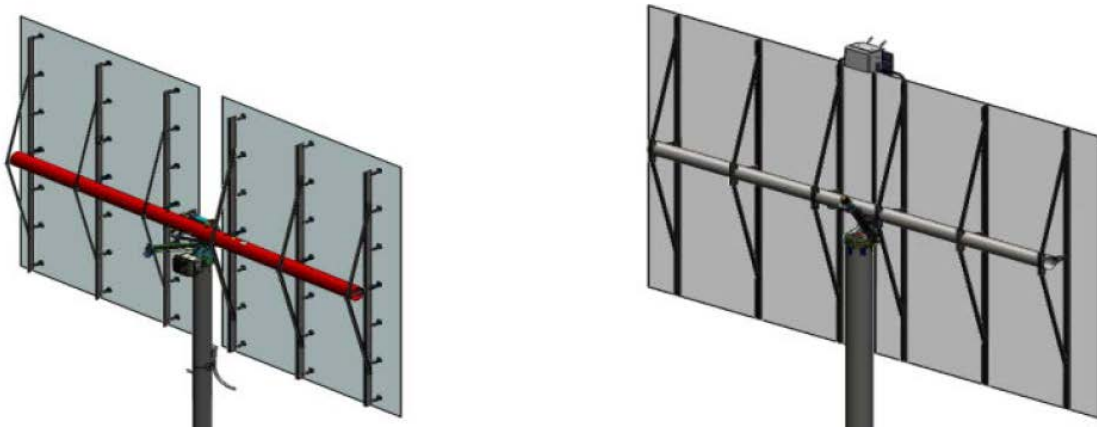


Figure 2. Brightsource 15.2 m² LH 2.2 heliostat (left) employed at Ivanpah, and the new 19.0 m² LH2.3 heliostat (right) [12]

Abengoa Solar has installed its 120 m² heliostat 'Sanlúcar 120' model at the PS10 and PS20 plants in Spain [19]. Each heliostat has 28 spherically curved facets. A new heliostat, the 140 m² 'ASUP 140' is being installed at the 50 MWe Khi Solar One plant in South Africa [20]. It has 4 extra facets, uses thinner glass on sandwich panel type facets, and is claimed to be 30% cheaper.



Figure 3. Abengoa Solar heliostats – the Sanlúcar 120 (left) [19] and the ASUP 140 (right) [21].

SENER's most recent heliostat design is the 115.7 m² heliostat deployed at the Gemasolar plant (Figure 4). Each heliostat is composed of 35 facets made of a 3mm thick mirror reinforced with a galvanized stamped steel support that is bonded to the rear mirror face [13]. The 20 MWe Gemasolar plant consist of 2650 heliostats, and a single 140 m high tower. It is also equipped with 15 hours thermal energy storage through a molten salt system.



Figure 4. 115.7 m² Sener heliostat (left) and 1.14 m² eSolar heliostat (right) [13, 22].

At a size of 1.14 m², eSolar's heliostat design is the smallest available commercially. The flat mirrors are individually tracked using a hybrid stepper motor system, and mounted on an h-frame as shown in Figure 4 [22]. The heliostats are supported on a truss structure, ballasted and shared with other heliostats. At this stage the eSolar heliostats have not been installed in a fully commercial plant, but eSolar demonstrated its technology at the 5 MWe Sierra SunTower, which has been operational since 2009.

4.2 Heliostats under development

We describe here a number of heliostats under development. Some have been offered commercially, and in certain cases deployed at pilot scale.

The DLR 'autonomous light-weight' heliostat [23] is a primary horizontal axis design, with cable driven rim drives on both axes and a single high accuracy (0.6 mrad slope error) curved laminated mirror panel made by Toughtrough [24]. It uses a wireless communication and energy supply system, developed by Trinamic [25]. Other features are a prefabricated concrete ground anchor, and a wind load reduction mechanism using a perimeter fence mounted on the heliostat.

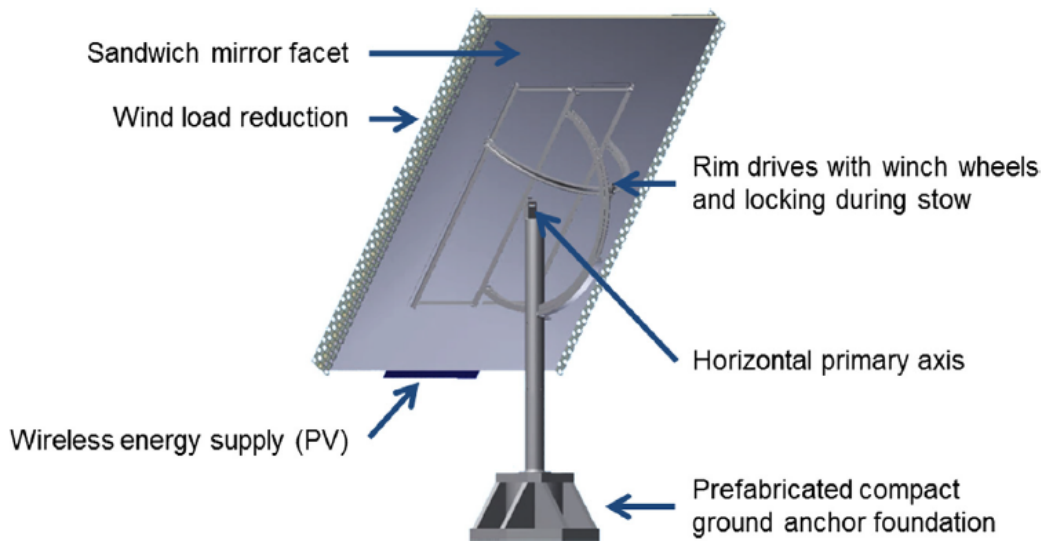


Figure 5. DLR's 8 m² 'autonomous light-weight' heliostat [23]

The Solaflect 'suspension heliostat' [26] is comprised of 16 x 1 m² glass facets held in position by cables tensioned from a compression element perpendicular and central to the mirror panels (Figure 6). The mirrors themselves are also in compression. The heliostats can be canted by adjusting the cable tension via threaded rods, although in a more recent design iteration, canting is fixed by use of precision pre-manufactured cables [27] (see Section 13.4 for more discussion of canting). It is claimed that material use is as low as 35-40% of that of a conventional heliostat.



Figure 6. Solaflect's 16 m² 'suspension heliostat' [26]

In 2010 and 2011, as part of the Australian Solar Institute foundation project, CSIRO constructed a 1 MW_{th} solar thermal array using the CSIRO heliostat design (Figure 7). Performance Engineering, a Central Coast NSW company, was selected to fabricate the heliostats [28].

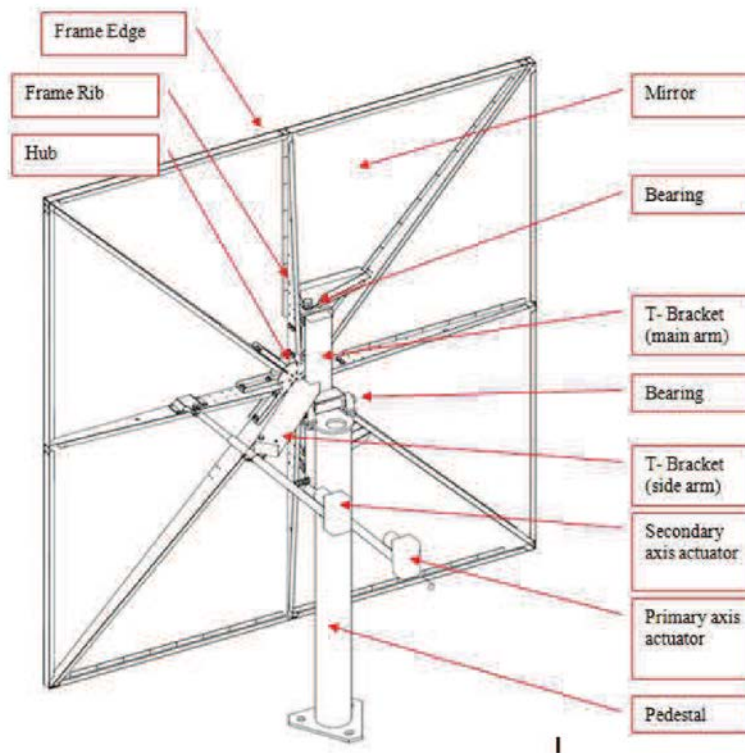


Figure 7. Schematic representation of the CSIRO heliostat [28]

The design parameters are given in Figure 8.

CSIRO HELIOSTAT DESIGN PARAMETERS	
Mirror Size	4.84 m ² (2.2 m × 2.2 m), considerable up to 5.76 m ² (2.4 m × 2.4 m)
Reflectivity	92 % solar weighted specular reflectivity.
Surface Error	Less than 1.2 mrad slope error (standard deviation of error of normal in one dimension)
Control Error	Less than 1.5 mrad (standard deviation of error of mirror normal in one axis)
Maximum Wind Rating	40 m/s (Structure and footing designed to meet AS1170.2; highest 50 year wind event in a non-cyclonic region is a gust speed of 44m/s. With a terrain/height multiplier of 0.91, the maximum design speed is 40 m/s.)
Operating Wind Rating	Structure has structural rigidity to maintain specified control error up to 15 m/s operating wind speed

Figure 8. The CSIRO heliostat design parameters [28]

The TitanTracker heliostat [29] is a 150 m² azimuth-elevation ‘carousel’ style heliostat (Figure 9), developed in Spain.



Figure 9. The 150 m² TitanTracker heliostat [29]

JPL & L'Garde have recently commenced a Sunshot supported project to develop a large faceted heliostat, with one innovative feature being facets that are designed to 'give' in winds greater than 35 mph (15.6 m/s) then relatch with a magnetic latch system (Figure 10) [8, 30]. Tension wires are used to minimise the mass of the structure and to impart curvature. Polymer reflective films are to be bonded to foam cored sandwich panels to form the mirror facets.



Figure 10. JPL/L'Garde heliostat concept [26]

NREL recently concluded a short investigation into a new heliostat design, funded under the Sunshot program (Figure 11) [8, 31]. The focus areas included a cable drive system, glass integrated structural design, a wireless control system, and an image based tracking system to allow use of low cost sensors.

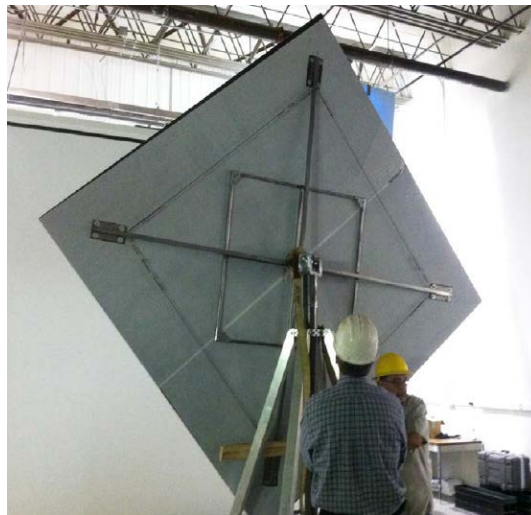


Figure 11. The NREL heliostat prototype [31]

HelioTower, an IP holding company spun off upon the demise of Solar Millenium, has developed a heliostat design (Figure 12) with key features being a horizontal primary axis tracking mode with both axes driven by linear actuators, a sheet metal fabricated pylon that is off-centric to allow the necessary range of tracking, and clipped reflector corners to allow denser spacing for minor loss of collector area.

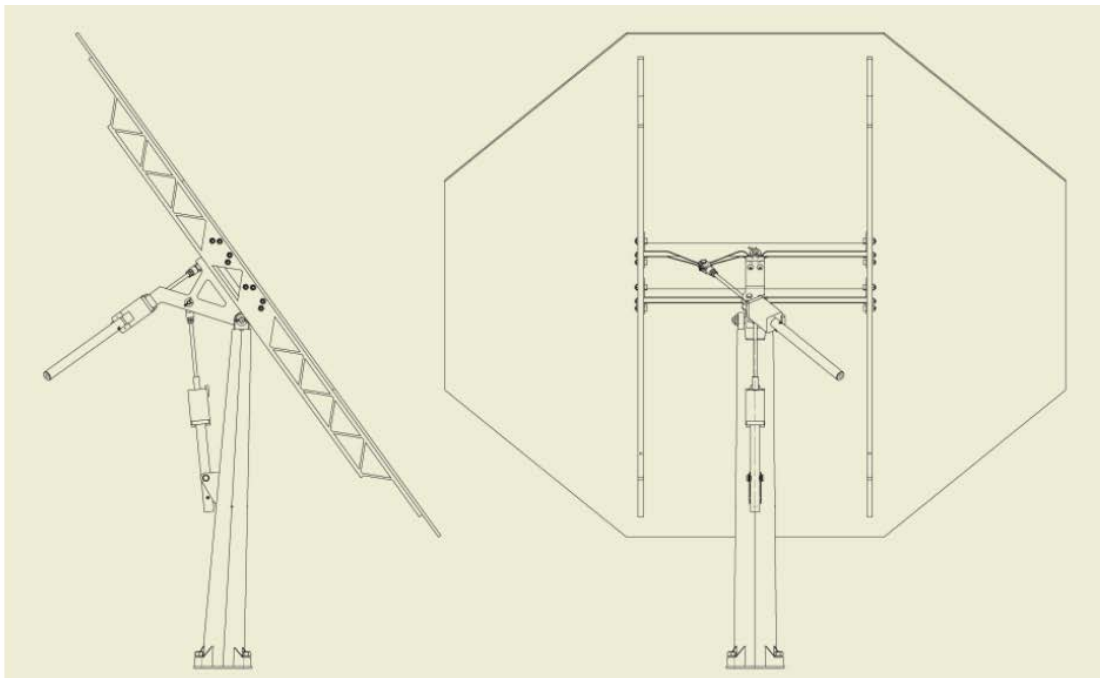


Figure 12. Heliotower's heliostat design [32]

The HydroHelio heliostat is a 'standard' pedestal mounted design, however it makes use of a hydraulic drive system (Figure 13) [33, 34]. An alternative version of this heliostat, where the hydraulic power unit and cylinders are incorporated in the cross beam to provide rotary motion via a chain drive, is described below in Section 14.6.

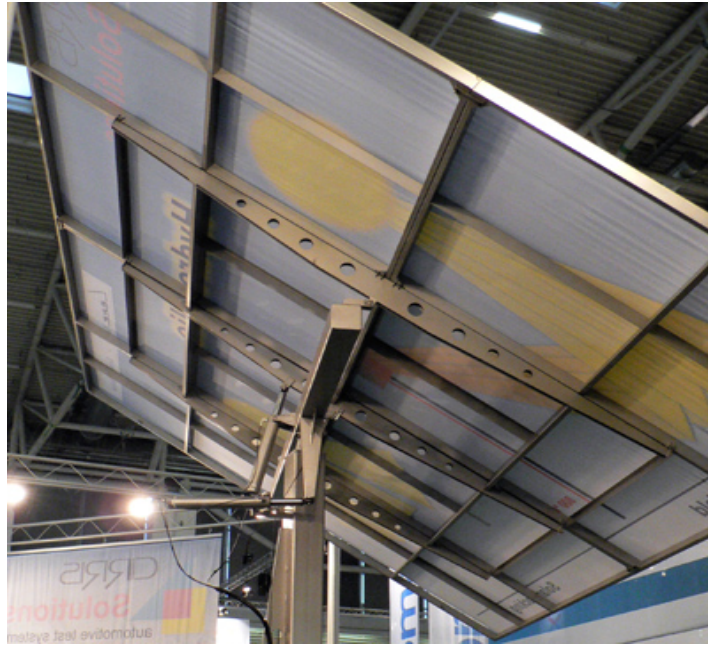


Figure 13. Hydrohelio heliostat [34]

Heliosystems is pursuing a 9 m² so-called “Passive Adjustment Toroidal Heliostat” (PATH), which uses the target-aligned tracking method described in Section 13.2. The prototypes shown in Figure 14 use the gravitational method of passive curvature adjustment, described in [35]. The target application is tower systems requiring concentration ratios higher than can be achieved with conventional heliostats. According to Alex Lehmann (personal communication, 01/08/13) there are 14 such heliostats under test in Cooma, and there is a project under development in China which will utilise 1000 heliostats. Another version of Heliosystems heliostat, under test in Cooma, has passive astigmatism correction using a ‘mechanical’ system that makes use of the elevation rotation [35, 36].



Figure 14. Heliosystem's passive adjustment toroidal heliostat (PATH) [photo: Joe Coventry]

The Google heliostat [37] is a 6 m² sandwich panel made entirely of glass, swivelled about a universal joint on a tetrahedron-like frame (Figure 15). The tracking is carried out via two

winch driven cables, tensioned by the unbalanced mass of the mirror. Google has concluded its research into power tower technology, citing both technical and commercial reasons.

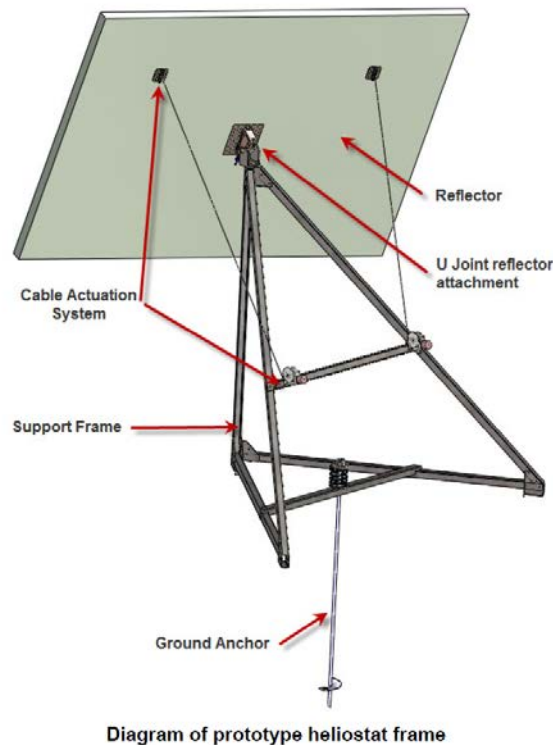


Figure 15. The Google heliostat [37]

5 The key to LCOE reduction

ANU takes the position that the key to achieving LCOE targets is not to achieve a single ‘breakthrough’ development, but to bring together as many of the performance improving, cost reducing design concepts as possible into a single package, integrating design decisions at a solar field level, an individual heliostat level, and subcomponent level.

5.1 Leverage of heliostat performance

It is worth comparing the difference in leverage of heliostat performance and cost on the LCOE. For example in a recent report on CSP in Australia [38], a sensitivity analysis about a 250 AUD/MWh baseline showed that a 10% improvement in annual generation, and a 10% reduction in capital cost have a similar impact on LCOE: 8% and 9% reduction respectively (in other words, the ‘steepness’ of the red and yellow lines in Figure 16 are reasonably similar when close to this baseline). However, the solar field makes up only about 38% of the direct capital cost in a power tower plant [9]. Therefore, in terms of LCOE reduction a design change that results in 1% performance improvement is equivalent to a design improvement that reduces solar field cost by about 2.3%. In other words the performance of the solar field has about 2.3 times greater impact on the LCOE than the field cost. The leverage of performance is important to consider at all times. It is probably relevant to most practical application for heliostat design decisions that relate to the optical performance, for example, selection of the mirror type, annual optical efficiency of the heliostat field, and cleaning regimes..

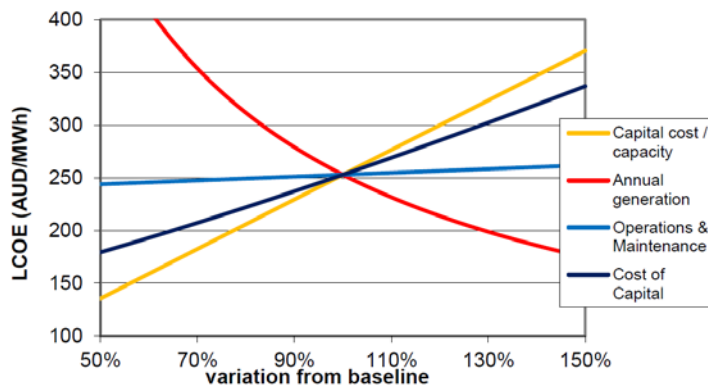


Figure 16. Variation of cost against an LCOE baseline of a Nevada Solar 1 type system at Longreach, from [38].

Despite these observations about the relative leverage of performance and cost reduction, capital cost reductions are emphasised by programs such as ASTRI and Sunshot, with targets of around 50% cost reduction. On the other hand, performance improvement, in terms of energy delivered by the heliostat field, is probably limited to less than 10%, through measures such as higher reflectivity mirrors, better solar field efficiency, and higher optical capture at the receiver. Therefore, despite the greater leverage of improved performance, because of the magnitude of potential cost reductions, continuing to drive down heliostat cost is critical to the future competitiveness of power tower systems.

5.2 The importance of O&M costs

In a recent paper, Zhu discusses the increased leverage of operations and maintenance (O&M) costs on LCOE as the cost of the plant comes down [39]. Zhu defines the annual investment energy return (IER) as the ratio of the annual net generated electricity of a solar power plant to the direct system cost of the plant. Figure 17 shows the LCOE as a function of annual IER for different variable O&M cost assumptions. While Zhu's study relates to linear Fresnel systems, Figure 17 is independent of the technology type (although it does represent a specific set of financial assumptions based on the default values from the DOE Sunshot program [40]).

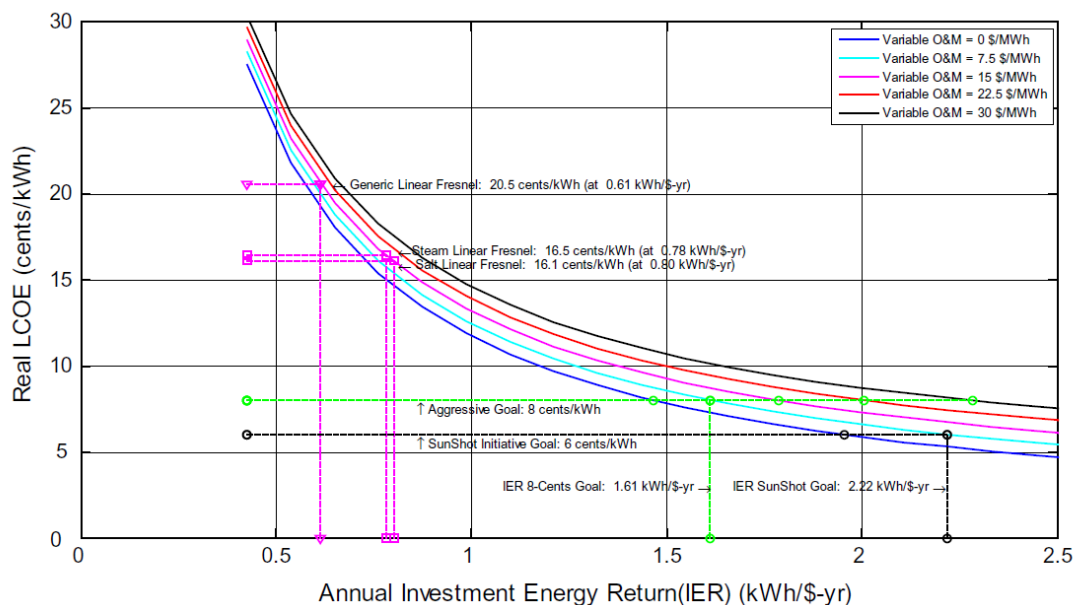


Figure 17. LCOE as a function of annual IER for different variable O&M cost assumptions [39].

A useful feature of this plot is that it mathematically separates physical system variation (such as collector design and efficiency) from the financial metrics. Zhu made a few key observations based on this curve:

- LCOE shows asymptotic behaviour as a function of IER, not linear behaviour. It drops quickly as a function of IER at low annual IER values (such as 0.5), but is less sensitive at fairly large IER values (such as 1.5).
- O&M costs have a dramatic impact on LCOE, particularly for higher IER values. For example, for an O&M cost of 30 USD/MWh it would seem impossible to reach an LCOE of 6 c/kWh, no matter how much the IER is boosted.

Another way of looking at this is to consider a particular LCOE target. For a LCOE goal of 8 c/kWh, IER ranges from about 1.6 to 2.3 for O&M costs ranging from 7.5 to 30 USD/MWh. This is a large increase (>40%) in the output required, assuming fixed capital cost, to cover increased O&M costs.

We can conclude that the design of the heliostat must take into account O&M considerations, particularly when aggressive LCOE targets apply. This is probably particularly important for cleaning systems – ease of cleaning should be a key objective.

6 Solar field design

Current CSP research programs have ambitious performance goals, such as > 50% power cycle efficiency using working fluids hotter than 650 °C for the SunShot program [4]. The supercritical CO₂ Brayton cycle is seen as a good prospect to achieve this aim [41, 42]. Critical factors for receivers operating at such high temperatures are a high concentration ratio (i.e. high optical accuracy from the solar field¹) and a low radiative view factor [43]. While both cavity and external receivers are feasible, better thermal efficiency is attainable with a cavity [43].

The design requirements of individual heliostats influence, and are influenced by, the design of the solar field layout and the receiver type. The two most common field layouts are the ‘surround field’ (e.g. Solar Two, Gemasolar, Ivanpah, Crescent Dunes) and the ‘polar field’ (e.g. Thermis, PS10, PS20, Julich). LCOE analysis comparing surround and polar layouts should take into account all factors – blocking, shading, cosine losses, atmospheric attenuation, tower height, latitude, plant size, etc. The best option varies case-to-case, as evidenced by studies and by continued commercial development of solar towers of both layout types [6, 44]. External-type receivers are suited to both field layouts. Cavity-type receivers are better suited to polar fields, although multiple cavities or downward facing cavities are feasible for surround fields [45, 46].

Assuming here a power tower optimized for high temperature, high efficiency energy conversion, we make the following observations regarding our new heliostat design:

- Heliostats deployed in >50% efficient power tower plants are more likely to be arranged in a polar field than a surround field, due to the compatibility with cavity receivers. However, surround fields are also feasible and it would therefore be unwise rule out this option at the start of the design process. The field layout impacts heliostat design factors such as the required range of movement, tracking type, and the required optical

¹ Although as noted below in 10.6, increasing mirror panel accuracy has limited benefit beyond a certain range.

accuracy (as polar fields have a greater average slant range² than surround fields of an equivalent total mirror area.

- Analysis of the optical requirements of the solar field for high efficiency systems suggests optically accurate focusing heliostats will be required (or else small heliostats relative to the receiver) to achieve high flux at the receiver with acceptable uniformity and light spillage [41].

7 Heliostat manufacturing and assembly

It has been estimated that as much as 80% of the cost of product development and manufacture is determined by the decisions made in the initial stages of design [47]. Design of a solar field is highly multi-disciplinary, involving engineers in the fields of mechanical, structural, manufacturing, electrical, communications, aerodynamics, optical analysis, plus many more. In that context, it is inconceivable that a quality, low-cost outcome for a new heliostat design could result from a traditional *sequential* type design process. *Concurrent engineering* processes are essential, i.e. engineers across disciplines working together from the earliest stages of product design, and throughout the design life-cycle.

We focus on an aspect of the concurrent engineering approach, known as design for manufacture and assembly (DFMA). Boothroyd discussed the results of a 1990 study of the automotive industry, that showed that there was a wide variation in automobile assembly-plant throughput, yet the level of automation accounted for only one third of the difference in productivity between plants [48]. He suggested that the key lesson from this was that no improvements in operation can make a plant fully competitive if the product design is defective. We believe this is a lesson that is also true for heliostat design.

In order for heliostats to reduce costs in the order of 50%, their manufacture and assembly must be highly efficient. A key feature of the DFMA approach is simplifying the product by reducing the number of separate parts and materials, and by increasing the utility of subcomponents (i.e. allowing them to be used for multiple purposes), perhaps by using more sophisticated manufacturing processes. It requires a fundamental understanding of the capabilities and limitations of materials and manufacturing processes, which is why concurrent engineering – design and manufacturing engineers working together from the earliest design stages – is particularly important.

Make-buy decisions (i.e. choosing between manufacturing a product in-house or purchasing it from an external supplier) are important and are part of the concurrent design process. The make-buy decision is not simply about reducing cost, but a range of factors as well [49]. A “buy” strategy allows sharing of costs, including R&D costs, with suppliers and access to a wider range of new ideas and technologies, but this is balanced up by the benefits of “learning by doing” and gaining a competitive advantage through development of IP and in-house expertise. Supplier capability is a key issue, and innovative suppliers with high expertise are typically those with a diverse range of customers across diverse industries. There is a lack of consensus in literature about the best make-buy strategy for new technologies [50]; in general most commercial heliostat developers appear to be quite vertically integrated and favour the “make” strategy.– They can therefore offer their own technology from heliostat design through manufacture and assembly, specialised components, tracking and alignment software, and even in some cases mirror cleaning systems. However, despite the status quo, the potential cost reduction benefits of low-cost country sourcing of heliostat components cannot

² Slant range is the distance from the heliostat to the receiver.

be overlooked, although savings may not be as great as expected as companies tend to underestimate the add-on costs [51, 52].

Strong long-term relationships based on trust between technology developers and their suppliers is generally considered critical to success, although there is some evidence this is less important where radical technologies are being developed [50]. Supplier confidence and trust has not been helped by the instability in the CSP industry in recent times.

A detailed review of a range of potential production methods for heliostat structure has been carried out by Flinders University – see Section 11.

7.1 Heliostat manufacturing case study 1: Brightsource Ivanpah

At Ivanpah Brightsource have installed a large fabric building to manufacture and assemble heliostats (Figure 18). The fabrication and assembly of the heliostats appears to have a reasonably high level of automation, although the design requires a number of manual processes (riveting, alignment and assembly processes, materials handling). A video of the assembly process is available online at www.youtube.com/watch?v=DWsqnomXFMg. Some snapshots from this video are shown below in Figure 19.



Figure 18. Brightsource's assembly hall at Ivanpah [12]

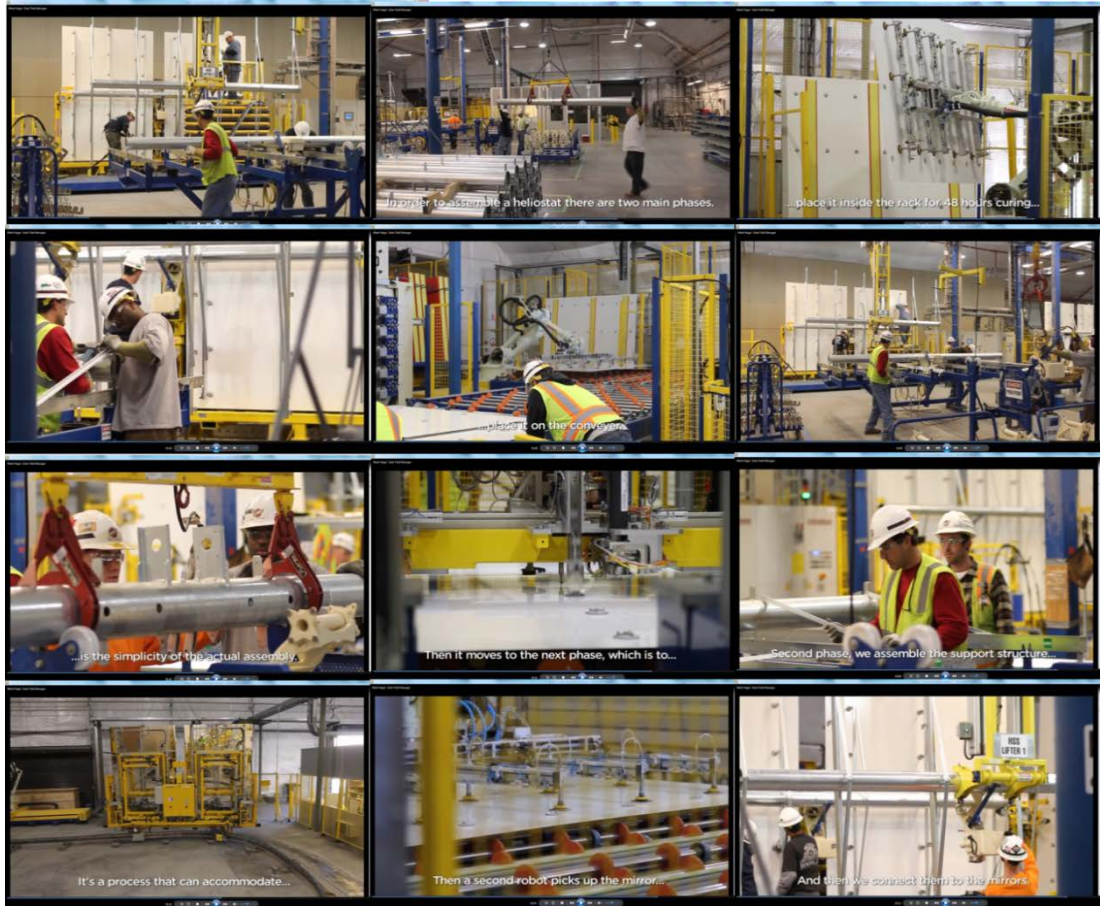


Figure 19. Manufacturing and assembling heliostats inside Brightsource's assembly hall at Ivanpah (screenshots from www.youtube.com/watch?v=DWsqqomXFMg)

7.2 Heliostat manufacturing case study 2: Brightsource FAST

Brightsource is developing a new manufacturing and assembly system in a project that is supported by the Sunshot program. It is called the Flexible Assembly Solar Technology (FAST) system [12].

The idea is to combine the final heliostat assembly and solar field installation processes using a mobile platform, and to remove the need for a large on-site assembly hall (as per section 7.1 above). The majority of the manufacturing and assembly steps would be carried out at a facility remote from the solar field, and the near complete heliostat units would be transported to the site for final assembly and installation.

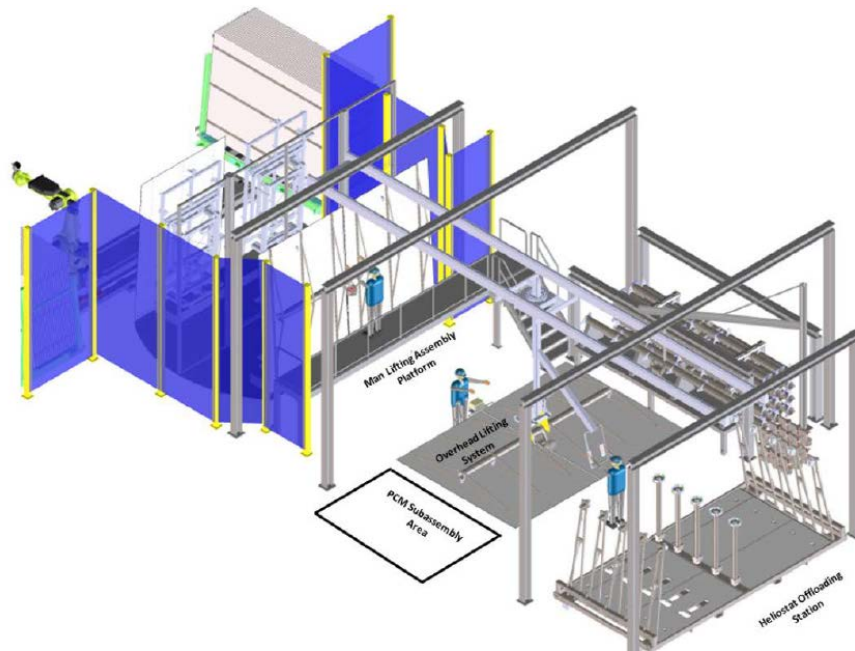


Figure 20. Brightsource's flexible on-site reflector assembly system.

According to Brightsource [53] FAST is designed to:

- Reduce heliostat assembly and materials costs
- Compress the solar field construction schedule by 25%
- Eliminate the need for a fixed assembly facility
- Provide flexible and scalable design to meet unique demands of each project
- Allow for easy relocation to multiple project sites

8 Heliostat size

It is noted in a number of recent reports [9, 54] that there presently appears to be no consensus regarding the optimal size of a heliostat. Operational heliostats range in size from 1.14 m² (eSolar) to 120 m² (Abengoa) with various sizes in between, e.g. 15.2 m² (Brightsource), 62.5 m² (Pratt&Whitney), 116 m² (Sener) [12-14, 22, 55]. Determining trends from industry is difficult. Some technology developers have recently upsized their existing heliostats – Abengoa from 120 m² to 140 m² [14, 20] and BrightSource from 15.2 m² to 19.0 m² [12] – perhaps to lower cost through less conservative, hence more efficient, use of customised components (such as the drive system). According to personal communications with Soledad Garrido (30/5/13), Sener's view is that increasing the size of the heliostat leads to lower solar field costs. However, the lack of a clear trend by the bigger technology developers is exemplified by Abengoa, who are simultaneously offering a 140 m² heliostat whilst developing an 18 m² heliostat [10]. A number of well-respected R&D institutions are presently developing very small heliostats: NREL ~6 m², DLR 8 m² and CSIRO 4.5 m² [8, 23, 56].

Throughout the 1980s, the prevailing view (at least in the US) was that heliostats should be very large to be cost effective. Sandia's analysis in the year 2000 confirmed this view, indicating heliostats should be at least 50 m², and preferably 150 m² [7]. The main driver to large scale heliostats was the cost per m² of the heliostat drive system. In efforts to reduce the cost of the drive, a number of customised drive products have been developed by companies

such as Sener [13], Flender Siemens [57-59], Winsmith [7, 60] and Cone Drive [61]. For smaller heliostats, the cost of the control and communication system also becomes an important cost driver favouring larger heliostats. Bhargav et al. [62] recently carried out a similar study, using the Sandia method, but with revised component costs based on recent quotations. They found minimum cost above about 32 m², preferably around 64 m².

The Sandia study [7] used the 148 m² ATS heliostat as its reference, and explored a size domain of 53 m² to 214 m². Figure 21 shows what happens when the relationships developed in this study are extended for heliostats smaller than 53 m². While outside the original domain of the Sandia analysis, the general trends are clear: specific cost escalates strongly as size falls, with the impact particularly noticeable for sizes below about 30 m².

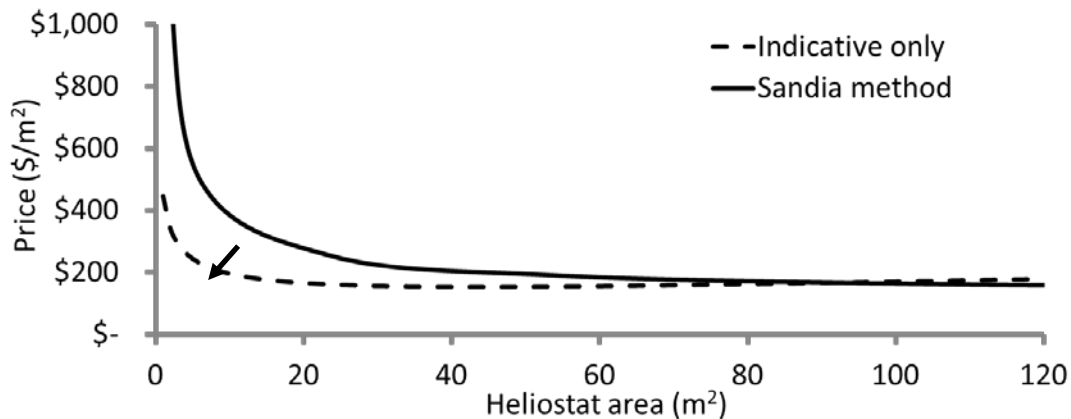


Figure 21. Heliostat price dependence upon area, using the method of Sandia (Scott Jones) [7] to extrapolate to smaller sizes (solid line). Note that as the intention is to show the trend, the values remain in year 2000 USD as per the original Sandia data. The dashed line is indicative only, showing forecast impact of cost drivers relating to manufacturing and assembly of smaller heliostats.

However, as size is reduced to a scale equivalent to other volume manufactured commodity items, a number of drivers relating to manufacturing and assembly become more relevant, such as:

- Production volume: smaller size means more heliostats, hence higher production volumes for components.
- Use of common-off-the-shelf (COTS) components: similarity to a wider breadth of industries helps when sourcing high volume manufactured COTS components e.g. motors, gearboxes, bearings, etc.
- Feasibility of a wider range of manufacturing processes: specialised components are of a size more likely to take advantage of low-cost manufacturing processes e.g. casting, stamping, roll forming (further details are given in Section 11).
- Feasibility of standard assembly processes: components better suited to automated assembly e.g. using robots, materials handling systems, smaller assembly buildings or even transportable assembly systems, such as the FAST system proposed by BrightSource [12].
- Simpler transport: logistics simpler, and off-site manufacturing more feasible.

These cost drivers all favour reduced scale, and have the impact of lowering specific cost for small sized heliostats (with the trend indicated by the arrow and dashed line in Figure 21). For example, a high volume COTS component is the linear actuator used in smaller heliostats. They are relatively inexpensive at small scale as they are mass-produced for a wide variety of industrial and domestic applications. There are a number of other drivers favouring smaller heliostats that are unrelated to manufacturing and assembly, including a lower design wind

speed, due to the wind velocity gradient and the closer proximity to the ground, and improved optical performance [7].

We believe that the combination of these drivers are behind the lack of consensus in the optimal size for heliostats, and perhaps also provide some guidance as to how to further reduce cost. The key trends in the specific cost curves (Figure 21) from the Sandia study are that the slope of the curve becomes steep as the heliostat size tends towards zero, and conversely, that the slope of the curve is gentler as the heliostat size becomes large. Based on these trends, we believe very small heliostats (say, less than about 10 m²) appear difficult to justify, and that looking for opportunities to *increase size* above this small base should be a design principle. However, we believe an equally important design principle is to seek *compatibility with volume manufacturing and assembly processes*, including the use of COTS components, which will have the tendency to reduce heliostat size. With these two equally important but competing design principles established, our answer to the question of optimum heliostat size is that, as long as a concurrent engineering / DFMA approach is adopted, the size will evolve naturally towards an optimum during product design.

9 Wind loads

The wind effects on the heliostats can be mainly divided into two parts, i.e., the static wind load and the dynamic wind load. In a heliostat field, due to the aerodynamically “bluff” shape of each heliostat, the heliostat arrays typically generate high aerodynamic drag. With an increase in the wind velocity, this drag increases significantly and dominates the structural loading on the array. The dynamic wind load, caused mainly by large-scale vortex shedding behind the heliostat, is important in the heliostat design. The stiffness and damping of a heliostat structure must be high enough to avoid wind-induced torsional divergence, flutter, and resonance of the structure itself or of upstream structures at any possible Reynolds Number [63]. Dynamic wind loading has the potential to cause structural failure, tracking errors, optical losses, and reduction of heliostat life.

9.1 Is it windy where it is sunny?

The wind effect on heliostats is a complex function of the wind condition, solar condition, and heliostat field configuration, all of which vary with time. As an example, the hourly wind velocity and the hourly direct normal solar irradiation (DNI) in Alice Springs, North Territory, Australia for the year 2012 were collected from Australian Government Bureau of Meteorology. A probability distribution of the wind velocity for DNI ≥ 200 W/m² is shown in Figure 22.

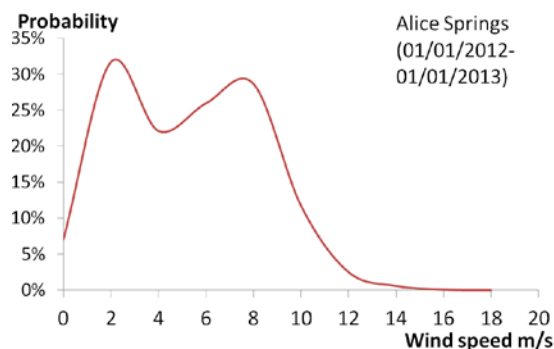


Figure 22. Probability distribution of the wind velocity when DNI ≥ 200 W/m² in Alice Springs, Australia, 2012.

It is clear to see from Figure 22 that the wind velocity was less than 10 m/s for most time of the year when DNI was greater than 200 W/m² in Alice Springs. Nonetheless, for 15% of the time the wind speed was greater than 10 m/s. Obviously the wind effects on heliostat become more significant at large wind speed. For example, assuming a 150 m² heliostat and 10 m/s as the wind speed, we calculate the loads as follows:

$$\text{Wind loading} = qSC_F \approx 18 \times 10^3 N$$

$$\text{Moment} = qSC_M L_{ref} \approx 1.5 \times 10^5 Nm$$

Here, q is the dynamic pressure of wind, S is the area of the heliostat, C_F is the drag coefficient of the heliostat, C_M is the moment coefficient, and L_{ref} is the characteristic length of the heliostat. These parameters are selected from previous literature [7, 64] as: area of the heliostat of 150 m², drag coefficient of 2, and moment coefficient of 1.6 at an elevation angle of 90° (defined in section 9.2).

Considering the self-weight of the mirror component ($\approx 2,000$ kg, or less) reported in [7] this significant wind effect on the heliostat cannot be ignored and becomes dominant both at higher wind speeds and when lighter mirrors are used in the heliostat field. Using the probability distribution of the wind velocity shown in Figure 22, the wind load acting on a heliostat with the same parameters can be added into the figure as shown in Figure 23. For most of the time in a year, the wind load acting on the heliostat panel is less than 18 kN. But, still on approximately 15% of the sunny days, the wind loading is greater than 18 kN, and at times exceeds 40 kN. These significant wind loads indicate high requirements for heliostat structure strength, supporting material strength, the drives and control system for accurate tracking. These calculations show that the structural costs can be expected to be dominated by wind load.

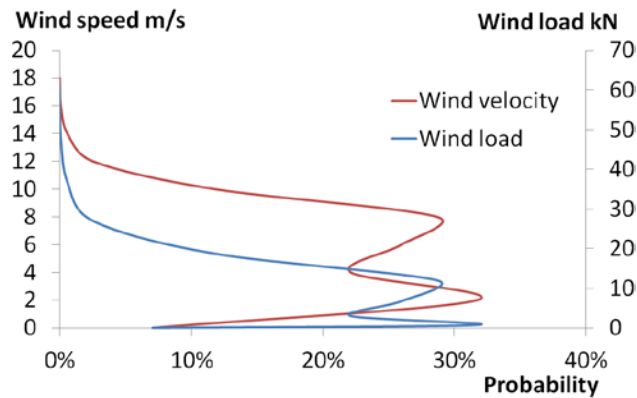


Figure 23. Probability distributions of the wind velocity and wind load when $DNI \geq 200 \text{ W/m}^2$ in Alice Springs, Australia.

For a concentrated solar power plant, the DNI is a very important factor in determining its cost effectiveness. But a place that is rich in solar energy is generally rich in wind energy. To identify the relationship between the solar irradiation and wind velocity in different locations, a statistical analysis has been performed using the same method example above, as summarized in Table 1.

Table 1. Average DNI and the probability when the wind velocity is greater than 10 m/s for various locations when DNI ≥ 200 W/m²

	Location	Recording period	Average DNI (W/m ²)	Probability (V>10m/s)
1	Oak Ridge, Tennessee	01/06/2012-01/06/2013	346.3	0.0%
2	Kalaeloa Oahu, Hawaii	11/01/2010-11/01/2011	416.9	0.0%
3	La Ola Lanai, Hawaii	14/12/2011-14/12/2012	433.3	4.0%
4	Golden, Colorado	01/06/2012-01/06/2013	450.4	5.2%
5	Rockhampton, Queensland	01/01/2012-01/01/2013	471.5	2.6%
6	Adelaide, South Australia	01/01/2012-01/01/2013	481.8	17.0%
7	Darwin, Northern Territory	01/01/2012-01/01/2013	485.8	7.8%
8	Aurora, Colorado	01/06/2012-01/06/2013	522.7	5.6%
9	WAGGA WAGGA, New South Wales	01/01/2012-01/01/2013	532.8	7.4%
10	Mildura, Victoria	01/01/2012-01/01/2013	556.2	10.0%
11	Pueblo, Colorado	01/06/2010-01/06/2011	594.6	6.0%
12	Las Vegas, Nevada	01/01/2012-01/01/2013	602.2	2.4%
13	Swink, Colorado	01/06/2012-01/06/2013	644.2	5.0%
14	Cedar City, Utah	01/06/2012-01/06/2013	685.8	11.0%
15	San Luis Valley, Colorado	01/01/2009-01/01/2010	695.8	9.5%
16	Alice Springs, Northern Territory	01/01/2012-01/01/2013	735.9	15.0%

Plotting this probability versus the average hourly DNI results demonstrates the relationship between the solar and wind profiles, as shown in Figure 24.

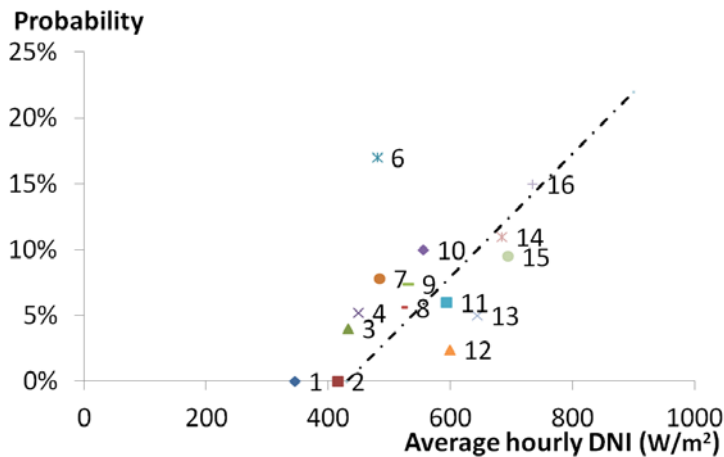


Figure 24. Probability when the wind velocity is greater than 10 m/s versus the average hourly DNI in different locations (filtering out data where DNI < 200 W/m²)

Considering only the wind effect, the ideal location for a concentrated solar power plant is a place with strong solar irradiation and weak wind condition. For example, comparing the data points 6 and 12 in Figure 24, which represent analytical result in Adelaide, Australia and Las Vegas, USA, respectively, it is reasonable to conclude that Las Vegas is a better place for a

heliostat field due to its stronger solar irradiation and weaker wind condition. It is not correct to state that a place is *always* rich in solar energy and wind energy at the same time; however, there appears to be some correlation.

9.2 Static wind load

Investigation of the wind effect on heliostats began in the late 1970's [65-68]. Due to the complex flow patterns of wind around a heliostat, most studies have been experimentally based, with the majority carried out in wind tunnels using turbulent boundary-layer flow scaled for model conditions. The wind forces of interest are typically the three dimensional wind forces and moments (C_{Fx} , C_{Fy} , C_{Fz} , C_{Mx} , C_{My} , C_{Mz}) at variable elevation angle and wind angle, as shown in Figure 25. Here, the elevation angle is the angle between the mirror plane and the ground surface (a perfectly horizontal ground is assumed). The wind angle is the angle between the nominal wind direction and the mirror normal, projected on the ground.

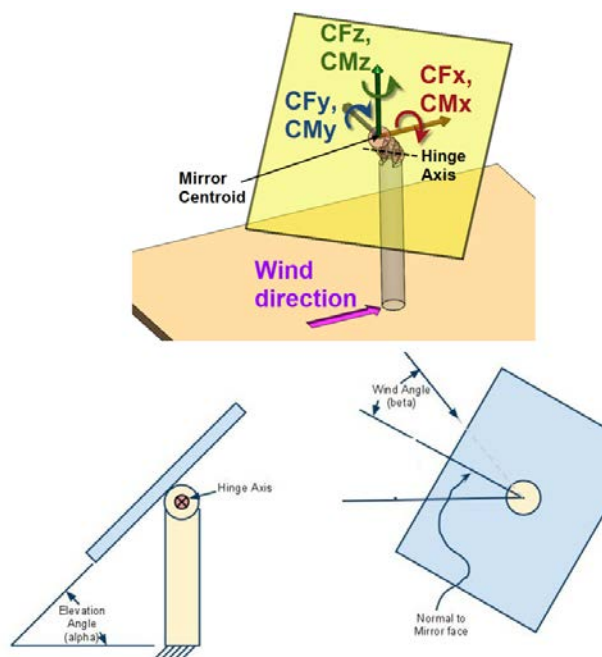


Figure 25. Definition of wind angle and elevation angle, from [37]

A key initial design decision is the determination of peak static wind loads. Structural loads depend on the square of wind velocity, hence even a small variation in the peak wind specification makes a significant difference to loads (and hence material cost), e.g. cf. 38 m/s [32, 69] and 40 m/s [6] peak wind, gives a load reduction of approximately 10%. As methods for determining peak wind loads relate to risk factors and are probabilistic in nature, a risk analysis for the specific site may be warranted to remove conservative factors inherent in codes. Analysis of historic wind data can also help, where it is available [70].

Conducting a wind tunnel model study is advisable, as design loads are more accurate than those derived from code and usually lower than code [70, 71]. Wind tunnel testing can be (and ideally should be) carried out as soon as the geometry of a new design is known, prior to the detailed structural design. This is particularly important when a DFMA approach is taken, as decisions relating to component manufacture can be costly to reverse. The structural design process should be interactive between structural and wind engineers.

Peterka et al. conducted a series of experimental studies on the reduction of wind load on heliostats [64, 72-76]. The mean wind loads on solar collectors were obtained through tests

carried out in a boundary layer wind tunnel. The wind loads were measured using a six component (force and moment) balance for an isolated heliostat, and for heliostats in array configurations. The effects of the proximity of the heliostats in the array arrangement, and the effects of the array perimeter fences and spoiler devices attached to the heliostats were investigated. Overall, the localized effects of the heliostat geometry on the wind loads were found to be limited. Based on the obtained results, the concept of a generalized blockage area (GBA) was defined based on the parameters of the perimeter and in-field fences. This was found important to the mean wind load on the heliostat field. The report also provided the force and moment coefficients induced by wind, for the studied heliostats, for varying elevation angles and wind directions. In the studies, a reduction of mean wind load on the heliostat panels was reported when internal and external porous fences with 40% porosity were employed as shown in Figure 26.

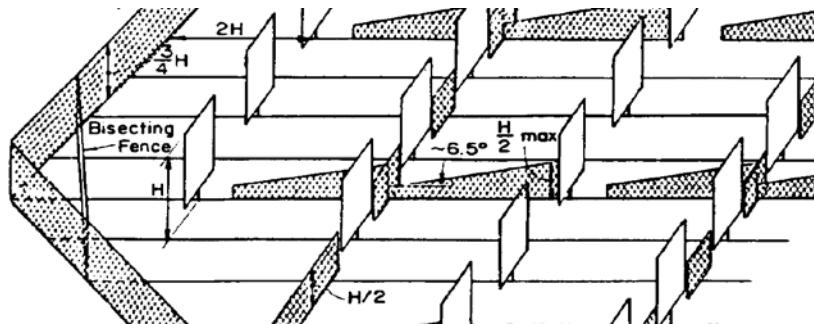


Figure 26. External and internal porous fences with 40% porosity in the reduction of wind loads [64]

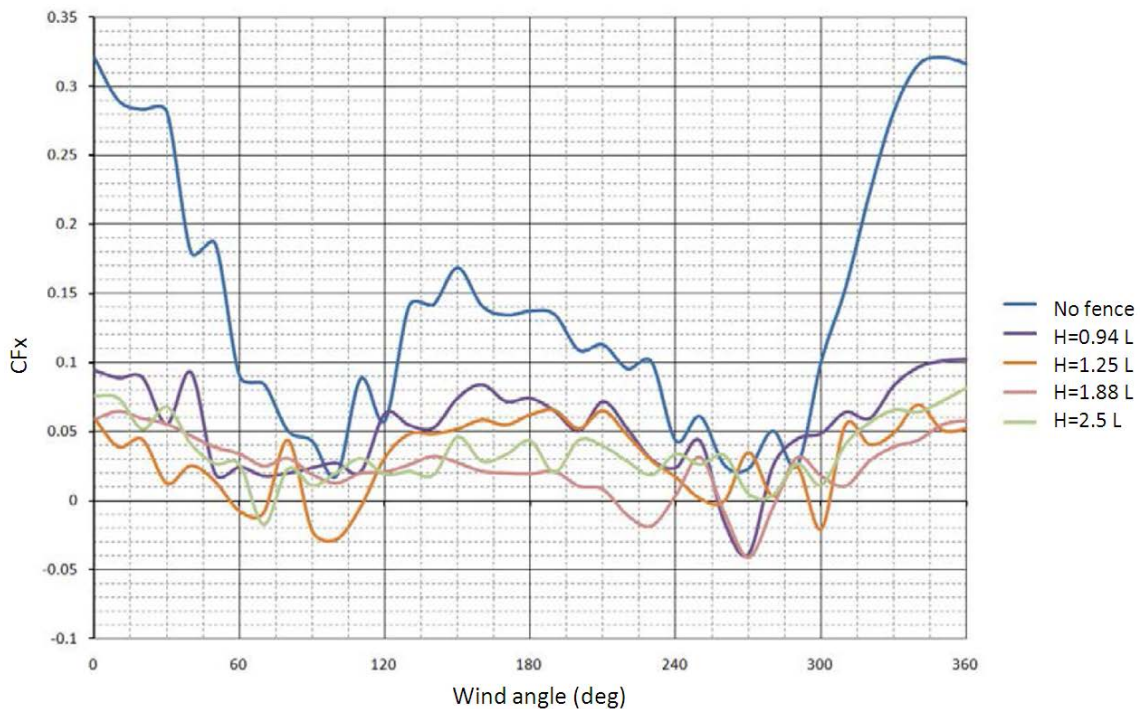


Figure 27. Drag coefficient of the heliostat with a solid barrier at different heights located in front of it and the tested heights (H) are presented on the right side of the figure (L is the characteristic length of the heliostat model) [37]

Similar investigations of the effect of fencing were conducted by Young et al. [37]. Figure 27 presents the results of drag coefficient of an isolated heliostat with a barrier of different heights located in front of it, which shows there is a reduction of wind load on the heliostat when barriers are employed. It was also found that the height of the barrier was important to the reduction of wind load on the heliostat. Further visualization of the flow pattern over a heliostat field with a barrier located in front also indicates that the flow is passing over the heliostat fielded, which then results in a reduction of the wind load on the heliostats located in the rear part (Figure 28). Hence, the wind load on the heliostat can be reduced by the application of barriers and this agrees well with the above mentioned reports.

Further investigations of porous fences in reducing the wind load on the heliostat panel have also been conducted, focusing on the porosity of the fences. Fence models with different porosity (Figure 29) were tested for reducing wind load and a good wind load reduction capability was reported using a 40-50% open area fence. However, the relationship between the wind load reduction and fence parameters has not been determined and there has not been an overall optimisation of the fencing effect considering all factors (i.e. location, shape, and height of the fence, reduction of wind load and financial evaluation). Moreover, the barrier also introduces extra dynamic loading on the heliostat panel, the effect of which has not been investigated and remains unclear.



Figure 28. Visualization of the flow over the heliostat field with a solid barrier placed in front [37]



Figure 29. Fence models used for porosity study (from left to right: 58%, 46%, 40% open area) [37]

The reduction of the wind load on the heliostat by the use of a fence/barrier in front of the field primarily results from the blockage effect of the fence, or deceleration of the flow passing the heliostat. This is also the reason that a lower wind load is found on the heliostat located in the inner layers of the field. As reported in [37], the 4th row of heliostats experienced a 90% reduction in total wind load compared to the 1st row of heliostats in the investigation. The drag coefficient of the heliostat at different locations within a field (90 degree elevation angle) is presented in Figure 30, from which it is clear that there is a lower wind load acting on the

heliostats in the rear part of the heliostat field. This reduction of wind load on the rear heliostats is mainly because the flow is not fully recovered in the wake after the heliostat panel. The distance between two heliostats is generally determined by the dimension of the heliostat, e.g. two or three times of the heliostat height. This distance is not enough for the flow to recover from the wake (in terms of the average velocity along the centreline), as the required distance is generally greater than 10 times of the characteristic height of the object [77, 78].

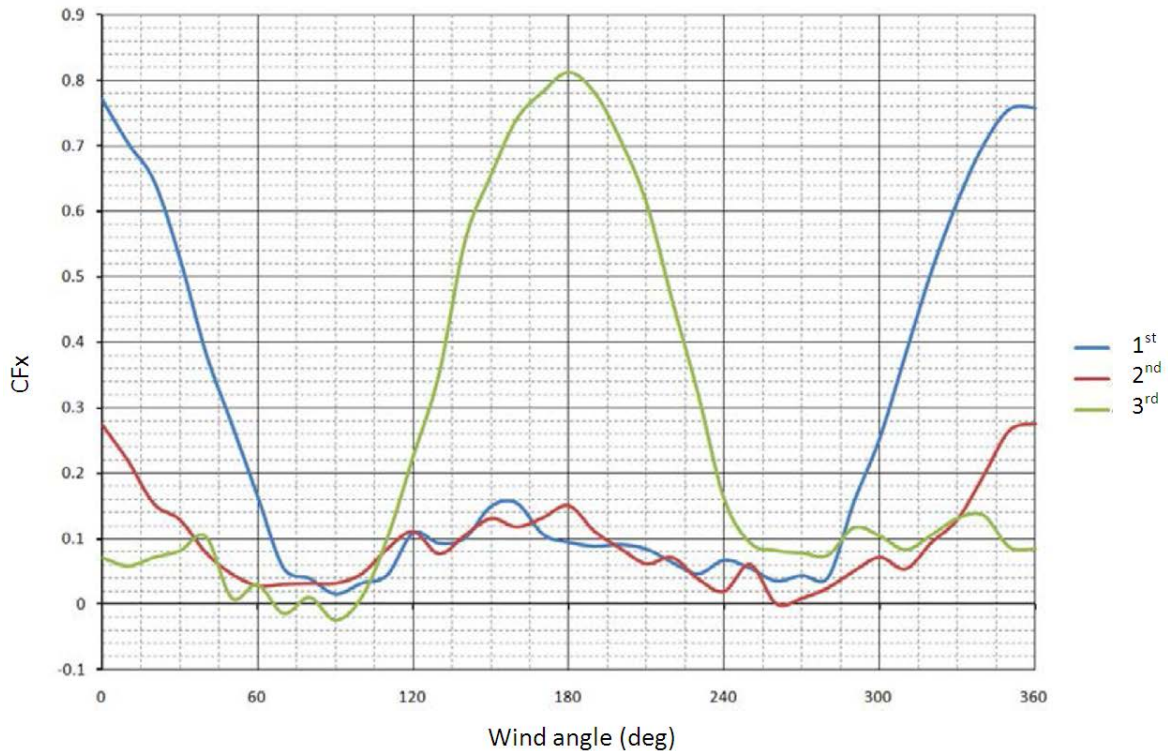


Figure 30. Drag coefficient of single heliostat locating in different rows of the field [37].

The reduced influence of the mean wind load acting on the heliostat located in the rear part of the field is also observed by the visualisation result of the flow over a heliostat field (Figure 31). The smaller magnitude of the mean wind load on the heliostats located in the inner region of a heliostat field indicates lower requirement for structural strength of these heliostats. However, when different configurations of the heliostat angular parameters are used, the force and moment coefficients are not significantly affected by the location of the heliostat [37]. Indeed, the wind effects on the inner heliostats are not well understood with respect to their precise location and orientation.



Figure 31. Visualization of the flow over a heliostat field

The application of a porous fence at the front edge of the mirror panel in reducing the wind loads on the heliostat was recently reported [23] (Figure 32). A maximum 40% reduction in the overturning moment was achieved, which would enable a 30% weight reduction of the supporting structure. However, the effects of the porous fence on the static wind loads reduction (drag and lift) have not been reported and hence, remain unclear. Together with the application of the external fence, this successful application of the aerodynamic attachment on the heliostat panel in controlling its wind loads indicates the feasibility of wind loads reduction using different attachments.

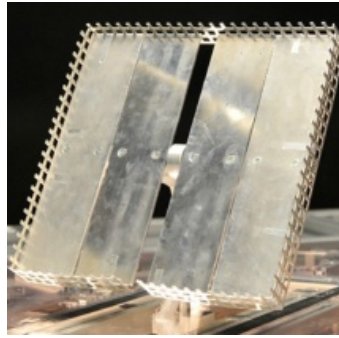


Figure 32. Heliostat model with porous fence at its edge used for wind loads reduction [23]

The spacing between mirrors of a heliostat have been considered in the past studies by Wu et al. [79]. The negligible effect of the gap between the mirrors on one heliostat panel on the wind loading was reported. It was found that a change of gap from 0 mm to 40 mm only resulted in a 2% reduction in the pressure coefficient on windward surface (model area = 300 x 300 mm). Therefore, due to the small magnitude of the change in load coefficient due to the gap effect compared to the overall wind load on the heliostat, it is not necessary to consider the gap effect in the design of the heliostat system.

In an investigation of the wind load on the heliostat at various Reynolds numbers [80], it was stated that the inclination of the mirror plane in stow position increased wind load due to the deflection of the heliostat's structure at high Reynolds number, and must be considered. Later, they also experimentally investigated the effect of the heliostat aspect ratios on the wind load (Figure 33) and reported that higher aspect ratios for heliostats were advantageous for the dimensioning of the foundation, the pylon and the elevation but disadvantageous for the azimuth drive [81].

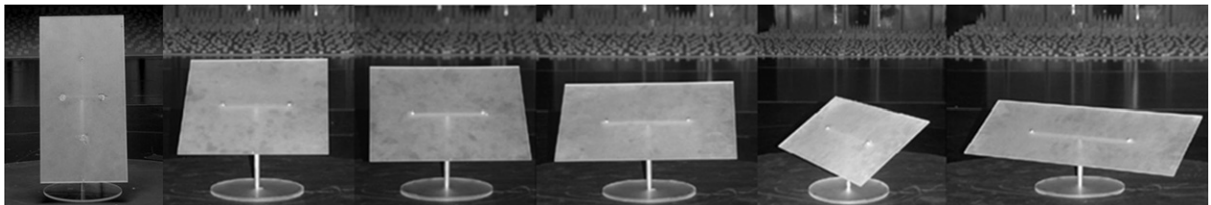


Figure 33. Heliostat models having different aspect ratios employed in the investigation of the wind loads [81]

The displacement/misalignment of the heliostat panel due to the wind load has also been investigated [58, 82, 83] The displacement/misalignment of the heliostat panel is generally proportional to the wind velocity. As reported in [83], for a second generation full-scale heliostat, a maximum misalignment of 4.7 mrad has been measured when the wind velocity is around 5 m/s. Therefore, for a heliostat having a distance of 1 km from the tower receiver, the displacement of the reflected beam of solar light is more than 4 metres, which indicates an

optical loss of the reflecting solar energy considering the window dimension at the entrance into the receiver [84]. Because of the weather condition, i.e., not many strong windy days in a year, and the control system of the trackers, this loss can be reduced, but cannot be avoided [58].

Aside from wind tunnel experiments, investigations of wind loads acting on heliostat panels have been carried out utilizing numerical simulations resulting from tools such as Computational Fluid Dynamics (CFD) [85] and Computational Structural Analysis (CSA) [86]. Wind tunnel tests are typically time-consuming, expensive, flow intrusive, and any modification in geometry, configuration, topography or load conditions needs a new set of tests with the corresponding additional time and cost. The results obtained are restricted to a limited set of points and variables, and most importantly, the dimensions and wind velocities in available boundary layer wind tunnels impose Reynolds numbers well below those occurring in open air full-scale structures of this type. This prevents a direct and fully accurate extension of the results to the characterisation of full-scale collector structures [87]. These wind tunnel shortcomings have made CFD an appealing alternative for determining wind load distributions over solar collectors.

Abengoa Solar recently stated that its design group relies on CFD analysis for predicting wind loads (Ken Biggio in a SolarPACES2013 presentation, 17/09/2013). Abengoa use XFlow, a commercial CFD program based on the Lattice Boltzmann method, where fluid dynamics are approximated by interactions between particles on a regular lattice, avoiding the need for the time-consuming meshing process [87]. The particles are constrained to move according to a finite, discrete set of velocities in an octree lattice. Smaller, unresolved turbulence scales are modelled by Large Eddy Simulation, and the boundary layer physics are modelled by means of generalised wall functions. Validation of this method was carried out using experimental data from a single 1:25 scale trough model, with mean load coefficients in agreement to <10%.

A CFD study carried out for both isolated heliostats and heliostat arrays is reported by Shademan et al. [85], and discusses the effect of wind direction and tracker inclination angle on the load on an individual panel. Lately, studies have been carried out to optimize the reliability and performance of the tracking system [88, 89]. Numerical simulation has also been employed to predict the velocity characteristics over a heliostat panel [80, 90]. For example, Figure 34 presents the simulated streamlines around a single heliostat in stow position.

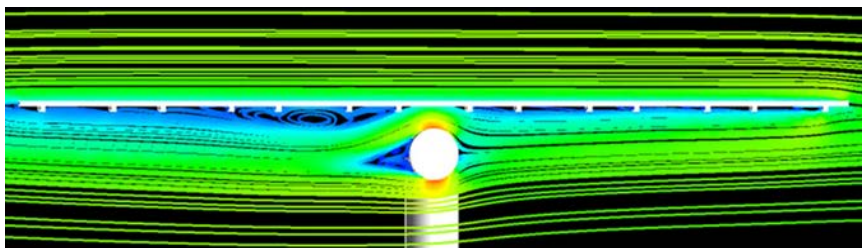


Figure 34. Simulation results of the streamlines around a heliostat in stow position [80]

9.3 The dynamic wind load on the heliostats

Previous work on heliostat aerodynamics has mainly addressed static wind load characteristics, while the dynamics of wind loading has not been fully understood and considered in the heliostat design. The dynamic wind load, or vortex induced vibration, is generally generated by large-scale vortex shedding around the heliostat panel as shown in Figure 35. Hence, the frequency and amplitude of the oscillation are related to the flow conditions. Such vibrations can lead to a higher load on the supporting structure and a reduction of the working efficiency.

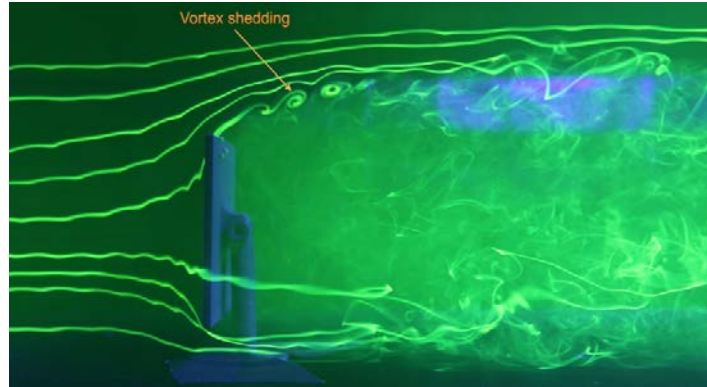


Figure 35. Vortex shedding observed on a heliostat perpendicular to the oncoming flow

The Strouhal number is a non-dimensionalised parameter describing the oscillating flow mechanisms and is given as:

$$St = \frac{fL}{U}$$

Here, f is the frequency of vortex shedding, L is the characteristic length and U is the velocity of the fluid.

For the air flow passing an inclined flat plate, the Strouhal number varies from 0.8 to 0.2 when the elevation angle of the plate is changed from 0 to 90 degree [91]. Where the frequency of the wind induced vibration matches a natural frequency of the heliostat structure, deformation or damage of the heliostat structure may occur. In fact, several drive failures in the heliostat field operation have been reported for cases in which only static wind loads were considered in the design. Resonant vibration has been emphasized as being important for heliostat design, particularly for large pedestal supported arrays [72].

Moreover, since the heliostats of a power tower are located in open terrain or suburban terrain, and the distance between the tower and heliostats can exceed 1000 m, any tiny torsion of a heliostat can lead to energy loss at the receiver, so wind-induced displacement of heliostats is a design priority. According to the experimental data reported in [58, 82, 83, 92] at a solar receiver of a 1 km heliostat field, the displacement of the projected light beam due to wind effects may achieve about 5 metres, when the velocity of wind is 5 m/s. With no doubt, the wind induced vibration of the heliostat will cause an unpredictable displacement on the beam reflection, because it depends strongly on the oncoming flow conditions. Therefore, it is important to devise effective means to control this vibration. It has also been observed that the areas of high quality solar resource are often also rich in wind energy (see Section 9.1), which means the wind induced vibration is likely to be significant in many potential sites.

As mentioned above, the heliostats which are located in the inner region of the field experience lower static wind load when the elevation angle is 90 degree. However, there is no evidence that the inner heliostats experience lower dynamic wind load. It can be seen that the flow passing an obstacle has the ability to change the flow pattern in the near field of the wake by vortex forming and shedding [93-97]. Vortex shedding generated by the first row of heliostats has an obvious effect on the heliostats behind. This is indicated by the experimental results reported in [37]. The measured force and moment coefficients of the inner heliostats at different wind directions do not show an obvious influence due to the heliostat location, except for the force coefficient with 90 degree elevation angle. Hence, it is not reasonable to conclude that the heliostats located in the inner region of a heliostat field experience less wind dynamic effects. Indeed, knowledge about the flow structure over a heliostat field, especially

the interaction between the heliostats on the bypassing flow pattern, is not well understood and further investigation is required.

One solution of controlling vibration is to increase the rigidity of the structure supporting the reflectors which, in general, will result in increased cost of a heliostat. An alternative solution is to adjust the flow field to reduce the vortex formation. The change of the flow pattern after a flat plate by applying different attachments [91] is shown in Figure 36, and indicates the feasibility of adjusting the flow field using aerodynamic methodology. This feasibility is also shown by the reduction of wind loads generated by porous fence at the frontal edge of the mirror panel [23]. Therefore, a comprehensive understanding of the flow characteristic of the heliostat is required, especially the vortex forming and shedding around the panel.

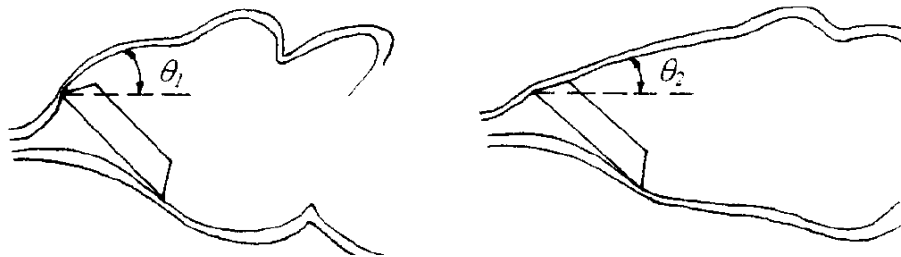


Figure 36. Sketched flow pattern after the flat plate with different attachments [91]

The natural frequency of a heliostat located at the National Solar Thermal Testing Facility at Sandia Labs was predicated and validated by Todd Griffith et al. [98]. The testing configuration of the heliostat varied in different bending modes with an elevation angle of 90 degrees. A good agreement between the pre-test predicted frequency and modal tested hammer frequency was reported. It was reported the natural frequency of the tested heliostat varied between 1.6 Hz and 4.6 Hz at different bending modes. Also, when compared to hammer data with calm winds, an increase in damping due to aerodynamics of the acting wind was reported in their study. Similar work was reported by Gong et al. [92] that the natural frequency of the tested heliostat varied between 2.6 Hz and 5.6 Hz with variable elevation angles and order of frequency (from first order to fifth order).

The wind-induced fluctuating characteristics of a heliostat, displacement of the heliostat structure, the equivalent stress and the structural natural frequency of the heliostat have also been investigated by Wang et al. [92, 99-101], and a mathematical wind load model for use in a finite element analysis of the heliostat was developed and validated. The wind vibration coefficient was reported [92] as an important factor in the study of the wind induced dynamic effect, which was defined as the ratio of the maximum displacement of the mirror panel over the mean value. The wind vibration coefficient at variable elevation angles (a) and wind directions (b) is presented in Figure 37, which indicates the complex relationship between the vibration conditions and angular phases of the heliostat.

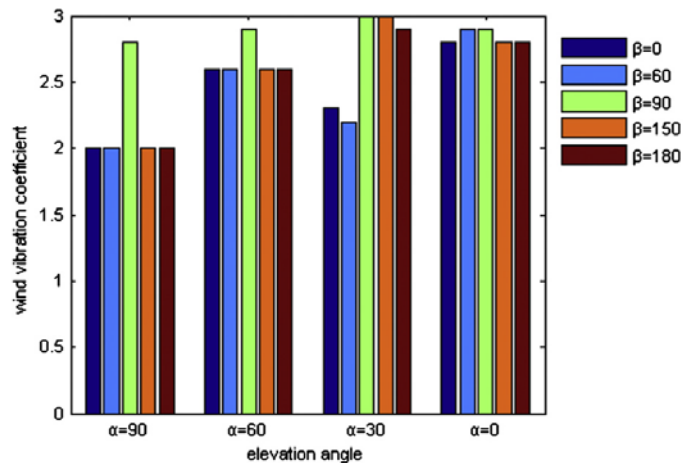


Figure 37. Wind vibration coefficient of a heliostat panel, which is defined as the ratio of the maximum displacement of the mirror panel over the mean value [92]

Aerodynamic loads obtained in low-turbulence flow are inappropriate and not conservative for heliostat design [102] as turbulence has a significant influence on heliostat loads [69, 70]. Therefore, wind tunnel tests typically attempt to simulate the turbulence profile; however, the methodology has been shown to be important. Turbulence intensity matching in wind tunnels, to simulate an open country profile, can artificially increase the predicted dynamic effects [103]. A number of well-cited experimental studies of heliostats involve turbulence intensity matching, and therefore potentially overestimate wind loads in the stow position [23]. Higher turbulence intensity than in codes has been measured for low wind speeds, which should be considered for estimation of operational loads [70].

10 Mirrors

To put into context the use of mirrors in the CSP industry, we have reviewed the many solar power plant installations globally, including only those completed and under construction (although there are many more announced but not yet underway). A summary of these facilities is included in Appendix A, including the types of mirrors and heliostats used [104-106]. It is apparent that there are very few suppliers of mirrors to commercial plants, and that thick (~4mm) glass mirrors are the dominant product.

10.1 Glass mirrors

We review here manufacturers of glass mirrors, noting also those who produce thin glass. While the use of thin glass is yet to be widespread, the use of thin glass (~1 mm) for mirrors offers a useful reflectivity advantage of around 1% [107] compared to thick glass (~4 mm).

10.1.1 RIOGLASS SOLAR

RioGlass Solar is based in Spain, with mirror manufacturing in both Spain and USA [108]. The mirrors use tempered glass with a “nanosilver” coating (developed with partners Samsung and CMS). This reduces silver particle size to <3nm compared to wet chemical deposition of the silver layer that results in a stack of silver particles >10nm. This reduces the scattering of reflected light, and hence increases overall reflectivity. Silicone edge sealing is also used. The reflectivity achieved is >94%. Rioglass reported mirror costs of €30-32/m² in 2010 [109].

10.1.2 FLABEG (NOW OWNED BY SUN & LIFE)

Saudi company ACWA's solar subsidiary, Sun & Life, recently acquired the solar mirror assets of German company Flabeg [110]. Flabeg uses annealed low iron float glass with a silver reflective layer. Mirrors for troughs use 4-5 mm thick glass, and are manufactured in Germany (noting the recent closure of the Pittsburgh facility) [107]. The Naugatuck (US) plant (still retained by the Flabeg group) manufactures thin flat mirrored glass, with reflectivity around 95.5% for 1mm thickness. The recently developed "duraGLARE" coating reduces soiling, as described below in Section 10.5.

10.1.3 SAINT GOBAIN SOLAR – COVILIS

Saint Gobain is based in France, with manufacturing in Germany and Portugal [111]. The SGG MIRALITE® SOLAR parabolic mirror are made of tempered low iron glass, with solar energy reflectance above 93% for 4 mm glass.

10.1.4 AGC (ASAHI)

AGC are based in Japan as part of Asahi Glass, with solar mirrors made in both Belgium and Japan [112]. AGC offer both thin (1mm) and thick glass mirrors (3 and 4mm) with reflectivity 95.5%, 94% and 93.6% respectively.

10.1.5 GUARDIAN

Guardian is based in Michigan USA. Its 'EcoGuard' product is a low-iron float glass, with thickness range from 0.95 mm to 4 mm, either annealed or tempered. They target a wide range of solar technologies, 4 mm back surface curved mirrors for parabolic troughs [113], and two flat mirror products: 1-4 mm back surface mirrors [114], 1-4 mm back surface mirrors laminated with PVB to 1.6-4 mm float glass [115].

10.1.6 RONDA

Ronda is based in Italy and has developed a new mirror technology developed in conjunction with ENEA [116]. A 1.1 mm thick glass sheet with reflective layer is adhered to a sheet-moulded composite (SMC) plastic panel for support (Figure 38). Reflectivity is claimed to be 96%. A 1.2 x 1.6 m panel weighs 16kg. This technology is reportedly used at the Archimede solar trough plant in Sicily.

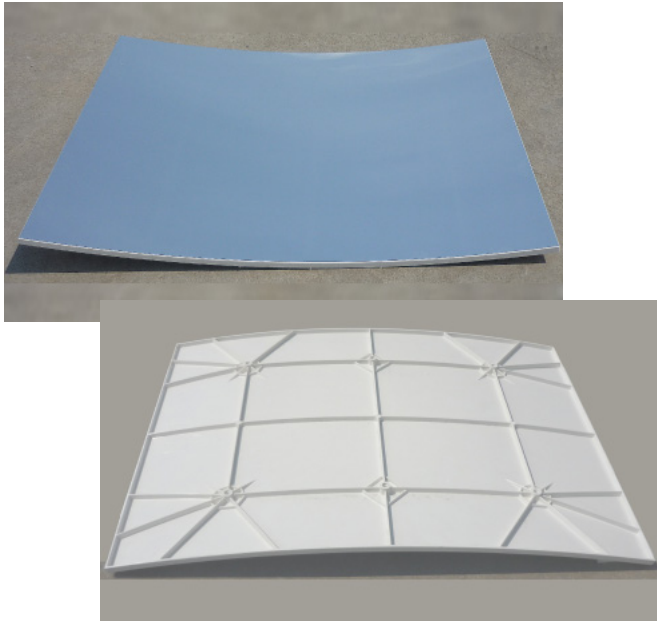


Figure 38. Ronda mirror system front (left) and back showing reinforcing structure (right)

10.1.7 DAMIN GLASS

Damin Glass is the first company in China to manufacture CSP reflectors [117], and claims to produce bent and tempered mirrors for troughs, as well as mirrors for dishes, LFRs and heliostats. Damin Glass is in the final phase of production of the first of three low-iron float glass lines, expected to come on line in late 2013.

10.2 Reflective films

Reflective films can be used as an adhered top layer on a metal substrate in order to avoid the weight and cost of glass mirrors. They are not breakable and therefore have lower repair costs, are lighter in weight which reduces the strength and weight requirements of the supporting structure, and are claimed to have at least as good reflectance properties as glass mirrors.

Reflective films have been received cautiously by the CSP industry to date, with all commercial-scale installations favouring glass mirrors (see Appendix A). Past studies have shown unfavourable reflectivity and specularity results for reflective films (and polished metal) relative to glass, particularly after abrasion testing [118] (although the standardization and improvement of test methods has been shown to be vital [119]). Key durability concerns are resistant to UV degradation, abrasion resistance (where abrasion in the field can be due to either dust or contact cleaning) and interlayer delamination [120]. However, manufacturers such as 3M and Reflectec claim significant improvement in the durability of silvered polymeric mirrors with a hard coat [120, 121], and specular reflectance equivalent to the best glass mirrors. The long term specularity of the reflective films is an important factor for use in heliostats, where the distance between the heliostat and target is great and the optical error “budget” is small (<3 mrad goal for SunShot [4]). Some question marks remain, but nonetheless the use of reflective films would open up a range of design options that are problematic for glass due to differing thermal expansion characteristics, for example, bonding film to lightweight and rigid fibre-reinforced plastic structures such as foam cored sandwich

panels, or direct bonding to shaped, closed-cell foam structures [30], and therefore the continued development and improvement of reflective films is certainly of interest.

Stretched membrane heliostats developed for R&D purposes, consisting of a stretched membrane tensioned to a large diameter ring, have used reflective film (e.g. the 3M ECP-300A silvered acrylic film) as well as polished aluminium and stainless steel sheets [122, 123].

10.2.1 3M SOLAR MIRROR FILM 1100

3M produces Solar Mirror Film 1100 for glass mirror replacement in solar thermal systems, consisting of a silver metalized polymer film [124]. The film can be manufactured at a width of 1245 mm [120]. 3M has also developed the 3M Anti-Soiling Liquid which has been designed to be field-applied and provides resistance to dry dust soiling [125].

3M claim solar weighted hemispherical reflectance for the film is 94.5%, and the specular reflectance at 25 mrad acceptance angle is 95.5% [120]. According to 3M [120] these results come from round robin testing by independent research institutes (presumably “Manufacturer A” in [119]). 3M is continuing development of its film technology through a Sunshot funded program [120]. The focus is to develop novel optical coatings for silvered polymeric mirrors with PMMA front surfaces, and to demonstrate manufacturing processes for these optical coatings and incorporate onto mirrors. Results to-date indicate significant improvement in durability compared to uncoated PMMA, with 35-80% improvement in abrasion resistance, and significant improvement in surface durability and uniformity (Figure 39).

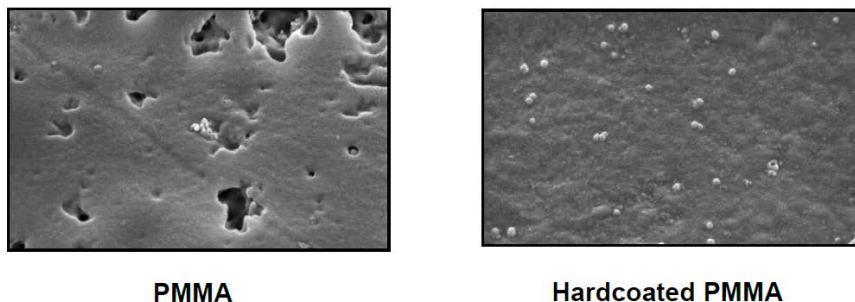


Figure 39. Surfaces of Weathered Samples 4000 h, 60,000 x Magnification, from [120].

In addition, 3M is working with Gossamer Space Frames to develop a full reflector system for solar thermal power generation. Gossamer’s X-Perf™ Reflective Panels [126] are a reflector for parabolic trough systems, but it is unknown if these have been installed commercially. The Large Aperture Trough (LAT) has been installed for trials at Daggett CA since October 2011 [127]. Abengoa Solar are testing the film at a number of trough facilities [120].

10.2.2 REFLECTECH MIRROR FILM

ReflecTech film consists of a silver reflective layer within multiple layers of polymer films that protect the silver layer from oxidation and UV degradation [128]. Reflectech claims specular reflectance at 25 mrad acceptance angle of 94% at 660 nm, and solar-weighted hemispherical reflectance of 93% [121]³. ReflecTech reported costs of \$18.84/m² in 2010 [109].

³ It is noted that ReflecTech have not published the solar-weighted specular reflectance.

Developed by NREL [129] and licensed to Reflectech, this reflective film has been installed as part of a Skytrough collector loop at SEGS II in Daggett CA since Feb 2010. Skyfuel has been contracted to utilise their Skytrough parabolic mirrors in a hybrid solar / gas installation in Canada [130]. The 1.1 MW installation will offset the gas use and correspondingly reduce emissions. They have also signed an agreement to install their parabolic troughs in Brazil in partnership with Braxenergy [131].

Skyfuel recently commenced a Sunshot funded project to further develop the layer that is the intermediary adhesion layer between the hard coat and the silver [8]. This is needed as the hard coats typically exhibit poor wetting and adhesion to bare silver. The scope of the project also includes methods of increasing reflectance by developing films that reflect more UV.

10.2.3 KONICA MINOLTA

Konica Minolta has developed a new reflective film and claims a solar weighted spectral reflectance of 94%, and higher durability than existing films [132].



Figure 40. Konica Minolta's new 1.3 m wide reflective film [132].

Details of the film are not provided on Konica's website, however a US patent [133] describes a process for forming a reflective layer, by calcining a coating liquid containing a silver compound, and using a protective layer over the top. We do not have confirmation that this method is used for their film, nor of Konica's commercial intentions for the film. However, it is understood the film is used in the beam down tower at Masdar for the secondary reflector, and possibly also for the heliostats [134].

10.2.4 EVONIK DEGUSSA

Evonik Degussa has developed a reflector based on two polymer layers with a metallic reflective coating in between [135]. This laminated structure forms a self-supporting reflector. Evonik's commercial / production intentions are not known.

10.3 Polished metal

Highly polished metal sheets are an alternative to reflective polymer films adhered to a substrate. Below are two companies that offer mirrors based on aluminium, with reflectivity enhanced by physical vapour deposition (PVD) of various coatings.

10.3.1 ALANOD SOLAR

Alanod produces surface-finished aluminium and copper sheet and supplies a range of industry sectors including automotive and solar industries. Alanod Solar produce a PVD-coated reflective aluminium sheet product for solar reflectors called MIRO-SUN[®] [136]. The coatings include a layer of silicon dioxide and titanium dioxide [137]. The aluminium is protected from corrosion by a lacquer. On its website, Alanod claims $\geq 84\%$ for solar weighted specular

reflectance [138] for this product. It is noted that test results by DLR and NREL published around 2009 by Alanod showed spectral reflectance around 87-88% and 83-84% respectively [139, 140]. The latter results are similar to DLR results [118] for two aluminium reflectors, although it is not known if any of these samples were Alanod products. Deterioration of spectral reflectance (0-3%) was observed over the test regimes at NREL [140]. Durability of the lacquer appears to be critical, and much development and testing is centred on this [136].

It appears by their website that Alanod reflectors have been used in a number small scale installations, but are yet to be utilised in large CSP plants [141].

10.3.2 ALMECO SOLAR

Almeco Solar is a division of the Ameco group, specialists in aluminium products particularly in lighting. Almeco Solar's 'vega' WR193 and WR293 solar reflector products are based on anodized aluminium with PVD coatings of 99.99% pure aluminium, a low optical index layer, a high optical index reflective layer and a weather resistant top coat [142]. Almeco claim the WR193 product has 88.3% specular reflectance (ASTM G173) based on testing at Fraunhofer ISE [143], and claims the WR293 product has "higher specular efficiency".

10.4 Plastic mirrors

Plastic mirror coatings have been developed for the automotive industry, driven by the cost-advantage of injection moulding complex shapes. For example, according to personal communication with Colin Hall (University of South Australia, 31/07/13), for car wing mirrors that include both planar and convex portions, it is significantly cheaper to form the shape from plastic and apply a reflective coating, than it is to use glass mirrors. Similar advantages could be envisaged for heliostats that make the most of the ability to form accurate and complex shapes by injection moulding, for example, features for lowering wind loads, helping the structural performance or improving the ease of connection to the mounting system. High reflectance and excellent durability are likely to remain key requirements.

10.4.1 PATRIOT SOLAR GROUP

Patriot Solar Group (USA) produce back-coated acrylic plastic mirrors [144]. Patriot reports up to 97% reflectivity in the range 400-1100nm, but does not give values for solar-weighted spectral reflectance. Reflective layers can be Al or Zn, with Patriot claiming Al coated on the back achieves 94% reflectance [109]. Patriot appears to be a smaller firm catering mostly to individual consumer applications, with some interest in the large scale power generation arena. The product no longer appears on Patriot's website, and it is assumed the product has not been successfully commercialised.

10.4.2 SMR AUTOMOTIVE

SMR produce first-surface reflective plastic rear vision mirrors for cars in Adelaide using a multilayer vacuum deposition process onto polycarbonate parts [145-147]. The polycarbonate substrate is hardcoated with an abrasion resistant resin, then sputter coated with $\text{SiO}_2/\text{CrZr}/\text{SiO}_2$. This multilayer structure has been developed with the correct stress profile to allow it to expand and contract with the underlying plastic substrate. Reflectivity is currently only 60%, as this is the design requirement for an exterior rear-view mirror.

10.4.3 UNIVERSITY OF SOUTH AUSTRALIA EXPERTISE

SMR's plastic automotive mirror was developed jointly by University of South Australia's (UniSA's) Mawson and Ian Wark Research Institutes in collaboration with SMR Automotive and

the Cooperative Research Centre for Advanced Automotive Manufacturing (AutoCRC) [146, 147].

Given the low reflectivity requirements for automotive mirrors compared to solar thermal applications, the challenge for this technology is to increase the reflectivity whilst maintaining the durability. To achieve this, UniSA researcher Colin Hall envisages an extension to the $\text{SiO}_2/\text{CrZr}/\text{SiO}_2$ stack so that an interference coating is realised that would achieve a broad wavelength reflective coating. Early UniSA modelling indicates reflectance in the order of 95% is feasible, but significant further work is required to realise this practically.

An example of the work which has occurred in the area of broadband reflectors is the patent by Vandehei [148], which describes a reflector for the visible and near infrared spectrum formed by multicoating copper with one fifth wavelength and three-quarter wavelength films. These films have alternating low and high refractive index. This coating enhances the reflectance in the visible range without appreciable degradation of reflectance in the near infrared, so that the resultant curve of reflectance-versus-frequency is substantially flat.

Recent work by UniSA in understanding abrasion and corrosion resistance of thin films includes:

- Corrosion resistance: in recent work it was shown a SiO_2 film with high compressive stress improves corrosion behaviour of multilayer films. The hypothesis is presented that in changing from low to a high stress, the structure of the SiO_2 transitions from an open porous layer to a dense layer, resisting penetration of “solvents” which would otherwise enter and dissolve the SiO_2 , causing the failure of the multilayer coating [149].
- Hard coating: in recent experiments a number of hard coating layers for plastic substrates have been tested for resistance to abrasion. Results indicate polymeric substrates with a hard coating can outperform a glass substrate, in one case, with double the resistance to abrasion [150]. Note this is a comparison with a front surface coated glass mirror (not a back surface mirror). Techniques for depositing chrome alloy coatings at low temperatures (required to be less than the glass transition temperature of the polymeric substrate) have been developed. Abrasion resistance using this technique rivals that of an as-deposited PVD CrN coating, which is a coating used to impart abrasion resistance to cutting tools [151].
- Characterisation and understanding of abrasion resistance: the resistance to abrasion of CrN_x layers was identified as being partially defined by the microstructure of the CrN_x layer within the multilayer system, with columnar structure more resistance than grain-like structure. Simple methods of characterising abrasion resistance were investigated, based on observation of surface roughness and measuring diffuse light scattering from the surface [152].

10.5 Anti-soiling coating for glass

Flabeg has developed a new product known as DuraGLARE, which is an anti-soiling coating that reduces the soiling rate of mirror surfaces and also facilitates easier removal of foreign matter [153]. Another characteristic of the product is that the peak reflectivity of a coated mirror is equivalent to the peak reflectivity of an uncoated mirror. Extensive laboratory and in-field testing has demonstrated the product’s soiling repellent and easy-to-clean characteristics. The product is aimed at reducing the solar plant operating and maintenance costs and / or increasing the plant performance.

Flabeg claim that the incorporation of the DuraGLARE product into a typical 50 MW parabolic trough plant could result in up to a 2% increase in the average reflectivity of the solar field for the same cleaning interval [153].

Another feature of the DuraGLARE product is its easy to clean characteristic. Soiling can be removed by rinsing the mirror with water, and a heavy rain event is sufficient to bring the mirrors up to a 100% cleanliness factor, as illustrated in Figure 41.

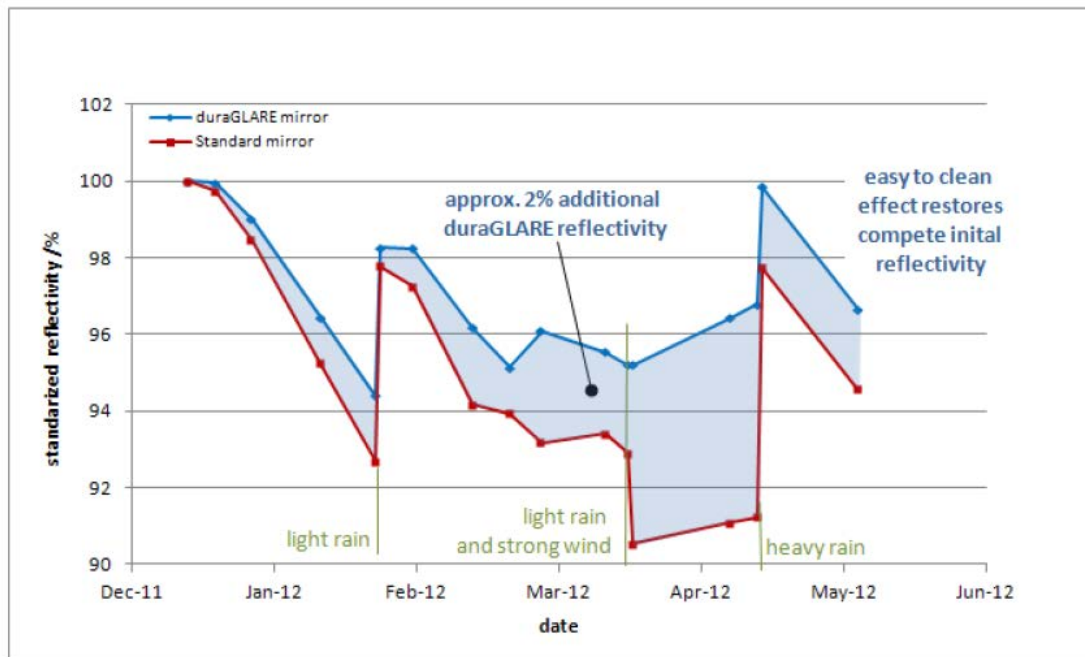


Figure 41. Standardized specular reflectivity for coated and uncoated mirrors during test campaign

A wide range of accelerated ageing tests have been conducted and are ongoing to help gain a better understanding of the coating life. Durability of the coating with regard to regular contact cleaning is an open question.

Note that as there is a parallel activity within ASTRI on mirror cleaning, we do not recommend further analysis of the costs and benefits of anti-soiling coatings within this node.

10.6 Structural mirror panels

As noted above in Section 0, thin (1mm) glass offers a useful reflectivity advantage over the more commonly used 3-4 mm glass. However, a supporting substrate is required due to the fragile nature of the glass. The glass may be bonded to another material to form a laminate, e.g. with steel or another thicker glass layer [115, 154, 155]. Alternatively, the glass is sometimes used directly as a face sheet in a sandwich panel structure [24, 156].

RioGlass Solar and Abengoa Solar have developed facets for Abengoa's new ASUP 140 heliostat [21]. According to personal communication with Jordi Villanueva from Rioglass Solar (18/09/2013) the panels are constructed with a 2 mm reflective glass sheet also acting as the front skin, a 40 mm foam core, and a 0.5 mm steel back skin. He indicated the cost is expected to be around 40 USD/m² at quantity. Assembly of the panels for the Khi One project is in South Africa.

Sandwich panels can be strong and very rigid, and may be designed to contribute significantly to the structure, as is the case for the ANU / Wizard Power Big Dish design [157]. Toughtrough has developed a steel and glass faced, polyurethane cored sandwich panel for heliostats (Figure 42) [107, 109]. The specific weight of the mirrors is less than 10 kg/m² and the foam core is designed with inhomogeneous density, i.e. the foam density is locally tuned according to structural requirements [23]. This development leverages expertise of one of their owners,

Brueggen, a manufacturer of insulated panels for trucks, for processes such as foaming the polyurethane and industrial scale vacuum forming. The glass mirror is embedded in the foam bed, and it is claimed that it achieves a slope deviation of $SD_x < 0.8$ mrad in the overall operational range and at wind speeds of up to 12 m/s. A frame is used as an additional stiffness element (assumed to be embedded in the polyurethane foam). Toughtrough mirror panels are used in the recent DLR developed heliostat [23].



Figure 42. Toughtrough mirror panels [158]

The cost of the mirror panels is estimated by DLR at about $\$40/\text{m}^2$, comprising steel ($\$12/\text{m}^2$), the mirror ($\$12/\text{m}^2$) and the core material ($\$15/\text{m}^2$) [23].

The Solaflect ‘suspension heliostat’ [26], described earlier, uses the mirror panels as structural members in compression.

Sener has used stamping techniques combined with an automated bonding process to produce a reinforced glass mirror panel [13]. This has allowed thickness to be reduced from 4 mm to 3 mm for increased reflectivity; however, the facets are not ‘structural elements’ in the sense that they substitute steel from the support frame. Very similar stamped mirror facets are currently being installed at Solar Reserve’s Crescent Dunes project by Cobra.



Figure 43. Sener facet containers [13].

Sandia is currently carrying out a project to develop low-cost mirror facets, primarily sandwich panel type facets, in conjunction with a number of small companies with suitable manufacturing capability [155]. These companies produce large flat products in high quantities such as tables, writing boards, packaging materials, large panels for outdoor signs, automobile and aircraft body panels, and other large flat, rigid products. The stated aim of the project is to reduce facet cost by 25% while maintaining surface slope errors of 1 mrad RMS or below. Figure 44 shows the facet cost/performance relationship of seven prototypes, as well as two facets used in currently deployed heliostats. Baseline facet cost was assumed to

be about 53 USD/m² for 1 mrad facets, and the cost of new designs were estimated by the manufacturers assuming production volume of 1,000,000 m² per year. Sandia has developed a figure-of-merit relating cost and performance of mirror facets to give equivalent LCOE using a baseline DELSOL simulation with most parameters taken from the Sunshot vision study. The blue, red and green lines in Figure 44 correspond to LCOE of approximately 0.08, 0.07 and 0.06 USD/kWh. It appears that, as long as optical quality is better than about 2 mrad, the cost of the facets is an important driver to achieve low LCOE. It is also noted that the benefit to LCOE of improving optical quality below 2 mrad is slight.

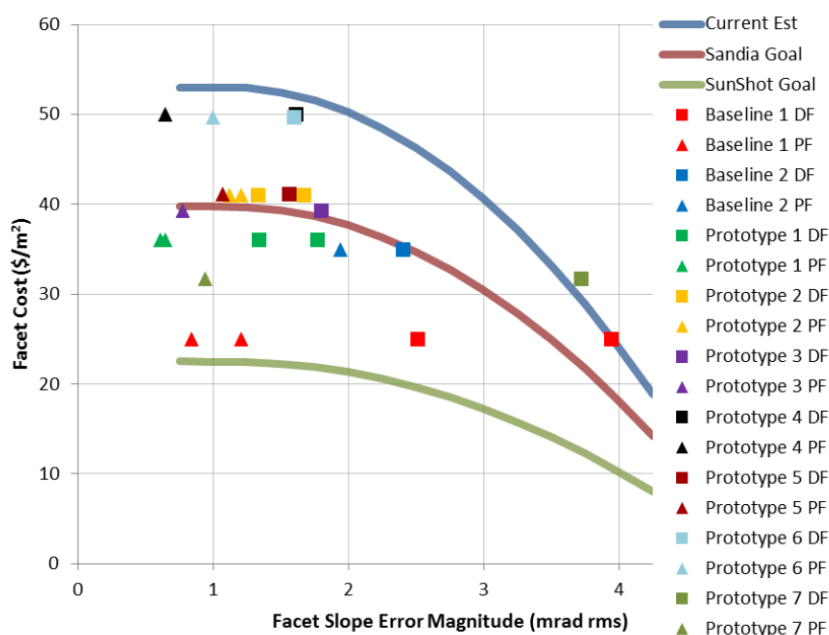


Figure 44. Facet cost/performance relationship derived from the study of the SunShot power tower scenario [155].

11 Production Methods for Mirror Supports

11.1 Introduction

The mechanical support of mirrors is a key part of the infrastructure within a solar thermal power plant. Traditionally this has consisted of large metal beams and foundations that support heavy glass mirrors. Here we review designs, materials and structures, and state of the art manufacturing methods that may be applicable for new heliostat concepts.

11.2 Design

The method of manufacture of reflector supports will depend on the design of the structure that supports the reflector, and the reflector material itself.

11.2.1 REFLECTOR MATERIAL

For example, if using a glass-based mirror, a stronger substrate will be required to support the weight of the glass, and to ensure that there is limited variability under thermal changes and variable wind loads.

Conversely, if using a reflective film on a lightweight substrate, a lighter weight support could be used, and therefore the manufacturing method would utilise thinner sheets of plastic or

metal, perhaps with lighter supports and less framing or ribbing on the back. In this case, other design features could be incorporated into the structure, including aerodynamic shapes and even holes in the surface to reduce wind load effects.

11.2.2 MODULARITY OF REFLECTOR SURFACE

If the reflector could be made of modular sections that fasten together to make the large reflector, methods such as injection moulding could be used to rapidly manufacture plastic supports for the reflector surface. Fasteners could be moulded into the part, making assembly easier. Added benefits of this method could be easier transport and assembly on site.

For large single reflectors, large panels would have to be made and assembled on supporting structures. These could be made of metal sheets or polymer-based composites which is a more labour intensive approach.

11.3 Plastics

There are two types of plastic materials that may be suitable for use as heliostat supports.

Thermoplastics – these consist of long chain molecules and soften when heated. This means that they can be processed into different shapes by heating to a sufficiently high temperature, and solidify when cooled. Examples are poly(ethylene terephthalate) (PET) (drink bottles), poly(vinyl chloride) (PVC) (pipes) and polyethylene (PE) (containers, tubing, car parts). These can form amorphous or crystalline structures. It is possible to re-heat and re-shape these materials many times. Reinforcing particles or fibres can be used to improve the mechanical properties of the resin.

Thermosetting polymers – these react to form 3-dimensional covalently bonded networks of molecules and, once reacted, cannot be re-shaped. Thermoset materials can be rubbery as in tyres, or very rigid, as in boat hulls. In the latter case, reinforcing glass fibres are used to add toughness and strength to the final product.

11.3.1 THERMOPLASTIC POLYMERS

Extrusion

Extrusion is the forcing of polymer through a shaped die. In order for polymers to flow, they must be heated (typically in the range 190-320°C, depending on the polymer), and because they are viscous, significant pressure is required.

The extruder consists of a heated barrel and screw, into which polymer and additives are fed at one end, and a homogeneous polymer mixture is extruded at the other. Extruders can also be used as continuous reactors for some chemical modification of polymers.

Extruders can produce pipe, profiles and sheets. The die is designed to take into account the large shrinkage of the polymer on cooling, and this is greater for polymers that crystallise (such as polypropylene (PP)). Thick flat sheets of some polymers can be produced by extrusion for later modification.

Sheet production utilises a series of rollers to ensure that an even thickness in the sheet. Sheets are typically 0.25 to 5 mm thick and up to 3 m wide. Multilayer sheets can also be made in this way.

The extruder is also a significant part of many other polymer fabrication techniques including:

- Film blowing
- Cast film
- Extrusion coating of another substrate

- Wire and cable coating
- Foam extrusion
- Injection moulding

Applicability – used to make continuous flat sheets or shaped sections.

Injection moulding

In injection moulding a polymer is injected from the barrel of an extruder into a metal mould at high pressure and then cooled. Once the material has solidified the mould is opened and the part is ejected, preparing the machine for the next cycle. Injection moulding is typically used to manufacture parts with complex shape and high tolerance, at high throughput rates. The cost of manufacturing metal moulds is high, and the cost of the machine increases with clamping pressure, which increases with part size.

Applicability – not suitable for large flat parts as the costs would be very high due to the size of both mould and machine.

Rotational Moulding

Rotational moulding is used to produce very large hollow parts, such as water tanks. Powdered polymer is rotated inside a metal mould, heated and sticks onto the walls of the mould, producing the required shape. The part can be removed from the mould when cooled.

Applicability – only useful if a large hollow structure is required.

Thermoforming

Thermoforming takes a sheet of polymer, heats it to the point of softening and re-shapes it as it drapes over a shaped metal mould. Methods of assistance can be used to increase speed and accuracy, including vacuum, air or top moulds.

Thermoforming is applied from small items, such as cups, food containers and trays, to large items, such as freezer liners, bath tubs and boats.

Applicability – useful for shaping large sheets into a final shape.

Casting

Casting is a process of polymerisation of a liquid monomer into the final product. This can be done by a batch process using a mould (such as lens making) or as a continuous process where the monomer solution is cast onto a moving belt. The latter process is used to make cast acrylic (PMMA) sheet which has excellent optical properties and is used in glazing applications. Nylon (polyamide) sheet can also be produced in this way.

Applicability – only useful for forming a polymer sheet, could be used to cast the acrylic material into a final shape directly from the monomer, but one side would have to be flat.

Conclusions about thermoplastic materials

The production of a large polymer sheet with precise shape could best be achieved with thermoforming or compression moulding of a pre-prepared flat sheet. This sheet could be made of any suitable thermoplastic material for use as a rear support for a reflective film. A material with high stiffness would be preferred in order to reduce variability in shape. Smaller modular sections of reflector support could be made by injection moulding.

11.3.2 THERMOSET POLYMERS

Materials

Thermosetting resins are similar to the acrylic casting materials described above. They are produced in the monomer form, and when catalyst and initiators are added, can be cured into a final shape. Rubbery materials include many rubbers and acrylics. Rigid materials include polyester, vinyl ester and epoxy resins that are hard and brittle. The properties of polyurethanes can be tailored as they contain both rubbery and rigid components.

These materials are cured in a mould to make the final shape.

Applicability – moulds are required to hold the resin while curing, and could be an expensive option. Parts may not have the required combination of mechanical properties.

Composites

In order to increase the toughness of thermoset resins, fibres can be added. Typically glass fibres are used, although in specialised applications carbon, Kevlar or specialist organic fibres can be used. The production of large flat parts from these materials requires hand 'lay-up' of sheets of the fibre and impregnation with the resin and curing additives. Sheets of fibre and pre-prepared resin called 'prepregs' can be used to shorten production time.

The laying of fibres in different directions within the part can be used to tailor the mechanical properties of the material in specific directions. As the curing process is exothermic, time must be allowed for each layer to cure when making thick parts.

Shape precision could be increased using higher precision methods such as vacuum-assisted autoclaving (e.g. carbon fibre composite panels for aerospace).

Applicability – this method is highly labour intensive, but can be used to make panels of any size with superior mechanical properties (stiffness, thermal stability).

Sheet moulding compound

A variation is where a thermoplastic (typically polypropylene) is layered with glass fibres and resin, in an alternating structure. This can be rolled up for later use. For producing the final shape, the pieces are trimmed from the roll, put into a metal compression mould and heated to initiate the curing process.

Applicability - this is a high capital cost process, due to the need for hot-platen press machines, and would be most suited to large production runs [159].

Compression, injection and transfer moulding

These methods are similar in the curing of the resin, but differ in the transport of resin to the mould. All of these methods use heated metal moulds and are therefore capital intensive, but can have cycle times as low as minutes.

Applicability – large metal moulds and press machine required for large panels, best for high volume manufacturing due to high cost of equipment.

Open mould processing

Lay up of composite materials for large structure (eg boats) typically uses this method. Little or no pressure is used, and curing occurs at ambient temperature. This includes processes such as filament winding for pipe making.

Applicability – useful for large structures, but labour intensive.

Pultrusion

Sheets or strands of fibre are wetted by resin and pulled through a heated forming die that creates the final shape.

Applicability – useful for producing continuous lengths of fibre reinforced material.

Resin Transfer Moulding

This forces resin into a mould pre-packed with reinforcing fibres in the desired layout.

Applicability – large moulds required for large parts, although moulds can be made of lower cost materials due to the low pressures used. Long cycle times are common.

Conclusions about thermoset materials

Thermoset materials can be used to make large area panels, including complex shapes. The methods used are labour intensive, but can achieve strong, stiff and lightweight structures.

11.4 Metals

11.4.1 HOT FORMING

Hot forming processes are not applicable here as they are used for the shaping of an ingot into structural shapes such as bar or sheet [160, 161]. It can include rolling or press forging, for example, and generally found in metal foundries.

11.4.2 COLD FORMING

Bending

Bending operations are most suited to forming large metal shapes from sheet starting materials. The bending will only be on one axis. A press is required, and in this case the die would be the same size as the panel [160].

Rolling

Rolling could also be used to form curved supporting structures, but would need to be carefully controlled so that the shape was accurate [160].

Stretching

Stretching would be used if the metal panel required a complex shape, with curves in more than one axis [160]. Stretch forming was developed by the aircraft industry to make large sheet metal parts economically in small quantities. A form block is required to act as a die for the final shape. Correct control of the process eliminates the compressive stresses that accompany bending or forming so there is very little spring-back. As the form block is in compression, it can be made from many materials including wood and plastic. It is possible to stretch form steel, stainless steel, titanium and aluminium.

Forming with a rubber tool or fluid pressure can be used to make deep parts with low cost tooling, which makes this method suitable for low volume manufacturing. However, the system must be fully enclosed so that the pressure can be applied to the whole part and force it onto the die.

Metal sheet from Bluescope has a maximum width of 1800 mm.

Stamping / Pressing

To create complex shapes or parts with cut-outs from flat sheet metal, stamping and pressing techniques would be used [160]. These types of designs would be used to add strength and/or remove excess weight from metal supporting structures. An example of this approach for supporting glass mirror panels used at the Crescent Dunes plant is shown in Figure 45. These methods require metal dies to be fabricated, and are often referred to as blanking or piercing when part of the sheet is removed. Many designs are possible; increased complexity and the use of specialised materials can increase the cost of tooling.

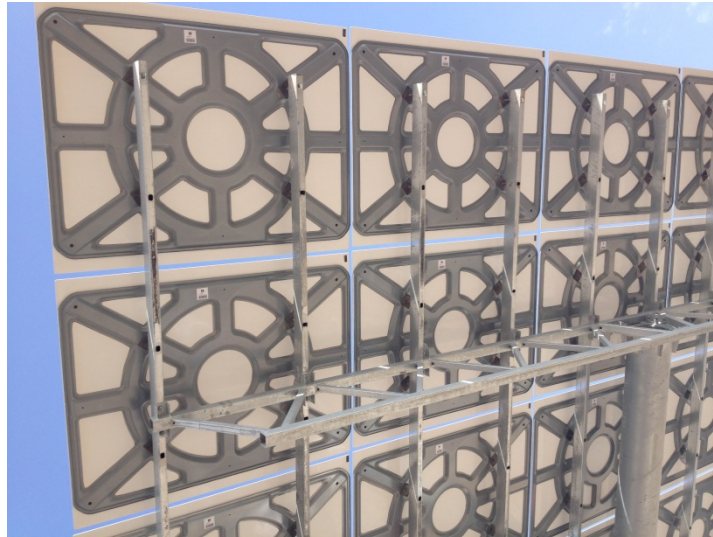


Figure 45. Mirror support structures at Crescent Dunes plant [photo: Joe Coventry]

11.4.3 CONCLUSIONS ABOUT METALS

Metal supports are traditionally used to support heliostats, and offer suitable ways in which to create large area supports for reflector panels. Simple bending methods could be used for large area panels required for solar thermal reflectors. The use of shaped panels with potentially complex shapes to support mirrors is also possible with simple stamping techniques.

11.5 Summary of production methods for heliostat supports

Thermoplastic Polymers

The production of a large polymer sheet with precise shape could best be achieved with thermoforming or compression moulding of a pre-prepared flat sheet. This sheet could be made of any suitable thermoplastic material for use as a rear support for a reflective film. A material with high stiffness would be preferred in order to reduce variability in shape. Smaller modular sections of reflector support could be made by injection moulding.

Thermoset polymers and composites

Thermoset materials can be used to make large area panels, including complex shapes. The methods used are labour intensive, but can achieve strong, stiff and lightweight structures.

Metals

Metal supports are traditionally used to support glass mirrors in thermal solar facilities, and offer suitable ways in which to create large area supports for reflector panels. Simple bending methods could be used for large area panels required for solar thermal reflectors.

Material combinations

There is also the potential for a combination of support materials. For example, the use of shaped metal brackets to supporting a polymer-based panel with an attached reflector film could be one way to combine lightweight design and stiffness in the support structure for film-based reflectors.

The materials and processes used for reflector supports will depend on the overall design approach chosen for the entire structure.

11.6 Issues to explore

Detailed analysis of each of the processing methods would include factors such as:

- Material costs
- Production costs
- Mechanical properties v. Thickness v. Weight
- Stiffness requirements (compared to glass)
- Durability / lifetime / environmental resistance
- Compatibility with reflective sheet
- Surface finish
- Dimensional stability with temperature, load

Capex for production, availability of outsourced manufacturing

12 Communications

12.1 Autonomous heliostats

Development of autonomous heliostats - i.e. heliostats that do not require power or communication wiring - has progressed markedly in recent years. Autonomous heliostats also do not require lightning protection.

In 2004 PSA tested a field of 92 radio-controlled heliostats [162, 163], and found capital cost savings of more than 50% were feasible for the power supply and communication system, compared to conventional hard wired systems.



Figure 46. A view of the PSA CRS heliostat field, which has 92 autonomous radio-controlled units.

A wireless mesh communication system has been tested at the solar tower plant in Julich by Trinamic [25]⁴, and a similar system is under development by NREL [31]. Advances to wireless communication technology and reduction in the cost of photovoltaics have made heliostat autonomy an attractive option. Brightsource has recently named development of autonomous heliostats as an “area of focus” [164].

12.2 Conventional communications systems

Heliostat fields have traditionally been controlled using standard industrial communication networks, based on buried copper wires or fibre optics [6, 163]. For example, the Gemasolar plant uses 26 fibre optic rings (Figure 47)– a method that gives a high level of redundancy [13, 165].

⁴ According to Michael Randt (personal communication 16/08/13) the wireless mesh system at Julich has since been dismantled.

Architecture:

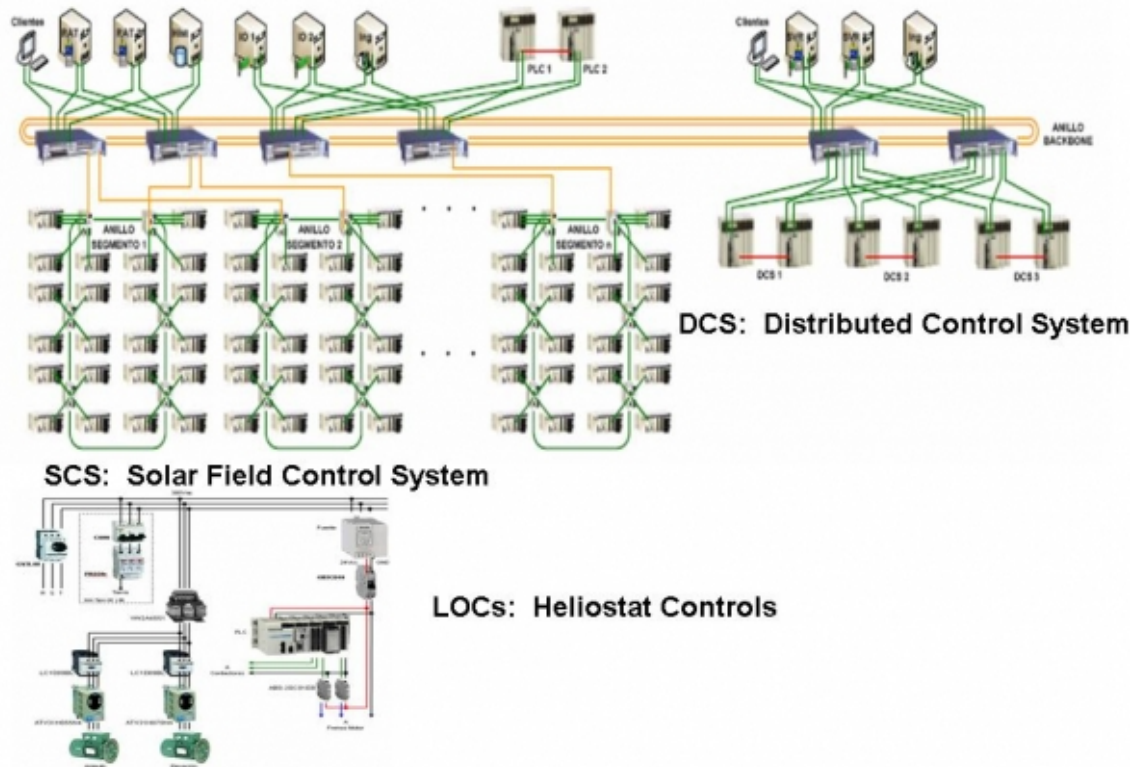


Figure 47. Architecture of the Gemasolar communications system by Schneider Electric [165]

At Ivanpah, Brightsource supply 50V power in mostly above ground cabling using a trickle charge system to power / control units equipped with capacitors. The communication system uses fibre optic cabling.

13 Sun tracking systems

The majority of heliostat systems – past and present – have used the so-called ‘azimuth-elevation’ style tracking, typically using the pedestal mounted design (Figure 48), for example, refer to current commercial designs in Section 4.1 and past heliostat designs documented in [6, 11].

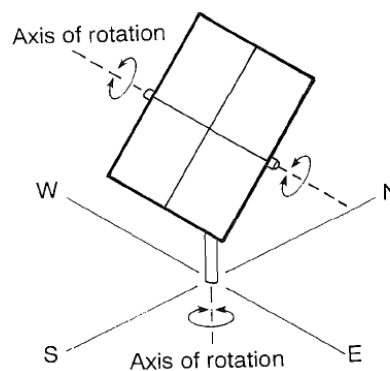


Figure 48. Azimuth-elevation tracking [166]

Other tracking systems were examined in the early days, but it was concluded that azimuth-elevation tracking systems were cheaper [6]. However, as is discussed in this section, there is renewed interest in alternative tracking systems for a variety of reasons.

13.1 Horizontal primary axis heliostats

Figure 49 shows another type of 2-axis tracking that has been used for a number of recent heliostat prototypes, the so-called horizontal primary axis heliostats. The right-most heliostat in Figure 49 has the azimuth-elevation style of tracking (or vertical primary axis), and the left-most heliostat has the horizontal primary axis style of tracking.

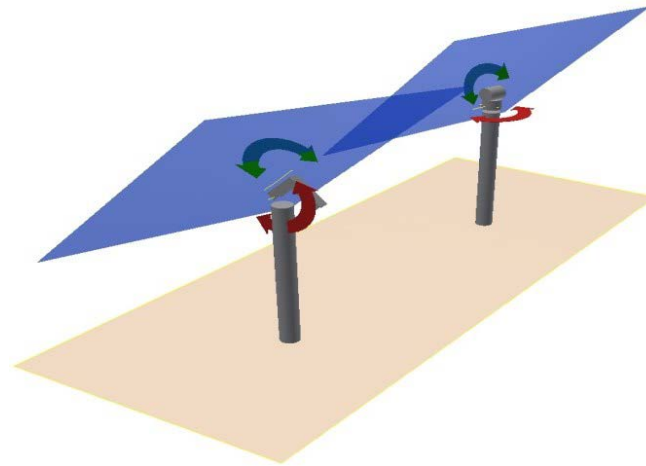


Figure 49. Heliostats with horizontal (left) and vertical (right) primary axis, from [32]

Heliostats with a horizontal primary axis of rotation allow up to 80% denser spacing without collision [32, 54, 167], which is particularly useful in regions close to the tower (refer to Figure 50 and Figure 51).

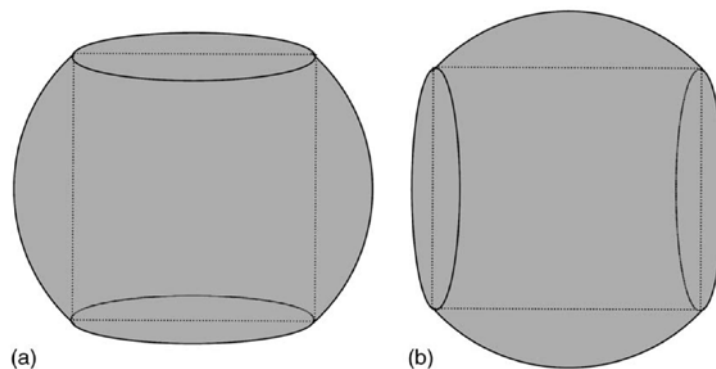


Figure 50. Unimpeded space volume needed by a reflector of an (a) azimuth-elevation tracking heliostat and a (b) primary horizontal axis heliostat [167].

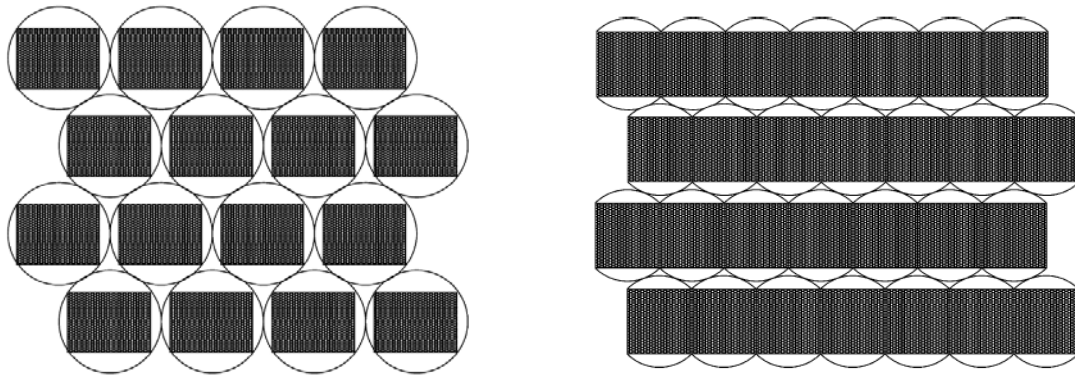


Figure 51. The maximum ground coverage of a heliostat field of azimuth-elevation tracking heliostats with rectangular reflectors (left) and a field of fixed horizontal tracking heliostats with square reflectors [167].

A hexagonal shape can theoretically increase ground coverage to 100% [167]. A number of small heliostats under development employ this type of tracking [23, 32, 56]. With optimal alignment of the primary axis, the range of motion for both axes can be brought within the feasibility limits of linear actuators [23, 32], allowing the use of cheaper components (discussed further below in Section 14.4).

13.2 Target aligned heliostats

Another tracking type with some merit for a high concentration solar tower is the so-called ‘target aligned’ heliostat approach [168, 169], where the primary axis of rotation points to the receiver. Target-aligned heliostats are also referred to as ‘spinning-elevation’ heliostats.

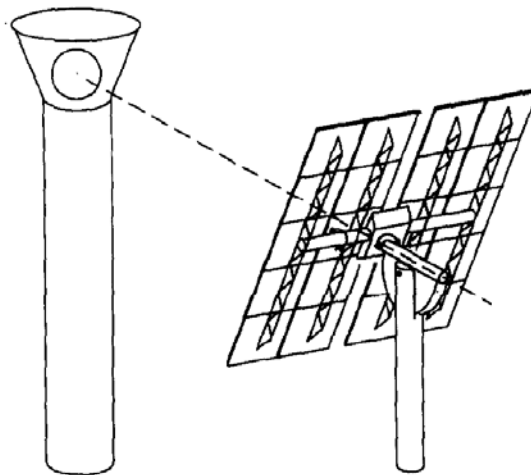


Figure 52. Target oriented mount where sagittal and tangential directions do not change with respect to the reflector. The first axis, fixed with respect to the ground, points towards the target. The second, fixed with respect to the reflector, is perpendicular to the first and tangent to the reflector [168].

As each heliostat tracks the sun, its sagittal and tangential directions do not change, and therefore it is theoretically possible to tune the curvature of each axis (so-called ‘toroidal’ heliostats) to minimise the average astigmatic aberration, which reduces the maximum spread and improves the uniformity of the reflected image from each individual heliostat. As is

apparent in Figure 53, which has results for a case study of a single heliostat in a field, sometimes the conventional heliostat focus is excellent (e.g. in the morning, when the tower is between the sun and heliostat), but sometimes it is very poor. The improved uniformity of the target aligned heliostat is likely to be advantageous for receiver design.

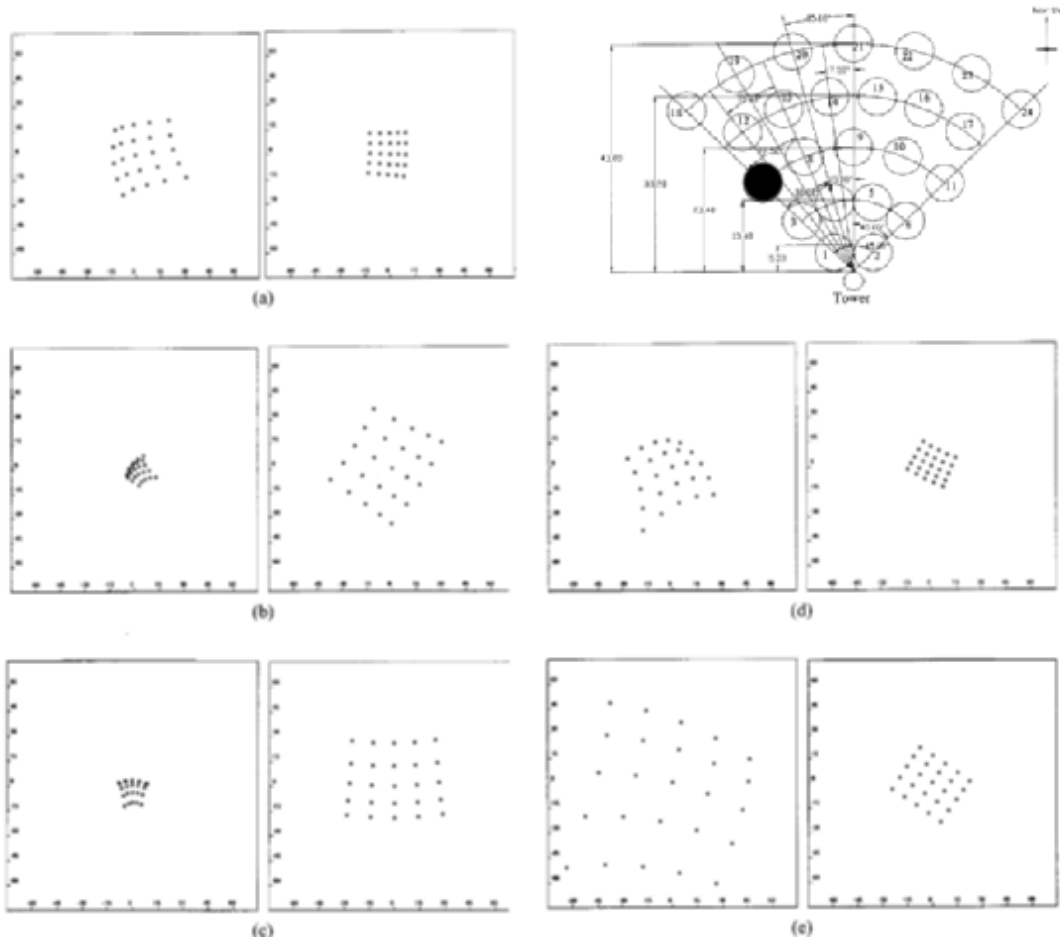


Figure 53. Comparison of image spread on a receiver target for heliostat 7 (ref. shaded heliostat in image top right) at different times on June 21. Each point represents the intersection on the target plane of a central ray from an individual facet. Left side is an azimuth-altitude heliostat, right side is a target aligned heliostat. (a) 7 am (b) 9 am (c) 11 am (d) 1 pm (e) 3 pm. [169]

For example, in a study by Zaibel [168] each individual heliostat was corrected such as to maximise yearly average concentration, with the results as per Figure 54. The target-aligned heliostats give higher concentration values than azimuth-elevation tracking heliostats in general, and in the northern part of the field has about 20%-50% higher concentration values, and in the southern parts of the field, an improvement by as much as 2-3 times.

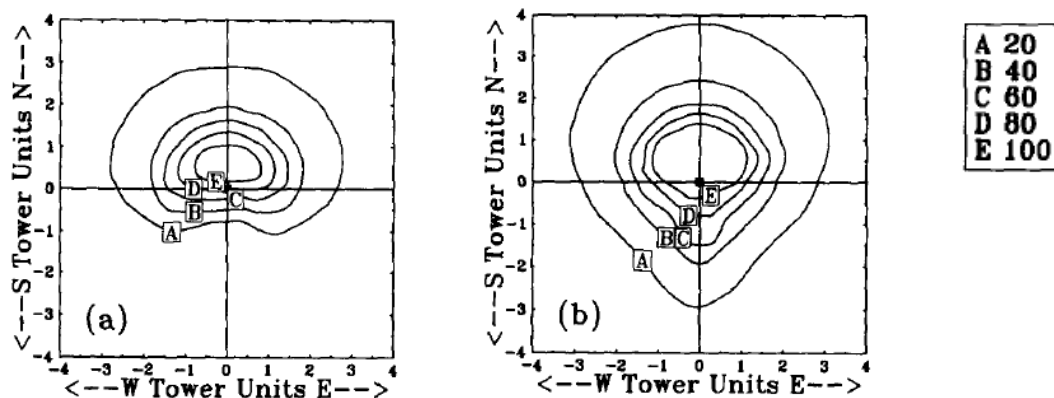


Figure 54. Lines of constant yearly average concentration for conventional azimuth-elevation heliostats (left) and astigmatically corrected target aligned heliostats (right). Field position is measured in terms of multiples of tower height, with the origin at the base of the tower. Correction was chosen such as to maximise yearly average concentration at each location individually [168].

Heliosystems is developing a ‘toroidal’ heliostat (i.e. different reflector curvature in the sagittal and tangential directions) which employs the target-aligned tracking approach (Figure 14) [35, 170]. Heliosystems has developed an algorithm to optimise the sagittal and tangential focal length of a given heliostat to cause the least beam spillage on average [171]. This software has been extended to create a simulation environment for designing full field layouts. It also includes ‘focal length contours’ for grouping heliostat rows to simplify manufacturing.

A study of tracking angle range for the target-aligned approach found the secondary axis could be actuated by a linear drive, but a slew drive is required on the primary axis [172]. Another study found a minor advantage with regards to power consumption: 5-10% less compared to conventional heliostat tracking systems [173].

Overall, the benefits of the target aligned tracking approach, annualized and averaged across the whole heliostat field, are not yet clear [169].

13.3 Heliostat shape

It noted that the shape of the heliostat can be important with regards to the annual optical efficiency of a solar field. One study found that for rectangular heliostats a horizontal-to-vertical aspect ratio of about 1.2 provides around 1% more energy to the receiver than a square heliostat [44].

Alternative shapes to a rectangle may also be advantageous with regards to the density of packing. Schramek and Mills [167] recommended hexagonal heliostats, which can theoretically allow ground coverage approaching 100% (Figure 55).

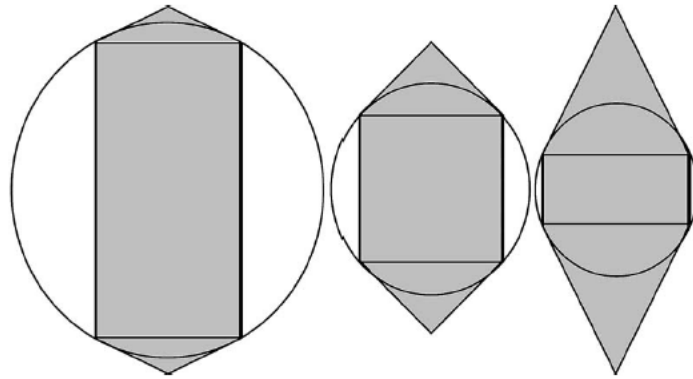


Figure 55. Three examples for the shape of a hexagonal reflector for 100% ground coverage, with the middle example recommended as the most practical [167].

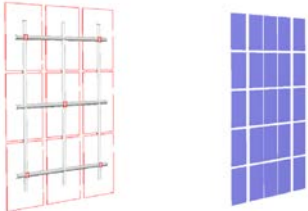
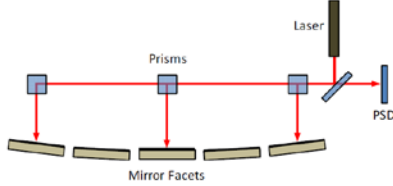
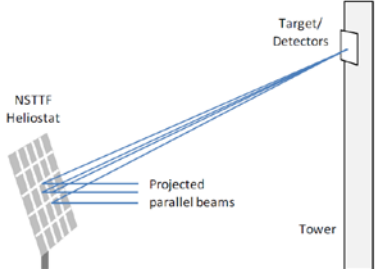
13.4 Canting

Canting describes the process of adjusting the alignment of individual facets on a multi-faceted heliostat. Yellowhair and Ho reviewed the various methods of heliostat canting [174]. The main two classes of canting are on-axis and off-axis alignment. On-axis alignment occurs when all mirror modules' normal vectors intersect at a point twice the focal distance from the mirror vertices. It is called on-axis because it is optimised for a geometry where the heliostat centre, the target, and the sun all fall along a line. Off-axis alignment is optimised for a geometry where the heliostat centre, the target, and the sun do not fall on a line. This type of alignment is normally implemented by tracking the sun and adjusting the aiming of each mirror module to minimise the size of the reflected beam upon a target. Both methods provide optimum heliostat performance for only one particular sun position.

A 1996 Sandia study show that if the canting is done at just the right time of the day, off-axis canting can achieve a better result for annual performance than on-axis canting [175]. However, the study concluded that in general on-axis canting performance is rarely exceeded, and is a 'safer bet'. Conversely, a 2009 DLR study concluded that for standard azimuth-elevation tracking, off-axis canting gives the best performance in most cases [176]. Yellowhair and Buck point out that these results emphasize that the best type of alignment strategy depends on various factors of the power tower design, such as size, geometry, heliostat configuration, application, etc. Yellowhair and Buck review a number of options for canting, and these are briefly summarised in Table 2.

Table 2. Summary of canting methods from [174]

Method	Description
Gauge blocks	With the heliostat frame facing up on a short pedestal, a reference plane is defined. The facet cant angles are pre-calculated, and gauge blocks with the correct thickness are used to tilt the facets from the reference plane before they are secured to the frame. Care is taken to account for gravity sag. The process is highly manual. Accuracy is limited by placement of blocks and by the accuracy of predicting the sag.
Electronic levels / inclinometers	Inclinometers are used to measure the facet angles. The facets are then adjusted to the pre-calculated angles, first vertical tilt then horizontal tilt, or vice versa. The process is highly manual. Facets can be canted to better than 1.5 mrad, but tedious to achieve this.
Linear displacement	Linear displacement transducers have been used to measure mirror edge

transducers	displacements from reference planes.
Photogrammetry	Photogrammetry uses multiple images of objects to determine the object geometric properties. ANU has significant experience with close range photogrammetry of mirrors. Photogrammetry has been combined with edge detection to find misaligned heliostat facets and fix the canting. The estimated surface normal is compared to the design surface normal to find the correction factor.
Deflectometry	A fringe pattern projected on a screen is viewed with a camera in reflection through a mirror whose surface is of interest. The images of the fringes are capture while modulating the fringes. In one method, the camera and a large screen are mounted on the tower. A camera projects the image on the screen from the ground. The surface normals across the heliostat surface are calculated, and can be fit to those of a target shape. Misalignments are seen as deviations from the target shape, and physical adjustments can be made.
Theoretical image overlay	 <p>A frame is positioned adjacent to a vertical heliostat. The frame has a number of cameras mounted on it, as well as targets with special patterns. The reflected images of the targets are compared to a theoretical image, and the facets are canted until the two images match. This is a new method developed by Sandia, based on a similar method that has been used previously for aligning trough facets.</p>
Scanning prism laser projections	 <p>This system consists of two or more prisms co-aligned to a laser, a beam splitter, and a position sensing detector (PSD). Outer prisms scan to measure facet angles, while the centre one remains fixed for reference. Nominally parallel beams are projected onto the facets. The reflected, deviated beams return back through the prisms and beamsplitter, and focus on the PSD. As the facets are adjusted in angle, the reflected laser spots on the PSD move accordingly. The shape of individual facets may be adjusted by this method too. This is also a new method proposed by Sandia in response to the cumbersome method of using an inclinometer for canting.</p>
Parallel laser beam projections	 <p>In an extension of the previous method, prisms are used to produce a regular grid of laser beams. The image of the beams on a target on the tower can be processed to align individual facets. The shape of individual facets may be adjusted by this method too. This is another concept proposed by Sandia.</p>
Camera look back	A camera at the top of the tower is pointed at a heliostat. The heliostat position is adjusted until the reflected image of the camera in the centre facet is centred in the camera field-of-view. With this reference established, the heliostat is moved multiple times such that the theoretical normal of each facet points to the camera. Facet tilt is adjusted such that the reflection of the camera is centred in the camera field-of-view. This method of canting proved slow during the Solar One heliostat alignment, and relies heavily on precision encoders for accurate

	canting.	
Target reflection		<p>A target is placed some distance from the heliostat. The heliostat is rotated until the reflected image in a tower-mounted camera is centred in the camera's field-of-view. The image is processed assuming a parabolic heliostat, and misaligned facets are adjusted until the image satisfactorily replicates the real target. This is another method proposed and trialed by Sandia.</p>

For the Gemasolar plant, Sener refer to the use of a “large volume metrology system” for canting, that checks hundreds of points with high precision [13]. The initial canting is done when the heliostats are in assembly, prior to field deployment. The system appears to be based on the use of a Nikon Metrology laser radar, which scans the surface of the heliostat, a process which takes about 5 minutes [143]. The data is processed in heliostat pointing correction software. The canting system employs different thickness washers. The software suggests the number and type of washers required for each facet support. This method allows a “long packing tightened bolted joint” which is able to withstand dynamic wind loads without loosening. The laser radar is used to do a final check of the heliostat surface after the adjustments are made.

13.5 Low profile mirror panels

Design loads for many heliostat components tend to occur in stow position, in order to survive infrequent high wind gust conditions stipulated by codes. In Figure 56, a range of concepts for achieving low profile mirror panels are shown [18].

<p>Vertically rotated horizontal secondary axis at ground level</p>	<p>Lifting jack pylon</p>	<p>Panel guidance at pylon and truss</p>
<p>Spatially fixed horizontal primary axis at ground level</p>	<p>Turning panel downwards along pylon</p>	<p>Pylon with central hinge</p>
<p>Spatially fixed horizontal primary axis at ground level, ganged facets</p>	<p>Lowering pylon below ground level</p>	<p>Pylon with base hinge and linear drive</p>

Figure 56. Approaches for lowering the mirror panels under storm conditions [18]

The advantages of low loads in the stow position should be assessed against the disadvantages, such as higher loads during tracking due to out-of-balance design, additional drives and other components, and added complexity [18].

14 Actuation systems

14.1 Pedestal mounted drive systems

As is discussed in Section 13, the majority of heliostats use a pedestal mounted azimuth-elevation tracking system. As noted in Section 8, a key driver to large scale heliostats is the drive system. In efforts to reduce the cost of the drive, a number of customised drive products have been developed by companies such as Sener [13], Flender Siemens [57-59], Winsmith [7, 60] and Cone Drive [61].

14.1.1 WINSMITH DRIVES

The Winsmith drive has been used on the ATS heliostat, and more recently the SES Dish-Stirling systems [60]. According to Sandia [7] the Winsmith drive has an “extremely clever” planocentric design with reduction between motor and outer ring of of 33,000:1 in a very small space.



Figure 5-1. Winsmith planocentric azimuth drive. One of the four small gears within the unit is driven by an external electric motor. The remaining three idler gears are connected to this drive gear by the center larger gear with the hole. The motion of each of the four small gears is connected to a plate via an eccentric race. This causes the plate to wobble back and forth and rotate the outer ring connected to the heliostat structure. The speed reduction between motor and outer ring is ~33000:1.

Figure 57. The Winsmith drive, from [7].

In 2007 Winsmith estimated the drive would cost \$5700 for production rates of 5,000 per year, or \$3,000 for 50,000 per year. Material costs were estimated at only \$360 per unit [7]. According to personal communication with George Tedesco Jnr (6/5/13), formerly of Winsmith:

“There were a number of specification issues that drove the cost of azimuth drives up during our development process:

- Life - Most specifications required consistent performance over a life of 20-25 years. Typical power transmission products were designed for around 5 years and generally had a two year warranty.
- Accuracy - This is one of the most difficult issues. Trying to keep gear wear low enough to maintain the high tracking accuracy required in most specifications was difficult to guarantee for the life requirements.
- Peak torque requirements - In an effort to handle these rare but necessary load occurrences the product size needed to grow.
- Low maintenance - Most specifications wanted the product to be lubed for life. This caused most products to have a sophisticated enclosure and seal system.

We were able to meet most of these specifications but at a high cost. If product life cycle costs were accurately computed we may have been more successful but the upfront costs were a problem”.

George was unsure of the level of involvement Winsmith currently has in the CSP industry, following the demise of SES.

14.1.2 FLENDER-SIEMENS DRIVES

According to personal communications with Andreas Pfahl of DLR, Siemens no longer offers drive systems for heliostats. According to Michael Randt, Trinamic has the last of the Siemens slew drives. Figure 58 shows the range of products offered in the past.

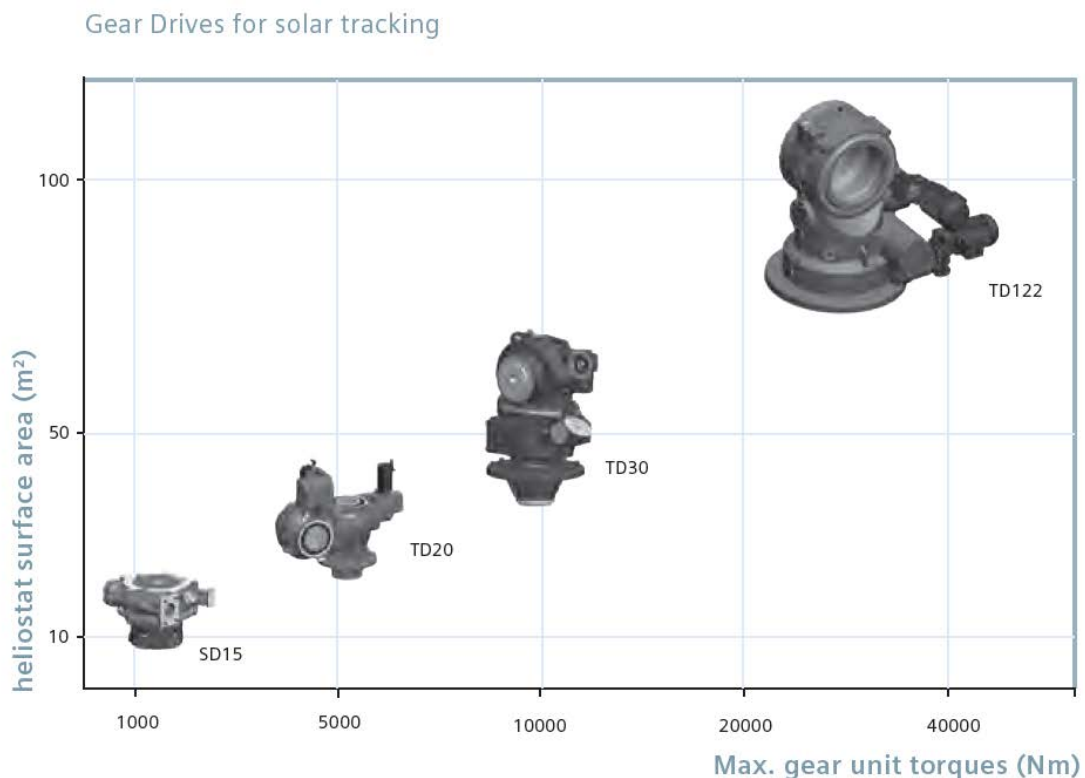


Figure 58. Siemens drives [57].

14.1.3 SENER DRIVES

SENER has developed a drive system, known as ‘MASS’, for use in its own heliostats but it also offers the drives to third parties. In personal communication with Soledad Garrido of Sener (30/5/13), it is claimed that the product is unique in the market due to “its high accuracy (zero backlash) even under strong wind, its high load capacity, high efficiency and low

maintenance". Sener has more than 3500 units in operation in commercial applications, for CSP and PV.

SENER delivers the complete drive (mechanism, motors (AC or DC), sensors, limit switches, lubricant) ready to be installed and operate. The model in Figure 59 is designed for a 120 m² heliostat. According to Soledad, Sener is developing a new MASS model with double capacity, increasing the heliostat size but maintaining a similar cost for the drive.



Fig. 5 SENER drive mechanism for the Gemasolar heliostat

Figure 59. The patented SENER drive, two AC asynchronous motors [13].

14.1.4 CONE DRIVE

Cone Drive Gearing Solutions claims to be the world leader in double-enveloping worm gear technology [61]. It has a number of ready-made product lines, but also develops custom gearing solutions as it did for Brightsource for the Ivanpah project [177].

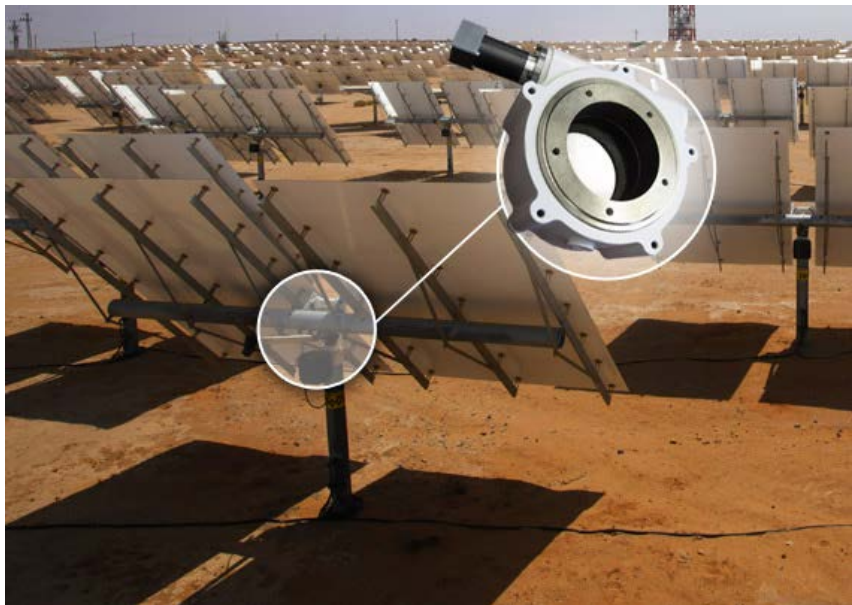


Figure 60. Cone Drive system for the Brightsource heliostats [61]

14.2 GFC

According to Michael Randt (personal communications, 16/08/13), GFC also supplied slew drives to the Ivanpah project. Michael says that Brightsource generally seek multiple suppliers for componentry, except where they have developed a product in-house. He also said that despite the large number of drives provided to Ivanpah, it was still a customised product with a dedicated production run, and production has now ceased.

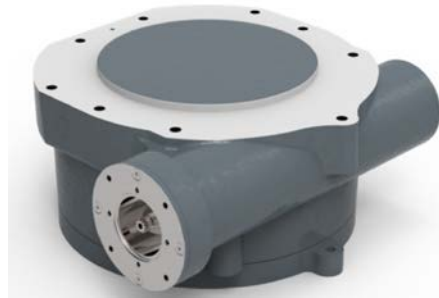


Figure 61. The DRW 100 slew drive from GFC [178].

14.3 Flextronics

Flextronics are assisting eSolar with design services relating to its next generation heliostats. Flextronics is an Electronics Manufacturing Services provider. According to Michael Randt of Trinamic (personal communications 16/08/13), Flextronics also provide linear actuators for the Brightsource Ivanpah project.

14.4 Linear drive systems

Some technology developers believe that using linear drive systems is cheaper than rotary drives [32]. Such systems may be used on a single axis, for example, the second axis in the Brightsource drives, or for both axes, for example in Julich, Germany and CSIRO.

A limitation of linear drives is the range of motion, which is practically limited to approximately 120° [32]. This can restrict the tracking range, as is shown for the case of the heliostat in Figure 62, assuming the primary axis is horizontal and driven by a linear actuator.

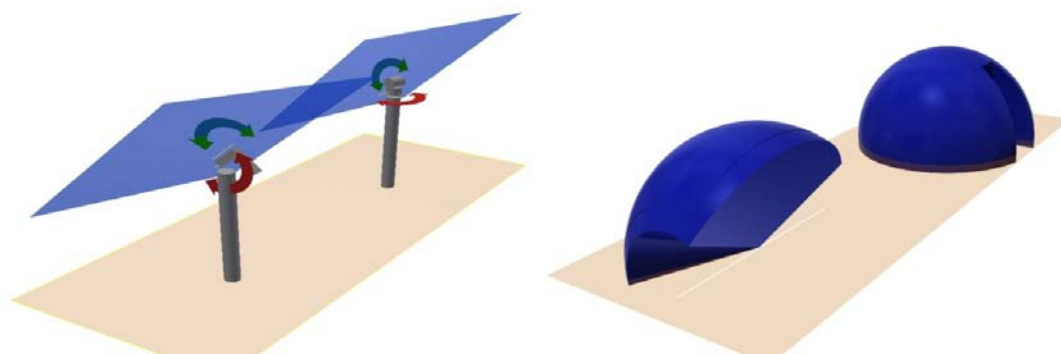


Figure 62. Heliostats with horizontal and vertical primary axes (left), and their movement range assuming a linear driven horizontal primary axis, and a rotary driven vertical primary axis (right) [32]

However, the impact of this limitation on the tracking range can be mitigated by strategies of alignment for the primary axis [32, 172]. In one such example case (Figure 63), assuming a

location in Mexico, around 6-12% of available radiation is missed with the east/west alignment, but in the optimised case availability approaches 100%.

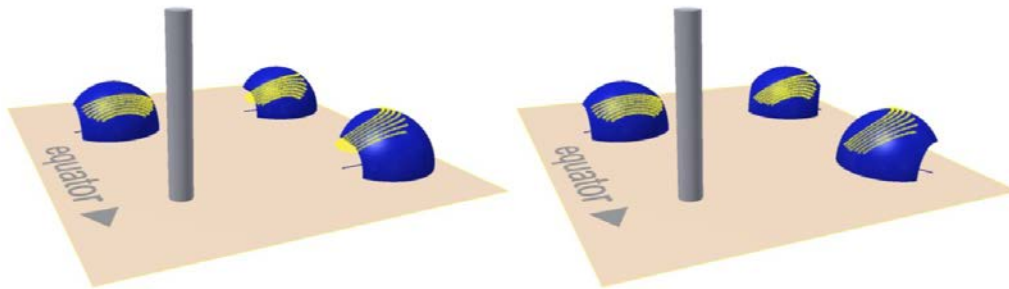


Figure 63. Physically limited movement ranges (blue) and sun tracking directions (yellow) of sample heliostat locations for an east/west orientation (left) and better optimised orientation of the primary axes (right) [32]

14.5 Rim drive systems

The concept of a rim drive is to improve the mechanical advantage compared to a conventional pedestal mounted slewing drive, lowering loads on bearings, the mirror panel, the upper part of the pylon and the stow locking device [23]. This allows the use of lower precision, lower cost drives. Another advantages for the elevation axis is that the rim partly counterweights the heliostat. However, use of a rim drive does add complexity to the design, requiring the rims, a guidance system, locking devices, and possibly protection from sand and dirt. A rim drive system may be used on one or both of the rotation axes. For example, the ‘Autonomous light-weight heliostat’ at DLR is rim driven on both axes [23] using a winch wheel system. The ‘Schlaich, Bergemann und Partner’ stressed metal membrane heliostat [11, 179] is rim driven on both axes, using a wheel driven rim for elevation, and a driven wheel and fixed rim (which is also part of the foundations) for azimuth rotation (Figure 64 and Figure 65). The Titan Tracker is rim driven on the azimuth axis only (Figure 9) [29]. Note that the ANU/Wizard Power Big Dish is also rim driven on both axes, with a driven wheel / fixed azimuth ring for azimuth rotation, and a rack and pinion system employing an off-axis circular back beam for elevation rotation (Figure 66) [157].

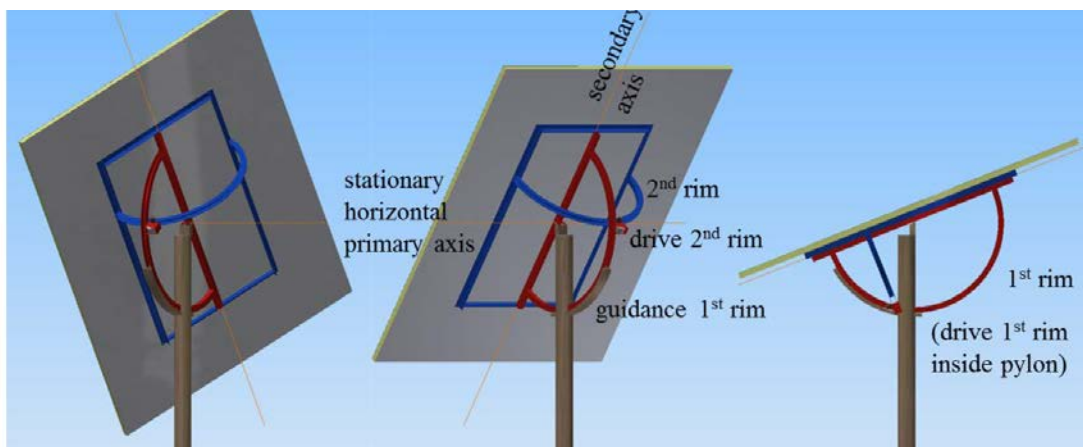


Figure 64. Rim driven heliostat under development at DLR [23].



Figure 65. Rim driven heliostat developed by Schlaich Bergermann und Partner [179]



Figure 66. The Big Dish at the ANU

14.6 Hydraulic drive systems

Hydraulic drives are well suited to solar tracking as they can be very precise, do not develop backlash over their lifetime, and can incorporate a pressurized reservoir for backup in case of power failure [33], although they may be better suited to larger heliostats due to both fixed cost components and maintenance requirements.

The HydroHelio design [33], developed in conjunction with DLR, encloses the entire hydraulic system in the cross beam of the heliostat (Figure 13 and Figure 67). The “transmission ratio” here is 1:10,000, as about 3 mm³ of fluid can be delivered by micro-valves into a cylinder with a volume 30,000 mm³ minimum (retracted). This corresponds to a positional accuracy of 0.01 mrad for elevation and 0.02 mrad for azimuth (i.e. extremely precise, albeit unnecessarily so). The fluid is kept under pressure in a spring accumulator, and only needs a refill every 30 minutes. This is energy efficient and provides backup in case of power failure. Fast movement is achievable if a discharge valve is installed. Azimuth over-torque can simply be dissipated by relief valves. The wind then just blows the heliostat to the neutral position. The fluid is natural or synthetic oil. The cross section of one cylinder is double the other one. Hence the chain is always pre-tensioned. Orientation feedback is via high resolution rotary encoders on both axes.

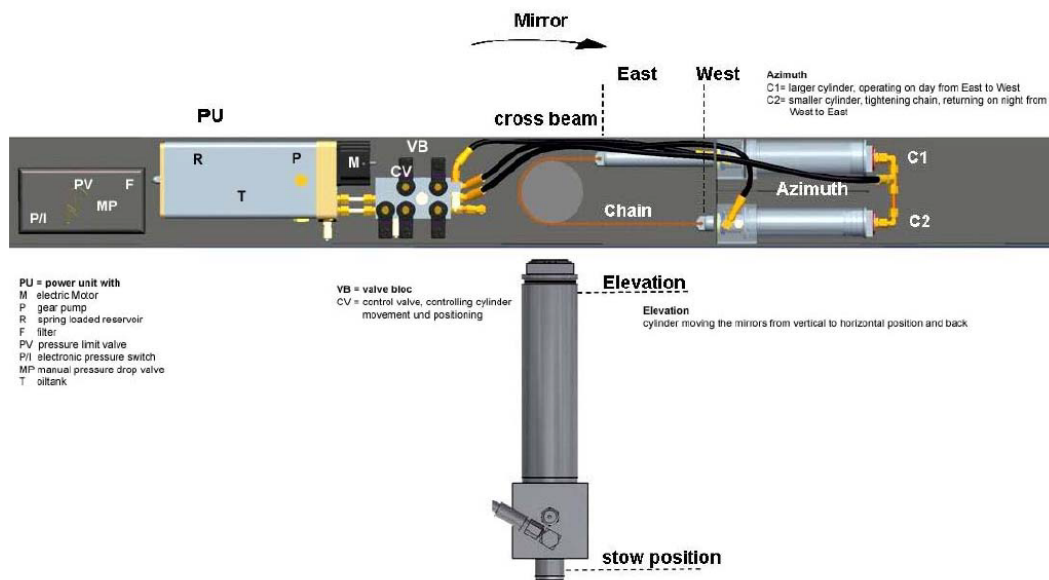


Figure 67. Cross-section of HydroHelio cross beam with integrated azimuth drive and pump unit

Abengoa Solar are using a hydraulic drive system for its new 140 m² ASUP140 heliostat design, currently being deployed at the Khi Solar 1 plant in South Africa [21].

14.7 Pipe-in-pipe drive system

The 2007 Sandia heliostat cost reduction study [7] identified the ANU’s “pipe-in-pipe” azimuth rotation system as a promising cost reduction measure. Figure 68 shows the ANU’s 20 m² dish, and the pipe-in-pipe design. The advantage of this system is distribution of overturning loads along the pedestal pipe, rather than a load concentration at a drive at the top of the pedestal. A disadvantage is that that an extra pipe is required within the pedestal.

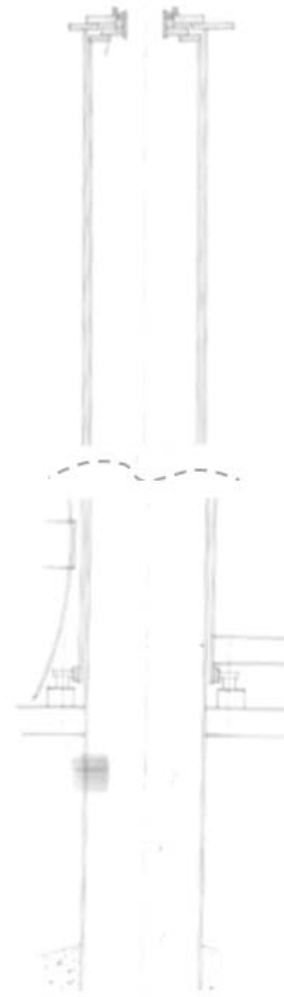


Figure 68. ANU's 20 m² dish (left), and the pipe-in-pipe azimuth rotation design (right)

14.8 Backlash

Backlash is a consequence of the space required between gears to avoid jamming and to provide space for lubrication [59]. Drives may be pre-tensioned with a spring to avoid tracking error due to backlash [18]. The elevation drive can be deliberately unbalanced so that gravity provides the pre-tensioning. Analysis is required to determine whether a backlash avoidance mechanism is justified, given the additional cost and complexity.

One such study was carried out by DLR and Siemens [59]. The study showed that with 3 mrad backlash, total yield losses are 5.4% for an unbalanced heliostat (compared to a 0 mrad backlash baseline), and 19% for a balanced heliostat. Hence there is the potential for very significant losses due to backlash.

Backlash is particularly important for the heliostats located in the outer reaches of a heliostat field [as the angular error produces a larger translational error at the receiver], as Figure 69 shows.

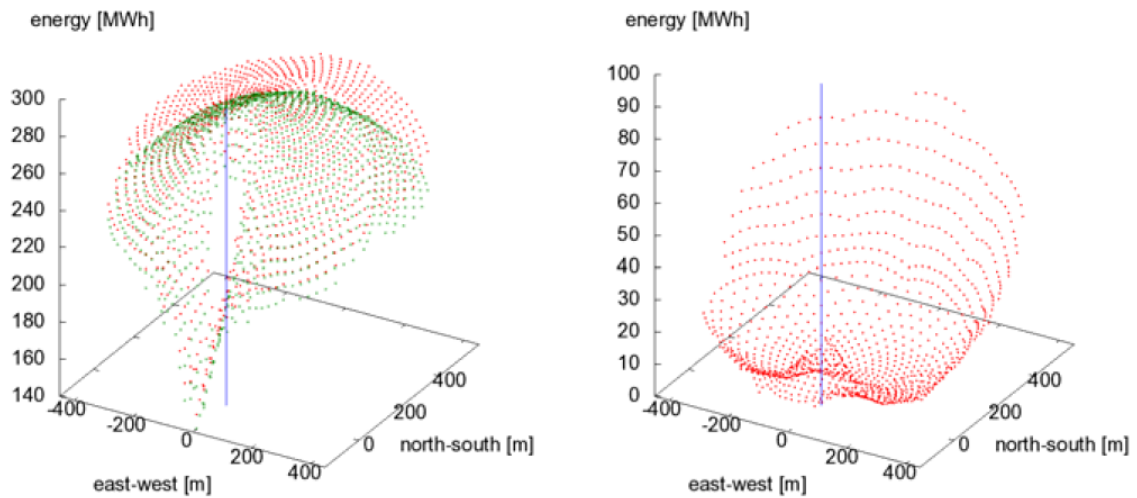


Figure 69. Annual optical yield of single heliostats with an ideal drive in an unbalanced situation. On the left, a system with 2 mrad backlash (green dots) is compared to one with zero backlash (red dots). The difference between the green and red dots is shown on the right in absolute terms (from [59])

Figure 70 compares the annual yield for various backlash scenarios, for both a balanced and unbalanced heliostat.

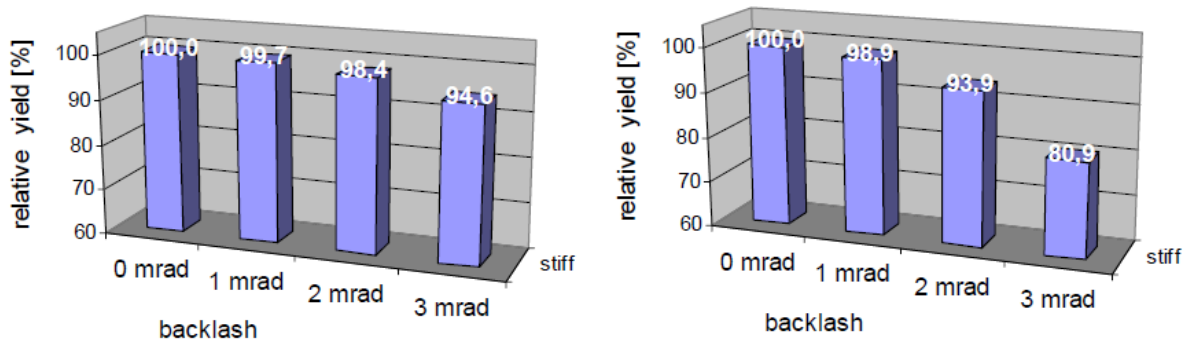


Figure 70. Influence of backlash on the total annual yield of an ideal drive, in the unbalanced (left) and balanced (right) cases.

As an example, according to the Siemens drive catalogue [57], backlash is between about 0.5 and 1.0 mrad for its range of drives. This would imply very low energy loss due to backlash in the unbalanced design (0.15-0.3%) and moderate losses in the order of 0.5 – 1.1% for the balanced case. For this drive, a pre-tensioning system may not be required.

15 Foundations

For foundations, the pedestal is typically mounted on a steel reinforced concrete pier (e.g. Sener [13]) or set directly below ground into concrete (e.g. ATS heliostat [7]). It is interesting to note divergent approaches in a number of recent heliostat designs.

Brightsource has developed a method of augering, then vibration hammering a thin walled pylon directly into the ground (Figure 71) [180]. An auger makes a hole, then reverses to keep the dirt in place. This protects the thin walled pylon when it is driven into the ground using vibration hammering. The hole diameter is at least 3 x bigger than the support member diameter. The pipe may be supported when it is hammered in, perhaps by another pipe inside or outside the pylon. The pylon has radially extending elements to resist rotation.

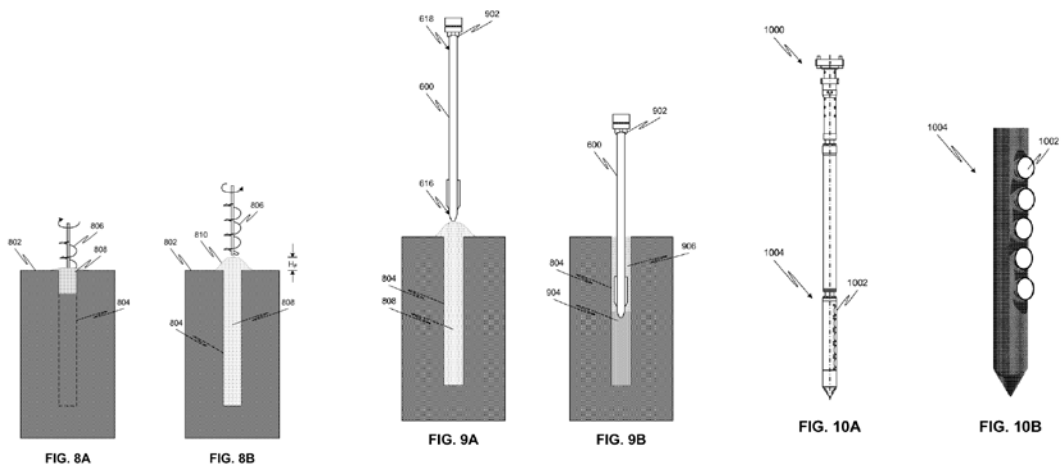


Figure 71. Brightsource method of direct installation of pylons [180]

eSolar's heliostats are mounted on an above-ground ballasted frame (refer to Figure 4)[22], and Abengoa's planned 18 m² heliostats will also have ballast type foundations [10].

DLR have opted for a pre-fabricated concrete ground anchor dropped in a hole, and further ballasted by natural site material (Figure 72) [23].



Figure 72. Pre-fabricated concrete ground-anchor foundation

16 Cost information

Reliable, contemporary heliostat cost information from current projects is not available in the public domain. Therefore we must rely upon other sources to establish base line costs

16.1 NREL (2013)

According to NREL current costs of heliostat fields are approximately 150 USD/m² [8]. No further detail is provided for this estimate.

16.2 Sandia (2011)

In the 2011 Sandia power tower roadmap [9] a baseline cost of 200 USD/m² was identified. This was based “primarily” on responses to a confidential questionnaire that was distributed by Sandia to power tower developers (inc. Sener, Abengoa, eSolar, Brightsource, Pratt & Whitney) in early 2010⁵, but also mentions the following sources:

- Escalation to 2010 dollars of power tower costs reported in a 1988 study by the Pacific Gas and Electric Company, reference not available, but well out-dated in any case.
- A 2010 Abengoa Solar study of the cost of molten-salt power towers [181], ref. section 16.3 below.
- A 2007 Sandia study of heliostats [7], ref. section 16.4 below.

16.3 Abengoa Solar (2010)

In 2010 Abengoa Solar did a detailed study [181] of a central receiver power plant to determine if supercritical heat transport fluids, in combination with ceramic thermocone storage systems, offer a reduction in LCOE over a baseline nitrate salt concept.

The study included estimates of the solar field cost, based on mid-2008 dollars. Heliostat costs were based on installed costs for the 122 m² heliostats at the PS10 and PS20 central receiver power plants, and were given as 224 USD/m² including foundations and controls, plus an additional 7.50 USD/m² for electric power distribution and field wiring (power, control, and grounding).

16.4 Sandia (2007)

In 2007 Sandia updated older studies of heliostat costs, with two base case designs: the 148 m² ATS heliostat (a pedestal type glass/metal heliostat) and the 150 m² SAIC second-generation heliostat (with a single, pedestal mounted stretched membrane). Estimates were given for two production quantities: 5,000 per year and 50,000 per year. The results, in 2006 USD, are summarised in Table 3.

⁵ We have a copy of the blank survey sheet issued by Sandia. It may be worthwhile re-issuing the survey as an ‘update’, perhaps with the support of Sandia.

Table 3. Summary of heliostat price estimates by Sandia in 2007 [7]

Type	5,000 per year	50,000 per year
ATS	164 USD/m ²	126 USD/m ²
SAIC	180 USD/m ²	143 USD/m ²

For these estimates, a breakdown of the costs in various categories was given. For example, for the ATS heliostat at 50,000 per year the breakdown is given in Table 4.

Table 4. Cost breakdown of ATS heliostat at 50,000 per year by Sandia in 2007 [7]

Item	Cost (USD/m ²)
Geardrive	27.11
Mirror Module	23.06
Torque Tube Assembly	10.78
Truss Assembly	6.75
Cross Bracing	3.68
Controls and Cabling	1.9
Drive Motors and Limit Switches	1.78
Pedestal	16.96
Fabrication Direct Cost	92.02
Overhead/Profit (20%)	18.4
Total Fabrication Cost	110.42
Foundation	2.33
Field Wiring	7.4
Field Assembly and Checkout	6.34
Total Installed Cost	126.49

16.5 Heliostat cost information from SolarPACES 2013

At the 2013 SolarPACES symposium, there was a panel discussion on the topic of “Cost Reduction Challenges and Approaches in CSP”. The key messages from the session were that LCOE costs are expected to fall below 100 USD/MWh by 2020, and will be required to do so for the CSP industry to survive. In the USA, with the investment tax credits, CSP costs are currently around 0.12-0.14 USD/kWh. Heliostat cost reductions of around 50% are sought to achieve the LCOE targets, and some companies see a path for costs around 75 USD/m² within the next few years.

16.6 Cost summary

Table 5 is a summary of the various cost data.

Table 5. Summary of cost data

Source	Original cost		Current cost*
	USD/m ²	Date	USD/m ²
NREL 2013	150	Apr-13	150.3
Sandia 2011	200	Mar-10	214.1
Abengoa 2010	224	Jun-08	238.5
Sandia 2007	126	Jun-06	144.7

* Indexed to May 2013 using U.S. CPI data

As is discussed in Section 3 there has been tremendous growth in the industry in the last few years. It is our expectation that heliostat costs from the main suppliers will have reduced, even since the time of the Sandia questionnaire and workshop with technology developers in early 2010. Hence, we believe the current cost is likely to be lower than 214 USD/m², perhaps approaching the 150 USD/m² recently estimated by NREL.

17 Key findings

Table 6 summarises some of the key findings from this report, and a view on the implication of each finding for future activities that may be undertaken under a future ASTRI heliostat cost down project.

Table 6. Summary of key findings, and recommendations for the follow-on heliostat cost down project within ASTRI.

Key findings	Report section	Recommendations for ASTRI based on the review
Most people in the industry believe the ASTRI cost target of 120 AUD/m ² by 2020 is realistically achievable.	3	This KPI is realistic for the ASTRI program, and should be retained.
The Sunshot cost target of 75 AUD/m ² by 2020 is seen as more of a stretch, although a number of people we have spoken to believe it will be met.	3	ASTRI should consider the concept of an additional stretch target, perhaps as an 'in-house' goal in the order of 90 AUD/m ²
The current cost of heliostats is estimated to be in the range 150-200 USD/m ² .	3 and 16	Perhaps the mid-point of this range is appropriate for a baseline model for ASTRI.
Heliostat performance has a strong leverage on LCOE, and as a result the use of mirror with high reflectance is important. The benchmark is 3-4 mm silvered glass mirrors with solar-weighted spectral reflectance around 93-94%, but there is the possibility of achieving higher reflectance through the use of thinner glass and reflective films.	5.1 and 0	The ASTRI heliostat cost down program should favour reflective materials that <i>currently</i> meet or exceed a reflectance benchmark of 93-94%, in order to have a realistic chance of meeting KPIs with the time frame of the program.
O&M costs have a strong impact on LCOE when aggressive LCOE targets apply. Compatibility with low-cost cleaning systems is an important design requirement.	5.2	Concepts for low-cost heliostat cleaning should be developed concurrently to a new design, and collaboration across the ASTRI nodes 1 and 4 is vital.
Heliostats deployed in power tower plants with >50% efficient power cycles are more likely to: <ul style="list-style-type: none"> • be arranged in a polar field rather than a surround field, due to the compatibility with cavity receivers. However, surround fields are also possible. • require optically accurate heliostats to achieve high flux at the receiver with acceptable uniformity and light spillage 	6	As achieving the ASTRI target LCOE is likely to require the use of highly efficient power conversion cycles, new heliostat designs developed in ASTRI should be compatible with both polar and surround solar field layouts, and should be focussing (or else small relative to the receiver).
Concurrent engineering processes are essential, i.e. engineers across disciplines working together from the earliest stages of product design and through the design life-cycle.	7	The ASTRI heliostat cost down program should include input from engineers across the most relevant design disciplines (mechanical, structural, manufacturing, electrical, communications, aerodynamics) and where suitable expertise is not available from within ASTRI, it should be actively sought out and budgeted for in the program.

		As an example, ANU would like to involve the Materials and Manufacturing group from the Research School of Engineering, to leverage expertise from the automotive manufacturing industry.
Make-buy decisions are important, and supplier capability a key issue. The benefits of low-cost country sourcing cannot be overlooked.	7	<p>A well-thought through make-buy strategy for all subsystems of a new heliostat design is vital to the success of the ASTRI heliostat cost down program, and should be developed as part of the program.</p> <p>ASTRI should seek to capitalise upon the strengths of its members to undertake the R&D side of a 'make' strategy for carefully selected subsystems of the heliostat design. Strategic partnerships with industry are likely to be beneficial for prototyping and cost sharing, and should be investigated as part of the program.</p> <p>However, for many elements of the heliostat design, a 'buy' strategy will be more cost effective – i.e. defining requirements and purchasing from an external supplier. This will allow cost sharing and access to a wide range of new ideas and technologies, as well as limiting the overall scope of the design task to a manageable level within the ASTRI resource constraints.</p>
<p>Currently operational heliostats range in size from 1.14 m² to 120 m², and there is no consensus regarding the optimal size of a heliostat. In the past, the studies indicated that heliostats should be very large to be cost effective, at least 50 m² and preferably larger. The main driver to large scale was the cost per m² of the heliostat drive system.</p> <p>However, as size is reduced to a scale equivalent to other volume manufactured commodity items, a number of drivers relating to manufacturing and assembly become more relevant, such as:</p> <ul style="list-style-type: none"> • Production volume • Use of common-off-the-shelf (COTS) components • Use of low-cost manufacturing processes • Use of standard assembly processes • Transport and logistics <p>These cost drivers all favour reduced scale, and have the impact of lowering specific cost.</p>	8	<p>The ASTRI program needs to take a reasoned position on heliostat size. This report recommends two key principles:</p> <ul style="list-style-type: none"> • Small heliostats (<10 m²) appear difficult to justify and we should look for opportunities to increase size above this. • We should seek compatibility with volume manufacturing and assembly processes – including the use of COTS components – which will have the tendency to reduce heliostat size. <p>With these two equally important – but competing - design principles established, it is our position that the size will evolve naturally towards an optimum during product design, as long as a concurrent engineering / DFMA approach is adopted.</p>
Structural costs can be expected to be dominated by wind load.	9.1	The cost of the structural elements (primarily pedestal, mirror supports, foundations) is higher than any other subsystem. Hence techniques that reduce wind loads are important to overall cost reduction. Further

		work is recommended in characterising wind and resultant loads as a function of location.
A key initial design decision is the determination of peak static wind loads, due to the sensitivity of loads (and hence material cost) to the wind specification.	9.2	As methods for determining peak wind loads relate to risk factors and are probabilistic in nature, a risk analysis (based on a 'typical' installation) is warranted to remove conservative factors inherent in codes.
Design loads derived from wind tunnel tests are more accurate, and generally lower, than those derived using building codes. For certain heliostat orientations, the inner rows of heliostats may experience a reduction in total wind load as high as 90% compared to the first row.	9.2	Given the University of Adelaide expertise, wind tunnel testing should be carried out as soon as new design geometry is known, prior to detailed structural design. Tests should include a heliostat array, to allow for the possibility of lower design loads for heliostats located with the heliostat field.
Wind load on a heliostat can be reduced by the application of wind barriers.	9.2	Further wind tunnel investigation of the impact of barriers on the static loads is warranted, as the relationship between the wind load reduction and fence parameters (location, shape, height, and porosity) has not been determined. In addition, the effect of wind fences on dynamic loading remains unclear.
The application of a porous fence at the edge of the mirror panel can reduce the overturning moment by as much as 40%.	9.2	Investigation of the feasibility of wind load reduction using different attachments is warranted.
With some significant effort, CFD simulations of wind effects in a solar field can be made reliable, and overcome many of the physical, time and cost restrictions of wind tunnel experiments.	9.2	Significant effort would be required to develop numerical modelling tools with an appropriate level of confidence, although such modelling may be warranted as it may allow design optimisation beyond what is achievable using wind tunnel tests alone. The level of R&D effort should be proportional to the potential for heliostat cost reduction. Care needs to be taken to limit the scope of CFD simulation to align with the main ASTRI goals.
Where the frequency of wind induced vibration matches a natural frequency of the heliostat structure, deformation or damage of the heliostat structure may occur. Adjusting the flow field to reduce vortex formation is an attractive alternative to increasing the rigidity of the structure. Previous work on heliostat aerodynamics has mainly addressed static wind load characteristics, while the dynamics of wind loading have not been fully understood and considered in heliostat design.	9.3	Understanding dynamic wind load effects is important, particularly when considering methods of reducing static wind loads, such as heliostat attachments, wind barriers, or designing inner field heliostats with lower static loads. In some cases, it may be that dynamic wind loads become more important than the static loads, and limit the usefulness of these techniques. Aerodynamic methods of reducing the vibration may also benefit the performance of the heliostats with regards to solar capture.
Mirrored glass and reflective film are the most suitable current (or near-term) options for heliostat reflectors. Polished metal and plastic mirrors both do not currently have adequate reflectance. There are around six suppliers of standard 3-4 mm low-iron mirrored glass for solar	0 to 10.4	Heliostat designs based on glass mirrors should be included in the future ASTRI heliostat program as a relatively 'safe' default option that is compatible cost reduction objectives. However, use of reflective film may open up design options, materials and reflector shapes not possible with glass, perhaps using plastic or

<p>applications. Three of these can also supply thin mirrored glass (~1 mm). Glass mirrors should be considered default reflector, as they are relatively inexpensive, durable, have high reflectance and are accepted by industry.</p> <p>There are approximately four suppliers of reflective film. Reflective film technology is still evolving and continuing to improve, particularly via an active research program by 3M, and encouraging durability results.</p>		<p>composite material as the substrate. ASTRI should consider both options, perhaps with parallel development streams.</p>
<p>Automotive plastic mirrors currently achieve excellent durability results and reflectivity of 60%. Early UniSA modelling indicates reflectance in the order of 95% is feasible, but significant further work is required to realise this practically.</p> <p>Significant practical limitations for CSP applications exist with the current process:</p> <ul style="list-style-type: none"> • Injection moulding typically limits size to about 0.1 m² in x-section, but 1 m² could perhaps be envisaged in future. • Both the injection moulding and PVD process limit throughput for complex shapes 	10.4.3	<p>UniSA is pursuing its own commercialisation plans for high reflectivity plastic coatings (regardless of the target industry), including filing of a recent patent and creation of a new company.</p> <p>Given the stage of development, and the existing commercial plans for this work, is recommended that ASTRI continues to watch this development closely, but that we presently avoid basing our heliostat development on this emerging plastic mirror technology.</p>
<p>There is a significant renewal of development in mirror facets based on sandwich panel type constructions. Two companies offer foam cored sandwich panels commercially. Sandia is also actively working with US manufacturers to develop new sandwich panel facets.</p> <p>Sandwich panel constructions have the following key advantages:</p> <ul style="list-style-type: none"> • Use of thin glass is feasible, hence there is improved reflectance. • Sandwich panels are very strong and rigid, and with good design can lower the mirror support costs. <p>In the past there have been durability issues, they have been considered too expensive to justify the advantages, and there have been no commercial supply options. However, all these issues are being resolved in current developments.</p>	10.6	<p>Investigation of the use of sandwich panel structures is warranted. ANU has a background of development in this area, although partnering with existing suppliers is also an option.</p>
<p>Structural mirror panels may also be made incorporating structural features with the largely planar mirror facets, either as integral</p>	11	<p>Within ASTRI there is experience with a range of materials and production methods that may be of interest. The ANU has worked</p>

<p>features or by bonding to the reflector.</p> <p>For example, pressed sheet metal structures support the glass at both the Gemasolar and Crescent Dunes projects. Various options exist with plastics, most likely in combination with a reflective film. For example, thermoforming or compression moulding of a pre-prepared flat sheet of a thermoplastic polymer may achieve suitable optics at a competitive cost.</p>		<p>extensively with the automotive industry in sheet metal forming, and both Flinders and UniSA have experience with polymeric materials and production methods.</p> <p>As discussed above, with regards to heliostat size, new designs should be compatible with volume manufacturing and assembly processes. Hence it is suggested that exploring options for manufacturing the mirror panels and/or the mirror panel supports is part of the heliostat cost down program, with industry partnering where it makes sense.</p>
<p>Development of autonomous heliostats – i.e. heliostats that do not require power or communication wiring – has progressed markedly in recent years.</p>	12	<p>The potential for significant cost savings favour the use of technologies enabling heliostat autonomy over conventional wired systems. It is suggested that ASTRI should leverage recent developments in autonomous heliostat technology, and partner with an organisation specialist in this area (rather than developing this subsystem within ASTRI).</p>
<p>The majority of heliostat systems have used the ‘azimuth-elevation’ style of sun tracking. However, other styles of tracking have been used in a number of recent prototypes. These include:</p> <ul style="list-style-type: none"> • Horizontal primary axis heliostats: suitability for linear actuators on both axes, and allows denser spacing. • Target aligned heliostats: minimises astigmatic aberration, improving overall solar capture and flux uniformity. 	13.1 and 13.2	<p>Pros and cons of these alternative approaches should be examined as part of the ASTRI heliostat program, and this will necessarily involve simulation of annual solar field performance for various geometries, including factors such as the physical limitation of tracking. CSIRO has expertise in this type of system modelling.</p>
<p>There are many methods for canting mirror panels (the review summarises 11 different methods).</p>	13.4	<p>Canting is a cost that in some cases can be avoided, for example, for single facet heliostats or systems assembled on a jig. Both the cost of canting, and the cost of avoiding canting, should be examined further in the ASTRI heliostat program.</p>
<p>Actuation systems have long been one of the key cost drivers for heliostats. The pedestal mounted azimuth drive system has been one of the main drivers to larger size heliostats. However, some technology developers believe linear drive systems are cheaper, and can completely replace azimuth drives. Alternative drive systems, such as rim drives with cables, have been proposed to avoid the cost of pedestal mounted systems. Hydraulic drive systems have been used cost effectively on large heliostats.</p>	14	<p>Avoiding unnecessary customisation and use of common-off-the-shelf components where possible should be guiding principles for tracking system design.</p> <p>Rim drives and linear drives have better mechanical advantage than slewing drives and are possibly good options.</p> <p>The ASTRI role here is likely to make sure a good systems engineering approach is taken to actuation system design, rather than development of specific components.</p>

18 Acknowledgement

For the many stimulating conversations, we would like to acknowledge our ASTRI colleagues Wasim Saman, Peter Murphy, Drew Evans, Sarah Miller, and Alex Burton. More broadly within the industry, we gratefully acknowledge Andreas Pfahl, Chuck Kutscher, Carsten Holze, Michael Randt, Cliff Ho, Soledad Garrido, Alex Lehmann, Peter Allenspach, George Tedesco Jnr, Jordi Villanueva, Peter Heller, Bhargav Ramachandra, Philipp Schramek, Mark O’Neil, James Fisher, Nick Borema, Steve Hollis, Graeme Wood, Tobias Prosin, Klaus Pottler, and Steffen Ulmer, all of whom have shown interest in the project and have provided invaluable input.

The ASTRI program has been supported by the Australian Government through the Australian Renewable Energy Agency (ARENA). The Australian Government, through ARENA, is supporting Australian research and development in solar photovoltaic and solar thermal technologies to help solar power become cost competitive with other energy sources. The views expressed herein are not necessarily the views of the Australian Government, and the Australian Government does not accept responsibility for any information or advice contained herein.

19 References

- [1] Australian National University (Solar Thermal Group). Heliostat Cost Down Scoping Study - Project Management Plan, 2013. Report number STG-3000 Rev 03
- [2] EurObserv'ER. Solar thermal and concentrated solar power barometer. 2013; Available from: <http://www.eurobserv-er.org/pdf/baro215.asp> [cited 27 June 2013]
- [3] National Renewable Energy Laboratory. Power Tower Projects. 2013; Available from: http://www.nrel.gov/csp/solarpaces/power_tower.cfm [cited June 25 2013]
- [4] U.S. Department of Energy. Strategy for CSP FOAs: Deconstructing 6 c/kWh. 2011; Available from: www1.eere.energy.gov/solar/pdfs/sunshot_csp_poster.pdf [cited 28 June 2013]
- [5] CSIRO. Australian solar thermal research initiative. 2013; Available from: <http://www.csiro.au/Organisation-Structure/Flagships/Energy-Transformed-Flagship/ASTRI.aspx> [cited 25 June 2013]
- [6] Falcone PK. A handbook for solar central receiver design, Sandia National Laboratories, 1986. Report number 86-8009
- [7] Kolb G, Jones S, Donnelly M, Gorman D, Thomas R, Davenport R, Lumia R. Heliostat Cost Reduction Study, Sandia National Laboratories, Albuquerque, New Mexico, 2007. Report number SAND2007-3293
- [8] U.S. Department of Energy. Sunshot Concentrating Solar Program Review 2013, Phoenix, Arizona, 2013.
- [9] Kolb GJ, Ho CK, Mancini TR, Gary JA. Power Tower Technology Roadmap and Cost Reduction Plan, Sandia National Laboratories, 2011. Report number SAND2011-2419
- [10] Abengoa Solar. Advanced baseload molten salt tower. In: Sunshot CSP program review. 2013. Phoenix, Arizona
- [11] Mancini TR. Catalog of Solar Heliostats, 2000.
- [12] Koretz B. Flexible Assembly Solar Technology. In: Sunshot CSP Program Review 2013. 2013. Phoenix, Arizona
- [13] Lata J, Alcalde S, Fernandez D, Lekube X. First surrounding field of heliostats in the world for commercial solar power plants - Gemasolar. In: 16th International SolarPACES Symposium. 2010. Perpignan
- [14] Abengoa Solar. Annual Report, 2009.
- [15] Solar Reserve. Web site. 2013; Available from: <http://www.solarreserve.com/what-we-do/csp-projects> [cited 5 August 2013]
- [16] NEM Energy. Heliostats. 2013; Available from: <http://www.worldfutureenergysummit.com/Portal/exhibitors/nem-middle-east.aspx> [cited 27 June 2013]
- [17] Kopilovsky K. AORA's tulips: solar energy in bloom. Earth Times 2012; Available from: <http://www.earthtimes.org/energy/aora-solar-energy-tulips/1997/> [cited 27 June 2013]
- [18] Pfahl A. Journal of Solar Energy Engineering 2013;136
- [19] Abengoa Solar. Annual Report, 2011.

- [20] Abengoa Solar. Annual Report, 2012.
- [21] Abengoa. Annual Report Section 06.3, 2012.
- [22] Schell S. *Solar Energy* 2011;85:614-619
- [23] Pfahl A, Randt M, Holze C, Unterschütz S. *Solar Energy* 2013;92:230-240
- [24] Holze C, Bruggen H, Misseeuw R, Cosijns B, Albers R, Isaza D. Laminated solar thin glass mirror solution for cost effective CSP systems. In: 18th annual SolarPACES symposium. 2012. Marrakesh
- [25] Kubisch S, Randt M, Buck R, Pfahl A, Unterschütz S. Wireless heliostat and control system for large self-powered heliostat fields. In: 17th annual SolarPACES symposium. 2011. Granada
- [26] Bender W, Chalifoux B, Schneider D. Suspension heliostat material efficiency. In: 2011 annual SolarPACES symposium. 2011. Granada
- [27] Bender B. Deploying low-cost suspension heliostats. In: Sunshot CSP program review. 2013. Phoenix, Arizona
- [28] CSIRO. Heliostat Benchmarking and Costing, excerpt from CSIRO ASI/ARENA report - provided in-confidence on 14 August 2013, 2013.
- [29] Titan tracker. Titan tracker heliostat model TT PTK-150 ATR. 2013; Available from: http://www.titantracker.es/v_portal/apartados/apartado.asp?te=699 [cited June 27 2013]
- [30] Ganapathi GB. Low-cost light weight thin film solar concentrators. In: SunShot CSP Program Review. 2013. Phoenix, Arizona
- [31] Kutscher C. Low-cost heliostat for modular systems. In: Sunshot CSP program review. 2013. Phoenix, Arizona
- [32] Cordes S, Prosinecki TC, Wiegardt K. An approach to competitive heliostat fields. In: 18th annual SolarPACES symposium. 2012. Marrakesh
- [33] Buck R, Wurmthoringer K, Lehle R, Gottsche J, Pfahl A. Development of a 30 m² heliostat with hydraulic drive. In: 16th annual SolarPACES symposium. 2010. Perpignan
- [34] Lehle GmbH. Website. 2013; Available from: <http://www.citytramp.com/solar/> [cited 31 July 2013]
- [35] Lehmann A, Allenspach P. Toroidal heliostat, 2012. Patent no.: WO 2012/139169 A1
- [36] Lehmann A, Shirvington T, Allenspach P. Development and validation of the passive adjustment toroidal heliostat (PATH). In: 50th annual Australian Solar Council (AuSES) conference. 2012. Melbourne
- [37] Google. RE<C: Heliostat Project Overview. 2013; Available from: http://www.google.org/pdfs/google_heliostat_project.pdf [cited 27 June 2013]
- [38] I.T. Power. Realising the potential of concentrating solar power in Australia, 2012. Report number 978-0-9873356-2-3 (ISBN)
- [39] Zhu G, Wendelin T, Wagner MJ, Kutscher J. *Solar Energy In press*
- [40] U.S. Department of Energy. Sunshot Vision Study, 2012.
- [41] Wagner M. Direct s-CO₂ receiver development. In: Sunshot CSP program review. 2013. Phoenix, Arizona

- [42] Turchi CS. 10 MW supercritical-CO₂ turbine project. In: SunShot CSP program review. 2013. Phoenix, Arizona
- [43] Ho CK, Iverson BD. Review of central receiver designs for high-temperature power cycles. In: 18th annual SolarPACES symposium. 2012. Marrakesh
- [44] Crespo L, Ramos F, Martinez F. Questions and answers on solar central receiver plant design by NSPOC. In: 17th annual SolarPACES symposium. 2011. Granada
- [45] Roger M, Amsbeck L, Gobereit B, Buck R. Face-down solid particle receiver using recirculation. In: 16th annual SolarPACES symposium. 2010. Perpignan
- [46] Tyner CE, Pacheco JE. eSolar's power plant architecture. In: 15th annual SolarPACES symposium. 2009. Berlin
- [47] Kalpakjian S, Schmid SR. Manufacturing engineering and technology. 6th ed. Prentice Hall, Singapore; 2010.
- [48] Boothroyd G. Computer-Aided Design 1994;26:505-520
- [49] Canez LE, Platts KW, Probert DR. International Journal of Operations & Production Management 2000;20:1313-1330
- [50] Perrons RK, Richards MG, Platts K. Management Decision 2005;43:670-690
- [51] Platts KW, Song N. Supply Chain Management 2010;15:320-331
- [52] Kusaba K, Moser R, Rodrigues AM. Journal of Supply Chain Management 2011;47:73-93
- [53] BrightSource. Press release: "Brightsource selected by Department of Energy for Sunshot research and development project". 2012; Available from: <http://www.brightsourceenergy.com/brightsource-selected-by-department-of-energy-for-sunshot-research-demonstration-project> [cited 12 July 2013]
- [54] Vant-Hull LL, Central tower concentrating solar power (CSP) systems, In: K. Lovegrove, W. Stein (Eds.) Concentrating solar power technology: principles, developments and applications, Woodhead Publishing, Cambridge, UK, 2012,
- [55] Gould WR. SolarReserve's 565 MWt molten salt power towers. In: 17th International SolarPACES Symposium. 2011. Granada
- [56] Schramek P, Mills DR, Stein W, Le Lièvre P. Journal of Solar Energy Engineering 2009;131:024505-024505
- [57] Siemens Geared Motors. Gear drives for solar tracking [product brochure], 2008, Available from: http://www.dut.ac.za/sites/default/files/space_science/Drivers%20for%20Solar%20Tracking.pdf. [cited 29 June 2013]
- [58] Teufel E, Buck R, Pfahl A, Boing G, Kunert J. Dimensioning of heliostat components under wind and gravity load: the map approach. In: 14th International SolarPACES Symposium. 2008. Las Vegas
- [59] Kunert J, Boing G, Pfahl A, Buck R. Dimensioning heliostat drives considering dynamic wind loads. In: 15th International SolarPACES Symposium. 2009. Berlin
- [60] Peerless-Winsmith. D-90 Type SE Worm Gear Speed Reducers, 2003, Catalogue number: 290J PWS-19350
- [61] Cone Drive. Tracking the sun with more teeth, more torque, more tech. 2013; Available from: <http://www.conedrive.com/97/solar> [cited June 18 2013]

- [62] Bhargav KR, Gross F, Schramek P. Life cycle cost optimized heliostat size for power towers. In: 19th annual SolarPACES conference. 2013. Las Vegas
- [63] Cook NJ. The designer's guide to wind loading of building structures. Part 1: background, damage survey, wind data and structural classification. 1985. Butterworths, London
- [64] Peterka JA, Bienkiewicz B, Hosoya N, Cermak JE. *Energy* 1987;12:261-267
- [65] Bhaduri S, Murphy LM. WIND LOADING ON SOLAR COLLECTORS, In, 1984,
- [66] Xerikos J, Tang HH, Cermak JE, Peterka JA. *Zement-Kalk-Gips* 1980;2:1173-1184
- [67] Xerckos J, Tang HH, Cermak JE, Peterka JA. IN: PROC. FIFTH INT. CONF. ON WIND ENGINEERING, (FORT COLLINS, U.S.A.: JUL. 8-14, 1979), J.E. CERMAK (ED.) 1979;2, New York, U.S.A., Pergamon Press, 1979, Session X, Paper 6
- [68] Edwards B. Electric Power Research Institute (Report) EPRI EA 1979:1319-1323
- [69] Huss S, Traeger YD, Schvets Z, Rojansky M, Stoyanoff S, Garber J. Evaluating effects of wind loads in heliostat design. In: 17th annual SolarPACES symposium. 2011. Granada
- [70] Rebolo R, Lata J, Vazquez J. Design of heliostats under extreme and fatigue wind loads. In: 17th annual SolarPACES symposium. 2011. Granada
- [71] Boggs D, Lepage A. Wind tunnel methods, American Concrete Institute (Ed.), 2008. Report number SP-240-6
- [72] Peterka J, Derickson R. Sandia National Laboratories, Albuquerque, New Mexico 1992
- [73] Peterka JA, Tan Z, Bienkiewicz B, Cermak J. NASA STI/Recon Technical Report N 1988;89:22179
- [74] Peterka JA, Tan Z, Bienkiewicz B, Cermak JE. 1988
- [75] Peterka JA, Tan Z, Cermak JE, Bienkiewicz B. *Journal of Solar Energy Engineering, Transactions of the ASME* 1989;111:158-164
- [76] Hosoya N, Peterka J, Gee R, Kearney D. NREL Report, NREL/SR-550-32282 2008
- [77] Krampa-Morlu FN, Balachandar R. *Journal of Hydraulic Research* 2007;45:270-278
- [78] Krampa FN, Balachandar R. *Canadian Journal of Civil Engineering* 2011;38:710-717
- [79] Wu Z, Gong B, Wang Z, Li Z, Zang C. *Renewable Energy* 2010;35:797-806
- [80] Pfahl A, Uhlemann H. *Journal of Wind Engineering and Industrial Aerodynamics* 2011;99:964-968
- [81] Pfahl A, Buselmeier M, Zschke M. *Solar Energy* 2011;85:2185-2201
- [82] Chuncheng Z, Zhifeng W, Xiaobing L. Design and analysis of a novel heliostat structure, In: Sustainable Power Generation and Supply, 2009. SUPERGEN '09. International Conference on, 2009, pp. 1-4
- [83] Strachan JW, Houser RM. Solar Thermal Test Department, Sandia National Laboratories, SAND92-1381 1993
- [84] Segal A.
- [85] Shademan M, and Hangan, H. Wind Loading on Solar Panels at Different Inclination Angles. In: Proc. 11th Americas Conference on Wind Engineering. 2009. San Juan, Puerto Rico

- [86] Velicu R, Lates, M., and Moldovean, G. Loading Cases and Forces on Azimuthal Solar Tracking Systems with Linear Actuator, In: Proc. 10th International Symposium on Science of Mechanisms and Machines, Brasov, Romania, 2009,
- [87] Mier-Torrecilla M, Herrera E, Doblare M. Numerical calculation of wind loads over solar collectors. In: 19th annual SolarPACES symposium. 2013. Las Vegas
- [88] Shingleton J. One-axis trackers—improved reliability, durability, performance and cost reduction, Subcontract Report SR-520-42769, National Renewable Energy Lab, 2008.
- [89] Kvasznicza Z, and Elmer, G. Optimising Solar Tracking Systems for Solar Cells. In: 4th Serbian-Hungarian Joint Symposium on Intelligent Systems. 2006
- [90] Sment J, Ho CK. Characterization of wind velocity distributions within a full-scale heliostat field, In, 2012, pp. 167-171
- [91] Chen JM, Fang Y-C. Journal of Wind Engineering and Industrial Aerodynamics 1996;61:99-112
- [92] Gong B, Li Z, Wang Z, Wang Y. Renewable Energy 2012;38:206-213
- [93] Ongoren A, Rockwell D.J. Fluid Mech.;191 , Jun. 1988:197-223
- [94] Ongoren A, Rockwell D.J. Fluid Mech. 1988;191 , Jun. 1988:225-245
- [95] Lasheras JC, Meiburg E. Physics of Fluids A 1990;2:371-380
- [96] Julien S, Lasheras J, Chomaz JM. Journal of Fluid Mechanics 2003:155-189
- [97] Tamaddon-Jahromi HR, Townsend P, Webster MF. Computers and Fluids 1994;23:433-446
- [98] Griffith DT, Ho CK, Hunter PS, Sment J, Moya AC, Menicucci AR. Modal analysis of a heliostat for concentrating solar power, In, 2012, pp. 415-423
- [99] Zang C, Wang Z, Liu H, Ruan Y. Applied Energy 2012;93:444-448
- [100] Gong B, Wang Z, Li Z, Zang C, Wu Z. Renewable Energy 2013;50:307-316
- [101] Wang YG, Li ZN, Gong B, Li QS. Key Engineering Materials 2009;400-402:935-940
- [102] Peterka JA, Tan Z, Cermak JE, Bienkiewicz B. Journal of Solar Energy Engineering 1989;111:158-164
- [103] Banks D. Measuring peak wind loads on solar power assemblies. In: 13th International Conference on Wind Engineering. 2011. Amsterdam
- [104] National Renewable Energy Laboratory. Concentrating Solar Power Projects. 2013; Available from: <http://www.nrel.gov/csp/solarpaces/> [cited 16 July 2013]
- [105] Tian Y, Zhao CY. Applied Energy 2013;104:538-553
- [106] Wikipedia. List of solar thermal power stations. 2013; Available from: http://en.wikipedia.org/wiki/List_of_solar_thermal_power_stations [cited 16 July 2013]
- [107] Flabeg. Solar mirrors for CSP and CPV - Catalogue, 2013, Available from: www.flabeg.com/uploads/media/FLABEG_Solar_en_05.pdf [cited 25 June 2013]
- [108] RioGlass Solar. Website. 2013; Available from: www.rioglassolar.com [cited 16 July 2013]
- [109] Procter T. Parabolic trough reflectors: Does glass still have the cutting edge? CSP Today 2010; Available from: <http://social.csptoday.com/technology/parabolic-trough-reflectors-does-glass-still-have-cutting-edge> [cited 22 July 2013]

- [110] Sun & Life. Sun & Life acquires FLABEG, the CSP Solar Technology Leader. 2013; Available from: <http://www.sunandlife.com/index-4.php?id=12&p=&search=#ontitle> [cited 21 October 2013]
- [111] Saint Gobain. Website. 2013; Available from: <http://www.saint-gobain-solar-power.com/> [cited 17 July 2013]
- [112] AGC Solar. Website. 2013; Available from: <http://www.agc-solar.com/> [cited 17 July 2013]
- [113] Guardian Industries. Guardian EcoGuard Solar Boost - MP, 2013, Available from: https://www.guardian.com/GuardianGlass/glassproducts/EcoGuardSolarEnergyGlass/EcoGuardCSPThermalSeries/EcoGuardSolarBoostMP/ssLINK/gi_009463 [cited 17 July 2013]
- [114] Guardian Industries. Guardian EcoGuard Solar Boost - CFM, 2013, Available from: https://www.guardian.com/GuardianGlass/glassproducts/EcoGuardSolarEnergyGlass/EcoGuardCSPThermalSeries/EcoGuardSolarBoostMP/ssLINK/gi_013412 [cited 17 July 2013]
- [115] Guardian. Ecoguard solar boost-CFL: concentrating flat laminated mirrors. 2010; Available from: https://www.guardian.com/GuardianGlass/glassproducts/EcoGuardSolarEnergyGlass/EcoGuardCSPThermalSeries/EcoGuardSolarBoostMP/ssLINK/gi_013417 [cited 28 June 2013]
- [116] Ronda. Website. 2013; Available from: http://www.ronda-hightech.com/it?page_id=27&lang=en [cited 17 July 2013]
- [117] Damin Glass. Damin Solar Mirror [brochure from SolarPACES2013 conference], 2013,
- [118] Meyen S, Lupfert E, Pernpeintner J, Fend T. Optical characterisation of reflector material for concentrating solar power technology. In: 15th annual SolarPACES symposium. 2009. Berlin
- [119] Meyen S, Fernandez-Garcia A, Kennedy C, Lupfert E. Standardization of solar mirror reflectance measurements - round robin test. In: 16th annual SolarPACES symposium. 2010. Perpignan
- [120] Chen D. Polymeric mirror films: durability improvement and implementation in new collector designs. In: Sunshot CSP program review. 2013. Phoenix, Arizona
- [121] DiGrazia MJ, Jorgensen G, Gee R, Bingham C, Loux C. Reflechtech® polymer mirror film advancements in technology and durability testing, In: 5th International Conference on Energy Sustainability, Washington, DC., 2011,
- [122] Schlaich J. Engineering Structures 1999;21:658-668
- [123] Alpert DJ, Houser RM, Heckes AA, Erdman WW, Beninga K, Konnerth Iii A. Solar Energy Materials 1990;21:131-150
- [124] 3M. 3M Solar Mirror Film 1100, 2012, Available from: http://multimedia.3m.com/mws/mediawebserver?mwsId=66666UF6EVsSyXTtnxMEmXf_EVtQEVs6EVs6EVs6E666666--&fn=SolarFilm1100_DMR.pdf [cited 17 July 2013]
- [125] 3M. 3M Solar Energy website. 2013; Available from: http://solutions.3m.com/wps/portal/3M/en_US/Renewable/Energy/Product/Films/ [cited 17 July 2013]
- [126] Gossamer Innovations. X-Perf™ Reflective Panels. 2013; Available from: <http://www.gossamersf.com/about-solar-power-products.htm#xperf-reflective-panels> [cited 17 July 2013]

- [127] Gossamer Innovations. Solar Power Products. 2013; Available from: <http://www.gossamersf.com/solar-power-products.htm> [cited 17 July 2013]
- [128] DiGrazia MJ, Gee R, Jorgensen G. Reflectech[®] mirror film attributes and durability for CSP applications. In: Energy Sustainability. 2009. San Francisco: American Society of Mechanical Engineers
- [129] Kennedy CE, Smilgys RV, Kirkpatrick DA, Ross JS. Thin Solid Films 1997;304:303-309
- [130] Skyfuel. Skyfuel's parabolic trough to save fuel in the gas city. 2012; Available from: <http://www.skyfuel.com/#/NEWS/PRESS%20RELEASES/> [cited 17 July 2013]
- [131] Skyfuel. Skyfuel and Braxenergy team to bring parabolic trough to Brazil. 2011; Available from: <http://www.skyfuel.com/#/NEWS/PRESS%20RELEASES/> [cited 17 July 2013]
- [132] Konica Minolta. Konica Minolta Showcases Newly Developed, Highly Durable Film Mirror for CSP at World Future Energy Summit as Reference Exhibit. 2012; Available from: http://www.konicaminolta.com/about/releases/2012/0116_01_01.html [cited 17 July 2013]
- [133] Honda M. Film mirror for reflecting sunlight and reflective device for solar thermal power generation, USA, 2013. Patent no.: US2013/0081612
- [134] Konica Minolta. Next-generation energy: solar thermal power generation. 2013; Available from: <http://www.konicaminolta.com/about/research/solar/> [cited 17 July 2013]
- [135] Numrich U, Arndt T, Arnold W, Olbrich M. Concentrator for solar energy generation and production thereof from polymeric materials, 2012. Patent no.: US 2012/0182607 A1
- [136] Alanod Solar. Miro-Sun[®], 2010, Available from: http://alanod-solar.com/opencms/export/alanod_solar/downloads/MIRO_SUN_engl_101112.pdf [cited 19 July 2013]
- [137] Wang U. Should CSP mirrors be glass or metal? Renewable Energy World 2010; Available from: <http://www.renewableenergyworld.com/rea/news/article/2010/08/should-csp-mirrors-be-glass-or-metal> [cited 22 July 2013]
- [138] Alanod Solar. Website. 2013; Available from: http://alanod-solar.com/opencms/opencms/Reflexion/Technische_Info.html [cited 22 July 2013]
- [139] Deutsches Zentrum für Luft- und Raumfahrt (DLR). Measurement of reflectivity of optical components for concentrating solar power technology, 2009. Report number DLR KTr 3001588
- [140] Alanod Solar. NREL testing of MIRO-SUN[®]. 2009; Available from: <http://www.alanod-solar.us/images/NREL%20MIRO-SUN%20Test.pdf> [cited 19 July 2013]
- [141] Alanod Solar. Website. 2013; Available from: <http://alanod-solar.com/opencms/opencms/Reflexion/index.html> [cited 19 July 2013]
- [142] Almeco Solar. Vega energy - solar reflective surfaces, 2013, Catalogue number: S302 - ENG - 05/2013 Available from: <http://www.almecosolar.com/Brochure/vegaenergy.pdf> [cited 22 July 2013]
- [143] Fraunhofer Institute for Solar Energy Systems. Spectral measurements of reflector samples and calculations of solar reflectance values - report concerning Offer AN10-0384, 2010. Report number MAO3-HEI-1005-E02
- [144] Patriot Solar Group. Solar Reflective Material, 2013, Catalogue number: DATA900802_REV001 Available from: www.patriotsolargroup.com/dataSheets/SolarReflectiveMaterial.pdf [cited 22 July 2013]
- [145] SMR. Website. 2013; Available from: <http://www.smr-automotive.com/exterior-mirrors.html> [cited 22 July 2013]

- [146] University of South Australia. Great science delivers automotive innovation to SA. 2011; Available from: <http://w3.unisa.edu.au/news/2011/230511.asp> [cited 22 July 2013]
- [147] Hall CJ, Field SD, Zuber K. Plastic automotive mirrors, 2011. Patent no.: WO2011075796 A1
- [148] Vandehei PT. Coated copper reflector, 1980. Patent no.: US 4,189,205
- [149] Hall C, Field S, Zuber K, Murphy P, Evans D. *Corrosion Science* 2013;69:406-411
- [150] Zuber K, Hall C, Murphy P, Evans D. *Wear* 2013;297:986-991
- [151] Zuber K, Hall C, Murphy P, Evans D. *Surface and Coatings Technology* 2012;206:3645-3649
- [152] Evans D, Zuber K, Hall C, Griesser HJ, Murphy P. *Surface and Coatings Technology* 2011;206:312-317
- [153] Schwarberg F, Schiller M. Enhanced solar mirrors with anti-soiling coating. In: 18th annual SolarPACES symposium. 2012. Marrakesh
- [154] Diver RB, Grossman JW. Sandwich Construction Solar Structural Facets, 1998. Report number SAND98-2845C
- [155] Yellowhair J, Andraka CE. Evaluation of advanced heliostat reflective facets on cost and performance. In: 19th annual SolarPACES symposium. 2013. Las Vegas
- [156] Lasich JB. A method of manufacturing mirrors for a dish reflector, 2001. Patent no.: WO 02/078933 A1
- [157] Lovegrove K, Burgess G, Pye J, Brunswick J, Coventry J, Cumpston J. A new 500 m² paraboloidal dish solar concentrator. In: 15th annual SolarPACES symposium. 2009. Berlin
- [158] toughtrough. Innovative Solar Mirror Technology [Data Sheet], 2013, Available from: http://www.toughtrough.com/index.php?eID=tx_nawsecuredl&u=0&file=fileadmin/pdf/Infosh eet_heliostat_toughTrough.pdf&t=1371885919&hash=99529a99807da494209cf0c6eab97469bf0d6327 [cited 28 June 2013]
- [159] Morton-Jones DH. *Polymer Processing*. Chapman and Hall; 1989.
- [160] DeGarmo EP, Black JT, Kosher RA. *Materials and Processes in Manufacturing* 7th ed. Macmillan, New York; 1988.
- [161] Amstead BH, Ostwald PF, Begeman ML. *Manufacturing Processes* 8th ed. John Wiley, New York; 1987.
- [162] Ciemat. *Plataforma Solar de Almería Annual Report*, 2004.
- [163] Garcia G, Egea A, Romero M. First autonomous heliostats field. PCHA project. In: *ISES Solar World Congress*. 2003. Goteborg
- [164] Bobinecz M. Ivanpah solar electric generating facility. In: *Engineering and Construction Contracting Conference*. 2012. San Antonio, Texas
- [165] Schneider Electric. *Torresol Energy - Concentrating Solar Power Plant*. 2013; Available from: <http://www.schneider-electric.com/solutions/ww/e/ref/4663701-torresol-energy-concentrating-solar-power-plant> [cited 9 September 2013]
- [166] Marion W, Wilcox S. *Solar Radiation Data Manual for Flat-Plate and Concentrating Collectors*, M.A. Dunlap (Ed.), National Renewable Energy Laboratory, 2009. Report number NREL/TP--463-5607

- [167] Schramek P, Mills DR. *Energy* 2004;29:701-713
- [168] Zaibel R, Dagan E, Karni J, Ries H. *Solar Energy Materials and Solar Cells* 1995;37:191-202
- [169] Chen YT, Kribus A, Lim BH, Lim CS, Chong KK, Karni J, Buck R, Pfahl A, Bligh TP. *Journal of Solar Energy Engineering* 2004;126:638-644
- [170] Heliosystems. Website. 2013; Available from: <http://heliosystems.com.au/products-and-services/> [cited 31 July 2013]
- [171] Lehmann A. Focal length and field optimisation for toroidal heliostats in high accuracy solar concentrators. In: 16th annual SolarPACES symposium. 2010. Perpignan
- [172] Haberstroh H, Keck T, Weinrebe G, Wohrbach M, Husenbeth C, von Reeken F, Balz M. Optimization of heliostat axes orientations to reduce annual angular ranges. In: 18th annual SolarPACES symposium. 2012
- [173] Chong KK, Tan MH. *Solar Energy* 2011;85:1837-1850
- [174] Yellowhair J, Ho CK. Heliostat canting and focusing methods: an overview and comparison. In: 4th International Conference on Energy Sustainability. 2010. Phoenix, Arizona
- [175] Jones SA. A comparison of on-axis and off-axis heliostat alignment strategies, 1996. Report number SAND--96-0566C; CONF-960455--1
- [176] Buck R, Teufel E. *Journal of Solar Energy Engineering* 2009;131:011001-011001
- [177] O'Brien B. Follow the Sun. *Traverse City Record-Eagle* 2011; Available from: <http://www.brightsourceenergy.com/site/images/btn-download.png> [cited 26 July 2013]
- [178] GFC. CSP-Slewing Gear Unit DRW 100 (Azimuth), 2013, Catalogue number: PM/EM2013 Available from: <http://www.gfc-drives.com/en/downloads/category/15-produkte?download=49:Datenblatt%20-%20DRW%20100%20> [cited 19 August 2013]
- [179] Schlaich bergermann und partner. 150m² metal membrane heliostat ASM 150. 2013; Available from: http://www.sbp.de/en/sun/sheet/699-150m%C2%B2_Metal_Membrane_Heliostat_ASM150.pdf [cited 5 August 2013]
- [180] Huss S. Systems and methods for inserting support members into the ground, 2012. Patent no.: WO 2012/095785 A1
- [181] Kelly B. Advanced thermal storage for central receivers with supercritical coolants, Abengoa Solar, 2010. Report number DOE/GO18149

Appendix A Mirror Technologies used in Solar Thermal Facilities Globally

Table 7. Parabolic Trough Power Plants – Completed and Under Construction

Project	Country	Size - units?	Completed	Mirror manufacturer	Substrate	Reflective layer	Solar collector (SCA) manufacturer
Abhijeet Solar Project	India	50	Not complete	RIO glass	tempered glass	silver	Ener-t International Ltd
Agua Prieta II	Mexico	14	Not complete	Rioglass	tempered glass	silver	Abengoa Solar (ASTRO)
Airlight Energy Ait Baha Plant	Morocco	3	Not complete				Airlight Energy
Andasol-1 (AS-1)	Spain	50	2008	Flabeg (RP3)	annealed glass	silver	UTE CT Andasol-1 (SKAL-ET)
Andasol-2 (AS-2)	Spain	50	2009				UTE CT Andasol-1 (SKAL-ET)
Andasol-3 (AS-3)	Spain	50	2011	Flabeg (RP3)	annealed glass	silver	Flagsol (SKAL-ET 150)
Archimede	Italy	5	2010	Ronda Reflex/RIO	1mm glass/plastic	silver	COMES (ENEA)
Arcosol 50 (Valle 1)	Spain	49.9	2011				Sener (SenerTrough)
Arenales	Spain	50	Not complete	Siemens	hot formed low iron glass	silver	Siemens (SunField 6)
Aste 1A	Spain	50	2012	Flabeg (RP3)	annealed glass	silver	Sener (SenerTrough)
Aste 1B	Spain	50	2012	Flabeg (RP3)	annealed glass	silver	Sener (SenerTrough)
Astexol II	Spain	50	2012				Flagsol (SKAL-ET 150)
Bokpoort	South Africa	50	Not				Sener (SenerTrough)

			complete				
Borges Termosolar	Spain	25	2012				Siemens (SunField 6)
Caceres	Spain	50	Not complete	Flabeg (RP3)	annealed glass	silver	Sener (SenerTrough)
Casablanca	Morocco	50		Flabeg (RP3)	annealed glass	silver	Sener (SENERtrough)
Colorado Integrated Solar Project (Cameo)	USA	2	2010	RIO glass	tempered glass	silver	
Diwakar	India	100	Not complete				SENERtrough (SNT0)
Enerstar (Villena)	Spain	50	Not complete	Flabeg (RP3)	annealed glass	silver	Sener (SenerTrough)
Extresol-1 (EX-1)	Spain	50	2010	Flabeg (RP3)	annealed glass	silver	UTE CT Extresol-1 (SENERTROUGH)
Extresol-2 (EX-2)	Spain	49.9	2010	Flabeg (RP3)	annealed glass	silver	Cobra Instalaciones y Servicios (SENERTROUGH)
Extresol-3 (EX-3)	Spain	50	2012	Flabeg (RP3)	annealed glass	silver	Cobra Instalaciones y Servicios (SENERTROUGH)
Genesis Solar Energy Project	USA	250	Not complete	Flabeg (RP3)	annealed glass	silver	Sener (SenerTrough)
Godawari Solar Project	India	50	Not complete	Flabeg (RP3)	annealed glass	silver	EuroTrough (ET-150)
Gujarat Solar One	India	25	Not complete	Flabeg (RP3)	annealed glass	silver	EuroTrough (ET-150)
Guzmán	Spain	50	2012	Flabeg (RP3)	annealed glass	silver	Sener (SenerTrough)
Helioenergy 1	Spain	50	2011				Abengoa Solar (ASTRØ)
Helioenergy 2	Spain	50	2012				Abengoa Solar (ASTRØ)
Helios I (Helios I)	Spain	50	2012				Abengoa Solar (ASTRØ)

Helios II (Helios II)	Spain	50	2012				Abengoa Solar (ASTRØ)
Holaniku at Keahole Point	USA	2	2009				Sopogy (SopoNova®)
Ibersol Ciudad Real (Puertollano)	Spain	50	2009	Flaberg/Rioglass	annealed glass	silver	Iberdrola (Iberdrola Collector)
ISCC Ain Beni Mathar	Morocco	20	2010	Rioglass	tempered glass	silver	Abengoa Solar (ASTR-Ø)
ISCC Hassi R'mel (ISCC Hassi R'mel)	Algeria	25	2011	Rioglass	tempered glass	silver	Abengoa Solar (ASTR-Ø)
ISCC Kuraymat (ISCC Kuraymat)	Egypt	20	2011	Flabeg (RP3)	annealed glass	silver	Flagsol (SKAL-ET)
KaXu Solar One	South Africa	100	Not complete	Rioglass	tempered glass	silver	Abengoa Solar (E2)
KVK Energy Solar Project	India	100	Not complete				SENERtrough (SNT0)
La Africana	Spain	50	2012				Sener (SenerTrough)
La Dehesa	Spain	50	2011	Rioglass	tempered glass	silver	Ingemetal (SAMCA-Trough)
La Florida	Spain	50	2010	Rioglass	tempered glass	silver	Ingemetal (SAMCA-Trough)
La Risca (Alvarado I)	Spain	50	2009	Flabeg (RP2)	annealed glass	silver	Acciona Solar
Lebrija 1 (LE-1)	Spain	50	2011	Solel			Solel
Majadas I	Spain	50	2010				Acciona Solar Power (SGNX-2)
Manchasol-1 (MS-1)	Spain	49.9	2011	Flabeg (RP3)	annealed glass	silver	Cobra Instalaciones y Servicios (Senertrough)
Manchasol-2 (MS-2)	Spain	50	2011	Flabeg (RP3)	annealed glass	silver	Cobra Instalaciones y Servicios (Senertrough)
Martin Next Generation Solar Energy Center (MNGSEC)	USA	75	2010	RIO glass	tempered glass	silver	Gossamer Space Frames (LAT 1)
Megha Solar Plant	India	50	Not				Albisa (AT-150)

			complete				
Mojave Solar Project	USA	280	Not complete	Rioglass	tempered glass	silver	Abengoa Solar
Morón	Spain	50	2012				
Nevada Solar One (NSO)	USA	75	2007	Flabeg	annealed glass	silver	Acciona Solar Power (SGX-2)
NextEra Beacon Solar Energy Project (Beacon)	USA	250	Not complete				
Olivenza 1	Spain	50	2012	Saint Gobain	glass		Siemens (SunField 6)
Orellana	Spain	50	2012				Sener (SENERtrough)
Ouarzazate (Phase I)	Morocco	160	Not complete				Sener (SenerTrough)
Palma del Río I	Spain	50	2011				Acciona Solar Power (SGNX-2)
Palma del Río II	Spain	50	2010				Acciona Solar Power (SGNX-2)
Palmdale Hybrid Power Plant (PHPP)	USA	50	Not complete				
Pedro de Valdivia	Chile	360	Not complete				
Saguaro Power Plant	USA	1.16	2006	Flabeg	annealed glass	silver	Starnet (LS-2)
Shams 1 (Shams 1)	UAE	100	2013	Flabeg (RP3)	annealed glass	silver	Abengoa Solar (ASTRO)
Solaben 1	Spain	50	Not complete				Abengoa (ASTRØ)
Solaben 2	Spain	50	Not complete				Abengoa (ASTRØ)
Solaben 3	Spain	50	2012				Abengoa (ASTRØ)

Solaben 6	Spain	50	Not complete				Abengoa (ASTRØ)
Solacor 1	Spain	50	2012				Abengoa (ASTRØ)
Solacor 2	Spain	50	2012				Abengoa (ASTRØ)
Solana Generating Station (Solana)	USA	280	2013	Rioglass	tempered glass	silver	Abengoa Solar (E2)
Solar Electric Generating Station I (SEGS I)	USA	13.8	1984				Luz (LS-1)
Solar Electric Generating Station II (SEGS II)	USA	30	1985				Luz (LS-1)
Solar Electric Generating Station III (SEGS III)	USA	30	1985				Luz (LS-2)
Solar Electric Generating Station IV (SEGS IV)	USA	30	1989				Luz (LS-2)
Solar Electric Generating Station V (SEGS V)	USA	30	1989				Luz (LS-2)
Solar Electric Generating Station VI (SEGS VI)	USA	30	1989				Luz (LS-2)
Solar Electric Generating Station VII (SEGS VII)	USA	30	1989				Luz (LS-2)
Solar Electric Generating Station VIII (SEGS VIII)	USA	89	1989				Luz (LS-3)
Solar Electric Generating Station IX (SEGS IX)	USA	89	1990				Luz (LS-3)
Solnova 1	Spain	50	2009	Rioglass	tempered glass	silver	Abengoa (ASTRØ)
Solnova 3	Spain	50	2009	Rioglass	tempered glass	silver	Abengoa (ASTRØ)
Solnova 4	Spain	50	2009	Rioglass	tempered glass	silver	Abengoa (ASTRØ)
Termesol 50 (Valle 2)	Spain	49.9	2011				Sener (SenerTrough)
Termosol 1	Spain	50	2013	Flabeg (RP3)	annealed glass	silver	Sener (SenerTrough)
Termosol 2	Spain	50	2013	Flabeg (RP3)	annealed glass	silver	Sener (SenerTrough)
Thai Solar Energy 1 (TSE1)	Thailand	5	2012	Guardian & AGC	low iron glass	silver	Solarlite GmbH (SL 4600)
Victorville 2 Hybrid Power Plant	USA	50	Not complete				
Yazd	Iran	17	Not				

			complete				
Shiraz	Iran	0.25	Unknown				
Ashalim	Israel	250	Not complete				
Solar 1 and Solar 2 decommissioned	USA	-	-				
Theseus	Greece	52	Not complete				

Table 8. Central Tower Power Plants – Completed and Under Construction

	Country	Size	Completed	Mirror manufacturer	Substrate	Reflective layer	Developer	Heliostat
ACME Solar Tower (Bikaner)	India	2.5	2011			glass		eSolar
Beijing Badaling Solar Tower	China	1.5	2012			G		Himin Solar
BrightSource Coyote Springs 1 (PG&E 3) (Coyote Springs 1)	USA	200	NOT COMPLETED			Glass	BrightSource Energy	
BrightSource Coyote Springs 2 (PG&E 4) (Coyote Springs 2)	USA	200	NOT COMPLETED			G	BrightSource Energy	
BrightSource PG&E 5	USA	200	NOT COMPLETED			G	BrightSource Energy	
BrightSource PG&E 6	USA	200	NOT COMPLETED			G	BrightSource Energy	
BrightSource PG&E 7	USA	200	NOT COMPLETED			G	BrightSource Energy	
Crescent Dunes Solar Energy Project (Tonopah)	USA	110	NOT COMPLETED				SolarReserve	
Gaskell Sun Tower (Gaskell)	USA	245	NOT COMPLETED			G	eSolar ; NRG Energy	
Gemasolar Thermosolar Plant (Gemasolar)	Spain	19.9	2011		Sheet metal stamped facet	G	Torresol Energy	Sener

Ivanpah Solar Electric Generating System (ISEGS)	USA	392	2014			G	BrightSource Energy	
Jülich Solar Tower	Germany	1.5	2008	<i>experimental plant</i>			Kraftanlagen München	
Khi Solar One	South Africa	50	NOT COMPLETED			?		Abengoa Solar
Lake Cargelligo	Australia	3	2011			?		
Palen Solar Electric Generating System	USA	500	NOT COMPLETED			G	BrightSource Energy	
Planta Solar 10 (PS10)	Spain	11.02	2007			Glass-metal		Abengoa (Solucar 120)
Planta Solar 20 (PS20)	Spain	20	2009			Glass-metal		Abengoa (Solucar 120)
Rice Solar Energy Project (RSEP)	USA	150	NOT COMPLETED			G	SolarReserve's Rice Solar Energy, LLC	Pratt Whitney
Sierra SunTower (Sierra)	USA	5	2009			G		eSolar
Supcon Solar Project	China	50	NOT COMPLETED			G	Supcon Solar	

G = assumption that it is glass – based on pictures and lack of mention of what heliostats are made from – i.e. if they were some sort of new material you would expect the project to mention it.

Table 9. Fresnel Reflector Power Plants – Completed and Under Construction

Project	Country	Size	Completed	Mirror Manufacturer	Substrate	Reflective layer
Alba Nova 1	France	12	X	Solar Euromed (AF1)	glass?	
Augustin Fresnel 1	France	250	2012	Solar Euromed (AF1)		
Dhursar	India	100	X			
eCare Solar Thermal Project	Morocco	1	X			
Kimberlina Solar Thermal Power Plant (Kimberlina)	USA	5	2008			
Kogan Creek Solar Boost (Kogan Creek)	Australia	44	X	AREVA Solar	?	
Liddell Power Station	Australia	9	2012	Novatec Solar	glass	
Llo Solar Thermal Project (Llo)	France	9	X	CNIM	?	
Puerto Errado 1 Thermosolar Power Plant (PE1)	Spain	1.4	2009	Novatec Solar España S.L.	glass	
Puerto Errado 2 Thermosolar Power Plant (PE2)	Spain	30	2012	Novatec Solar España S.L.	glass	

Table 10. Stirling Dish Power Plants – Completed and Under Construction

Project	Country	Size	Completed	Mirror manufacturer	Substrate	Reflective layer	Developer / System
Maricopa Solar Project (Maricopa)	USA	1.5	2010	AGC	glass	silver	Stirling Energy Systems (SES) (SunCatcher™)
Tooele Army Depot	USA	1.5	X				Infinia Corp (PowerDish™)

FOR FURTHER INFORMATION

Contact Name

Joe Coventry

t +61 2 6125 2643

e joe.coventry@anu.edu.au

Contact Name

Sarah Miller

t +61 2 4960 6000

e sarah.miller@csiro.au

w www.astri.org.au